Stony Brook University

Cholinergic modulation and integration of excitatory inputs to basolateral amygdala

A Dissertation Presented

by

James David Lederman

to

The Graduate School

in Partial Fulfillment of the

Requirements

for the Degree of

Doctor of Philosophy

in

Neuroscience

Stony Brook University

August 2014

Stony Brook University
The Graduate School

James David Lederman

We, the dissertation committee for the above candidate for the
Doctor of Philosophy degree, hereby recommend
acceptance of this dissertation

Lorna Role, PhD - Dissertation Advisor
Professor and Chair, Department of Neurobiology and Behavior

Mary Kritzer, PhD - Chairperson of Defense
Professor, Department of Neurobiology and Behavior

David Talmage, PhD
Professor, Department of Pharmacology

Alfredo Fontanini, MD, PhD
Professor, Department of Neurobiology and Behavior

Holly Moore, PhD - Outside Member
Professor of Neuroscience, Department of Psychiatry, Columbia University

This Dissertation is accepted by the Graduate School

Charles Taber
Dean of the Graduate School

Abstract

Cholinergic modulation and integration of excitatory inputs to basolateral amygdala

by

James David Lederman

Doctor of Philosophy

in

Neuroscience

Stony Brook University

2014

The amygdala, a subcortical structure in the anterior temporal lobe, plays important roles in integrating sensory information from different brain areas, assigning emotional valence and effecting adaptive behavioral, physiological, and cognitive responses. Sensory inputs from cortical and thalamic sources, carrying highly processed sensory information and low level, more direct sensory information, respectively, converge in the basolateral nucleus of the amygdala (BLA). Here, neuromodulation by acetylcholine (ACh), released from inputs arising from the nucleus basalis of Meynert (NBM) in the basal forebrain, plays a major role in synaptic integration during different emotional arousal states. Using patch-clamp electrophysiology in acute brain slices from adult mice, I took advantage of the fact that these inputs project through spatially distinct fiber tracts, and stimulated either or both of these pathways while recording excitatory post-synaptic currents (EPSCs) in BLA

pyramidal neurons. I found that while both the cortical and thalamic inputs have a similar baseline synaptic strength, they differ in their plasticity to patterned stimulation. Whereas cortical inputs readily potentiate, thalamic inputs are much more variable, showing either potentiation, depression, or no response at all. I subsequently used ChAT-Cre mice transfected with a floxed channelrhodopsin construct targeted to the NBM to compare the response of these inputs to optogenetic stimulation of endogenous cholinergic inputs to the BLA. I found that these inputs are oppositely modulated by endogenous ACh; while cortical inputs show synaptic potentiation, thalamic inputs show synaptic depression. Finally, optogenetic stimulation or inhibition of cholinergic inputs to BLA bidirectionally altered learning and memory in a cued fear conditioning paradigm. In sum, my work suggests that the influence of ACh on integration of inputs in the BLA is potent, input specific, and a key component of behavioral adaptation to fearful stimuli. With disorders such as PTSD an ever increasing problem, the amygdaloid circuitry underlying sensory integration and behavioral adaption represents an especially promising target for clinical intervention.

Dedicated to Emily

I am deeply indebted for your unwavering love and support through the past 3 years.

Your encouragement and gentle prodding has helped me get to the finish.

to my Mom and Dad

You have always given me everything in your power to give.

Without you I could not be here, writing this, proud to be your son.

and to my sister

You are brilliant and wonderful.

I look forward to joining you on one of your adventures.

Table of Contents

List of Figures

List of Abbreviations

AAV	Adeno-Associated Virus
ACh	Acetylcholine
AChR	Acetylcholine receptor
ANOVA	Analysis of Variance
BLA	Basolateral Amygdala
ChAT	Choline Acetyltransferase
CS	Conditioned Stimulus
CNS	Central Nervous System
EPSC	Excitatory Post-Synaptic Current
GABA	Gamma-Aminobutyric Acid
LTP	Long-Term Potentiation
mAChR	Muscarinic Acetylcholine Receptor
mPFC	Medial Prefrontal Cortex
nAChR	Nicotinic Acetylcholine Receptor
NBM	Nucleus Basalis of Meynert
PTSD	Post-Traumatic Stress Disorder
US	Unconditioned Stimulus

Acknowledgments

Without the help and support of many people, this thesis would not have been possible. I would first like to thank my mentor, Professor Lorna Role. I am fortunate to have had her guidance, understanding and encouragement through all the difficulties I faced in completing my work. I would also like to thank my co-PI, Professor David Talmage. His insights and ability to concisely frame complex problems have been invaluable. I would like to express my deepest appreciation for my committee chair, Professor Mary Kritzer, and committee members Professor Alfredo Fontanini and Professor Holly Moore. Thank you for your time and efforts spent guiding me to complete this dissertation.

I am grateful for the tutorship of Li Jiang, and for some of his work that he has graciously allowed me to reference in this dissertation. He helped me assemble the electrophysiology rig used in my experiments and taught me the basics of patch-clamping.

I am honored to have worked with an undergraduate research assistant, Noel Joseph. His dedicated help running preliminary behavioral experiments was invaluable to me. Noel is a bright, highly motivated student who has a productive career ahead in medicine.

Thank you to Professor Shaoyu Ge for providing the oChIEF constructs, and for his and Yan Gu's help and advice in setting up optogenetic behavioral experiments.

I owe a significant debt of gratitude to my girlfriend, Emily Benjamin, who has been unwavering in her support of me while writing this thesis. I am especially appreciative for her personal sacrifices in helping me see my dissertation through to the end.

I am thankful for all the friends I've had the pleasure of meeting and working with in the laboratory and at Stony Brook. I would like to especially thank Mel Haley for her help proofreading parts of this document and her friendship through the past several years. I would also like to thank all the members of the Department of Neurobiology and Behavior office staff, especially Diane Godden and Odalis Hernández, for their assistance navigating a tremendous amount of paperwork.

All the mice sacrificed to conduct these experiments deserve a special acknowledgment. Working with animals has been a cherished privilege.

This work was funded by NIH Director's Pioneer award and NS22061 to LWR.

Chapter 1 - Introduction

The amygdala is a collection of nuclei in the anterior portion of the temporal lobe and is a part of the limbic system (Aggleton, 2000). The importance of the amygdala was first realized in the 1930s by Heinrich Kluver and Paul Bucy conducting experiments in which they removed the temporal lobe from rhesus monkeys. They described several aspects of altered behavior in these animals: a lack of preference for interesting vs. uninteresting objects; a preference for exploring objects with the mouth instead of hands; a seemingly irresistible need to attend to whatever was in their field of view at the moment; emotional changes, *e.g.* lack of fear, more placid demeanor, and lack of facial expression; hypersexuality; and changes in diet, including a preference for normally inedible items such as rocks (Bard, 1928). In the 1950's human patients with temporal lobectomies or damage resulting from cancer, injury or stroke exhibited a similar set of symptoms, eponymously named Kluver-Bucy syndrome. Around this time Lawrence Weiskrantz repeated the Kluver-Bucy experiment lesioning only the amygdaloid complex in monkeys and replicated the same symptoms (Weiskrantz, 1956). In the following decades many studies examined the role of the amygdala in a variety of other cognitive processes, particularly regarding attention, assigning emotional valence to objects and events, emotional learning and memory, and addiction (J. LeDoux, 2007). In spite of its small relative size in the brain, the amygdala can have profound effects on circuits throughout the CNS due to the numerous long-distance reciprocal connections it forms with many other regions throughout the central nervous

system (Davis, 1992; J. E. LeDoux, 2000; McDonald, 1998; Swanson, 2003), even including the spinal cord (Burstein & Potrebic, 1993).

The amygdala plays a key role in assessing the salience of sensory stimuli encountered in an animal's environment (Aggleton, 2000; J. LeDoux, 2007; J. E. LeDoux, 2000). The amygdala receives sensory information of all modalities: visual and auditory information is conveyed directly from the lateral and medial geniculate nuclei of the thalamus, respectively, and from auditory and visual cortical areas; olfactory information is conveyed by direct projections from the olfactory bulb and olfactory cortex; somatosensory information is conveyed from somatosensory cortex, ventral posteromedial nucleus of the thalamus, and brainstem areas; and nociceptive information is conveyed primarily from nociceptive thalamic areas and spinal cord (Aggleton, 2000). The majority of long-distance outputs from the basolateral nucleus are to prefrontal cortex, hippocampus, striatum, substantia innominata and diagonal band of Broca (Rogan, Staubli, & LeDoux, 1997). These outputs are known to play a key role in many forms of learning and memory including associative, spatial, and operant learning (McIntyre, Power, Roozendaal, & McGaugh, 2003; Pare, 2003). For this reason, the amygdala has been described as a sensory gateway to the emotions (J. E. LeDoux, 2000; Mishkin, 1986).

Neural activity arising from sensory stimuli enters the amygdala by two distinct anatomical pathways, directly from sensory thalamic areas via the internal capsule, and indirectly (with the exception of direct olfactory bulb projections) from sensory and multi-

modal cortical areas via the external capsule (Davis, 1992; J. J. Kim & Jung, 2006; J. E. LeDoux, 2000; McDonald, 1998). Glutamatergic axons from these areas converge onto the dendritic trees of pyramidal neurons in the basolateral complex of the amygdala (Mahanty & Sah, 1999), as well as inhibitory GABAergic interneurons (Ehrlich et al., 2009; J. E. LeDoux, 2000). Synaptic connections from thalamic vs. cortical sources appear to be randomly distributed on the dendritic trees of these neurons (Humeau et al., 2005). These connections and their capacity for plasticity underlie the ability of these neurons to integrate sensory signals and, in turn, send appropriate outputs via glutamatergic projections to other nuclei in the amygdala, especially the central nucleus, and to other brain areas, effect adaptive behavioral, cognitive, and physiological responses (Aggleton, 1992, 2000; J. LeDoux, 2007; McKernan & Shinnick-Gallagher, 1997; Quirk, Repa, & LeDoux, 1995; Rogan et al., 1997; Rumpel, LeDoux, Zador, & Malinow, 2005; Shumyatsky et al., 2005; Tsvetkov, Carlezon, Benes, Kandel, & Bolshakov, 2002).

The cortical and thalamic inputs to these cells have notable differences in biochemistry, physiology and plasticity. Dendritic spines that receive inputs from thalamic sources are larger, and express high levels of R-type voltage-dependant calcium channels that cortical input-receiving spines do not (Humeau et al., 2005; Humeau & Luthi, 2007). This suggests that these synaptic inputs drive BLA neurons more strongly than cortical inputs. In the lateral nucleus of the BLA, both pathways robustly potentiate in response to pairing pre-synaptic stimulation with post-synaptic depolarization (Shin, Tsvetkov, & Bolshakov, 2006). Long-term potentiation (LTP)

mediated by NMDA-receptors, perhaps the most well-characterized mechanism underlying LTP in the CNS, has been demonstrated in both the cortico- and thalamo-amygdala pathways (Huang & Kandel, 1998; Humeau, Shaban, Bissiere, & Luthi, 2003; Watanabe, Ikegaya, Saito, & Abe, 1995). However, under some induction condition conditions, NMDA receptors do not appear to be necessary (Chapman & Bellavance, 1992; Huang & Kandel, 1998). Synaptic potentiation induced in the thalamo-BLA pathway by presynaptic patterns of activity has been found to be mediated by GluR5-containing kainate receptors, and manifests presynaptically as an increase in probability of vesicle release (Christian, Alexander, Diaz, & McCool, 2013; Shin et al., 2010). In the cortico-BLA pathway these same patterns of activity induce a postsynaptic potentiation that does not depend on kainate receptors (Shin et al., 2010).

A critical component of synaptic integration at cortico- and thalamo-BLA synapses is modulation by a variety of other neurotransmitters. These neuromodulators, which include dopamine, cortisol, norepinephrine, endocannabinoids, and acetylcholine, are released during different emotional arousal states and alter circuit dynamics by facilitating or impeding synaptic transmission and plasticity, or by modulating neuronal excitability. Neuromodulators influence synaptic integration in the BLA by directly interacting with synaptic, perisynaptic, and somatic receptors to modulate membrane excitability and synaptic transmission. Indirectly, they exert their influence by relieving or enhancing inhibition by GABAergic interneurons whose activity strongly opposes establishment of long-term synaptic potentiation at inputs to pyramidal neurons (McGaugh, 2004; Pape & Pare, 2010). The term “neuromodulator” is used to refer to

class of transmitters that do not directly excite or inhibit neurons, but rather change the state of a neuron or circuit, altering its behavior in response to stimulation (Ito & Schuman, 2008; Siggins, 1979). My dissertation focuses on the role of the least studied of these modulators, acetylcholine. I have focused on the effects of ACh in the modulation of BLA circuitry because comparatively little is known about synaptic mechanisms of ACh and because there is extensive cholinergic innervation to the BLA.

Acetylcholine, the first neurotransmitter ever identified, has a wide range of functions in the nervous system. The role of ACh was first known in the peripheral nervous system at the neuromuscular junction, where it is released by motor neurons to induce muscle contraction. ACh's role in the central nervous system (CNS), however, is more complex. ACh is involved in a wide range of cognitive functions including learning, memory, attention, and anxiety (Barros, Pereira, Medina, & Izquierdo, 2002; Barros, Ramirez, & Izquierdo, 2005; Levin, McClernon, & Rezvani, 2006; van der Zee & Luiten, 1999). ACh is synthesized from choline and an acetyl group transferred from acetyl-coenzyme A, catalyzed by the enzyme choline acetyltransferase (ChAT). Expression of ChAT is the defining feature of cholinergic neurons. Cholinergic neurons represent approximately only 5% of the total neurons in the mammalian CNS. However, many of these neurons have extensive axonal arbors (Mesulam, 1995; Zaborszky, 2002). Thus, a small number of cholinergic cells can influence innumerous circuits throughout the CNS. The cholinergic system is divided into two subsytems, the pontomesencephalic subsystem which innervates subcortical areas; and the basal forebrain which innervates the entire cortical mantle, as well as hippocampus, amygdala and the olfactory bulb

(Woolf, 1991). Cholinergic synapses with direct point-to-point transmission in the CNS have been difficult to demonstrate (Arroyo, Bennett, & Hestrin, 2014; Bloem, Poorthuis, & Mansvelder, 2014; Jiang, Lopez-Hernandez, Lederman, Talmage, & Role, 2014; Picciotto, Higley, & Mineur, 2012) but see: (Huh, Danik, Manseau, Trudeau, & Williams, 2008; Klein & Yakel, 2006). Rather, ACh primarily modulates neuronal excitability and synaptic transmission by interacting with receptors located on cell bodies, axons, and dendrites, or at sites on dendritic spines and axon terminals of glutamatergic and GABAergic synapses (Picciotto et al., 2012). Thus, the precise nature of acetylcholine's effects depends on the particular composition of receptors it binds to and where these receptors are located, which varies depending on brain region and cell type.

Acetylcholine receptors (AChRs) are divided into two classes, nicotinic (nAChR) and muscarinic (mAChR). The nicotinic receptors, named for their high affinity to nicotine, are ionotropic multimers, each subunit of which can be one of several members of two classes in the CNS, α and β. There are 9 α (α 2 thru α 10) and 4 β-type subunits (β2- β5) that comprise the CNS nicotinic receptors (Gotti & Clementi, 2004; Gotti et al., 2007; Picciotto et al., 2012). A great diversity of subunit permutations are found throughout the mammalian CNS. Each isoform has unique properties, particularly in regards to calcium permeability. Of note, the α7 subunit bestows high calcium permeability and α7 pentamers are potent modulators of glutamatergic transmission in the BLA (Jiang & Role, 2008). Modulation of internal calcium concentration can profoundly alter the probability of vesicle release, a calcium-dependant process, at pre-synaptic sites (Barik & Wonnacott, 2009; Dajas-Bailador &

Wonnacott, 2004; Wonnacott, Drasdo, Sanderson, & Rowell, 1990; Wonnacott, Sidhpura, & Balfour, 2005). Muscarinic AChRs are G-protein mediated metabotropic receptors comprised of 5 isoforms, M_1 through M_5. Despite the limited number of isoforms, there is no less diversity in mAChR function, due to the diversity of α subunits and G-protein effectors with which this receptor interacts (Wess, 2003). Activation of mAChRs typically leads to net neuronal inhibition, but in some cases can also lead to a mix of excitatory and inhibitory effects, or, in the case of M_1, excitation alone.

The BLA receives the vast majority of its cholinergic innervation from cells in the nucleus basalis (NBM), a basal forebrain nucleus. Ultrastructural localization studies have shown that cholinergic axons from these cells primarily target the dendritic shafts and spines of pyramidal neurons, with a small subset of terminals targeting perikarya and interneurons (Muller, Mascagni, & McDonald, 2011; Muller, Mascagni, Zaric, & McDonald, 2013). At cortico- and thalamo-BLA synapses in the BLA, presynaptic nicotinic as well as pre- and post-synaptic muscarinic receptors modulate synaptic transmission (Fig. 1.1). Nicotinic receptors are expressed on a subset of pyramidal neurons (Klein & Yakel, 2006) and on interneurons (Pidoplichko, Prager, Aroniadou-Anderjaska, & Braga, 2013). BLA nicotinic receptors include α7-containing (abbreviated as α7*) and α4β2* types (Hill, Zoli, Bourgeois, & Changeux, 1993; Seguela, Wadiche, Dineley-Miller, Dani, & Patrick, 1993). Activation of nicotinic receptors in the BLA has been shown to increase the frequency of miniature excitatory post-synaptic currents in GABAergic interneurons and facilitate glutamatergic transmission at cortico-BLA synapses (Barazangi & Role, 2001; Jiang & Role, 2008).

There is extensive evidence suggesting that nicotinic receptors can be localized to pre-synaptic structures within terminal fields, where their activation and/or desensitization can modulate the extent of transmitter release, changing release probability by altering local calcium (Dajas-Bailador & Wonnacott, 2004; Wonnacott et al., 2005). Of the muscarinic cholinergic receptor subtypes, only M_1, M_2 and M_3 are expressed in the BLA (Buckley, Bonner, & Brann, 1988; McDonald & Mascagni, 2011; Muller et al., 2013; Spencer, Horvath, & Traber, 1986). The M_1 receptor is highly expressed and is of particular interest due to its necessity for memory consolidation (Boccia, Blake, Baratti, & McGaugh, 2009). Ultrastructural localization by electron microscopy has found that it is expressed on axon terminals, 90% of dendritic shafts, a majority of dendritic spines, and on nearly all pyramidal cell bodies (Muller et al., 2013). Moreover, the M_1 receptor is primarily found in apposition to cholinergic release sites, although it can also be found more distantly from release sites (Muller et al., 2013). M_1 receptor activation is generally excitatory, inducing a slow depolarization of the cell membrane, but in some contexts has been found to suppress synaptic transmission, though perhaps by indirect mechanisms (Park, Nam, Choi, & Lee, 2004). The M_2 receptor, while expressed in lower numbers than M_1, (McDonald & Mascagni, 2011), is also required in the BLA for memory consolidation. The M_3 receptor is also found in the BLA in low numbers (Buckley et al., 1988). There is limited evidence as to its function here, but one study shows that its activation induces a slow non-selective cationic conductance in pyramidal neurons, suggesting a role in increasing membrane excitability (Yajeya et al., 2000).

Both the amygdala and the cholinergic system have been implicated in many cognitive disorders including generalized anxiety disorder, phobias, obsessive-compulsive disorder, and post-traumatic stress disorder (Hull, 2002; J. E. LeDoux, 2000). Given the amygdala's role in routing information primarily from sensory stimuli throughout the CNS, it is not surprising that a common theme of these disorders is a failure to appropriately process and respond to salient sensory stimuli. In the amygdala, acetylcholine is implicated in modulating the formation of emotional memories during periods of arousal. In humans, both cholinergic and amygdalar activity is increased in stress, mood disorders, depression, and post-traumatic stress disorder (PTSD). Post-mortem studies of patients with depression show an increase in nAChR occupancy by ACh (Dani & Bertrand, 2007), and increasing cholinergic tone by inhibition of acetylcholinesterase induces depression and PTSD-like symptoms (Deutsch et al., 1983).

My work examines cholinergic signaling in the BLA in the context of fear learning and extinction of learned fear. Fear learning occurs when a conditioned stimulus (CS), such as an auditory cue, is paired in time with an unconditioned stimulus (US), such as a painful electrical shock (J. E. LeDoux, 2000; Maren & Quirk, 2004). Future exposure to the previously innocuous CS will then induce a fear response. Extinction learning occurs after repeated exposure to the CS without pairing of the US (Milad, Rauch, Pitman, & Quirk, 2006). The learned fear is inhibited and the fear response to the CS decreases. In this regard, both the amygdala and cholinergic signaling are known to be important in fear learning and extinction of fear memory. The lateral nucleus of the

basolateral complex of the amygdala is considered the site of initial associative memory formation (Blair, Sotres-Bayon, Moita, & Ledoux, 2005; Blair, Tinkelman, Moita, & LeDoux, 2003; Sigurdsson, Doyere, Cain, & LeDoux, 2007). Lesion studies show that either the thalamo-BLA and cortico-BLA pathways to the BLA are sufficient for fear learning to occur (Romanski & LeDoux, 1992). In contrast to the lateral nucleus (LA), the basolateral nucleus (BLA), where there is vastly more cholinergic signaling, is not *required* for fear learning. The cholinergic input to the BLA is thought to play a modulatory role in the acquisition and expression of learned fear. The BLA is, however, a necessary component for extinction learning (Sierra-Mercado, Padilla-Coreano, & Quirk, 2011). LeDoux and colleagues showed that pairing optogenetic activation of pyramidal neurons in LA with a cue is sufficient to induce fear conditioning, even in the absence of any aversive unconditioned stimulus (Johansen et al., 2010). The BLA, which receives extensive inputs from LA, modulates the expression of these fear memories through its extensive connections to the central nucleus of the amygdala, the "output" nucleus of the amygdala primarily responsible for the autonomous expression of fear behavior, and through its reciprocal connections to higher brain areas, thought to underlie the cognitive and behavioral aspects of the fear response (J. E. LeDoux, 2000; Tye et al., 2011). For extinction learning, the reciprocal connectivity between BLA and medial prefrontal cortex (mPFC) is essential. Acetylcholine is known to be important for modulation of fear learning, expression of fear, and extinction learning in the BLA (Carballo-Marquez et al., 2011; Lalumiere & McGaugh, 2005). In rodents, nicotine is known to potentiate cortico-amygdala glutamatergic transmission (Jiang & Role, 2008; Mansvelder, Keath, & McGehee, 2002), enhance contextual fear learning (Gould 2008)

and delay extinction of fear learning (Gould 2014). Muscarinic receptors in the amygdala are known to be important for contextual fear learning and trace fear conditioning (Baysinger, Kent, & Brown, 2012; Fuchs, Feltenstein, & See, 2006; Pare, 2003; Power, McIntyre, Litmanovich, & McGaugh, 2003; Roozendaal et al., 1997; Vazdarjanova & McGaugh, 1999; Young & Thomas, 2014). Microdialysis studies have shown that ACh is elevated in the amygdala during stress and after fear learning (McIntyre et al., 2003). Nicotinic signaling also plays a role in modulation of fear memory (Lima et al., 2013). The nicotinic receptor antagonist mecamylamine decreases amygdala activity measured by *c-fos* immunoreactivity (Mineur, Somenzi, & Picciotto, 2007). These studies provide evidence for a strong link between cholinergic signaling in the amygdala and modulation of affective behaviors, but an understanding of how ACh modulates amygdala circuitry over different timescales and in distinct behaviors remains elusive.

Pharmacological techniques have yielded great insight into the possible effects of endogenous ACh on circuits, cells, synapses and behavior in the BLA and throughout the CNS. However, these methods have several drawbacks. The timescale of receptor activation or inactivation cannot be precisely controlled, effects of receptor desensitization may not be distinguishable from receptor activation, and there is limited specificity as to which receptors on which cells are being activated or inactivated.

Direct study of the effects of endogenous ACh are only beginning thanks to the recent introduction of cell type selective activation techniques. There have been

multiple roadblocks to studying the cholinergic system using traditional stimulation methods. Cholinergic neurons, even in so-called “cholinergic nuclei” such as the NBM and diagonal band of Broca represent only a fraction of the neurons within these areas and the cholinergic neurons are interspersed among other cell types. Moreover, the projections from these cholinergic neurons have extensive arbors that project to terminal fields with a heterogeneous mix of other afferents. Thus, neither drugs nor electrical stimulation is able to specifically stimulate these neurons or their projections without also stimulating neighboring neurons and inputs.

To examine the endogenous cholinergic circuitry in the BLA, I have taken advantage of new optogenetic methods that allow selective activation of cholinergic structures with high temporal and spatial precision. My studies have focused on utilizing this technique to directly activate or inhibit cholinergic axon terminal fields from genetically targeted ChAT expressing neurons in the NBM. Optogenetics, a recently developed technology, relies on the targeted expression of modified channel-rhodopsin encoding genes. Channelrhodopsins are light-activated ion channels naturally found in single celled organisms (Williams & Deisseroth, 2013). These channel proteins have been genetically engineered for faster kinetics and low desensitization (Yizhar, Fenno, Davidson, Mogri, & Deisseroth, 2011). By coupling channelrhodopsin genes to neuronal promotors and packaging them in a virus, such as adeno-associated virus, they can be delivered to and expressed in targeted populations of neurons. Genetic specificity can be achieved by flanking the channelrhodopsin gene with lox-p sites. When injected into

transgenic mouse lines that express cre-recombinase in specific subsets of cells, only those cells will express the optogenetic construct.

My dissertation work uses a knock-in ChAT-Cre recombinase mouse line (Jackson Labs, stock #018957)to specifically express either oChIEF, an excitatory channel opsin, or halo-rhodopsin 3.0, an inhibitory channel opsin, in NBM neurons that express choline-acetyl transferase (ChAT), the defining feature of cholinergic cells. The opsins, oChIEF and halorhodopsin3.0, are engineered variants of channelrhodopsin2 and halorhodopsin, respectively (Lin, Lin, Steinbach, & Tsien, 2009). The advantage of optogenetics over traditional electrical stimulation or pharmacological activation or inhibition of receptors is that optogenetically labeled cell bodies and their axons can be specifically stimulated or inhibited with light with high temporal precision and without affecting surrounding tissue. Optogenetic methods do not necessarily supplant electrical and pharmacological methods of investigating neural systems, but rather can complement these approaches as in my dissertation studies.

To examine the basic synaptic properties of the two major input pathways to the basolateral nucleus of the amygdala I employed patch-clamp electrophysiology in acute slices prepared from adult mice. Taking advantage of the spatial separation between the cortical and thalamic inputs, I independently stimulated either pathway while recording the evoked EPSCs in a BLA pyramidal neuron. The majority of these inputs in both tracts are excitatory (glutamatergic), while inhibition in the BLA arises from a small

population of GABAergic interneurons. In all my experiments I used bicuculine, a GABA-A receptor antagonist, to isolate excitatory synaptic currents arising from electrical stimulation of either the internal or external capsule. I show that under baseline conditions, synapses from cortical sources are weaker than those from thalamic sources. Moreover, these synapses respond to plasticity-inducing patterns of stimulation in different ways. Cortical inputs readily potentiate to both 100 Hz tetanic and theta-burst stimulation. Thalamic inputs, on the other hand, show much more variable responses, with synaptic depression the more frequently observed result. I next asked if there is an interaction between these inputs when they are coactivated, in a paradigm known as input-timing dependant plasticity (ITDP) (Cho et al., 2012). Coactivating these inputs at a low frequency potentiated thalamic inputs while depressing cortical inputs.

The second part of my dissertation investigates the role of acetylcholine (ACh) in modulating the cortical and thalamic inputs to BLA. The BLA is an ideal locale for investigating the role of endogenous ACh in synaptic integration for two reasons. First, this nucleus is particularly rich in cholinergic afferents originating from the NBM. Second, there are no cholinergic interneurons in the BLA, eliminating confounds from having multiple sources of ACh, and from feed-forward or feedback effects of stimulating neurons in the BLA or their inputs. Because the cholinergic inputs to BLA arise from NBM, cholinergic axons in the BLA are severed from their cell bodies in the slice preparation. Despite this fact, initial studies revealed that addition of cholinergic antagonists to the slice altered the profile of synaptic transmission implying that

cholinergic axons are still active in the slice. Thus, I addressed the role of endogenous cholinergic activity in the BLA by examining the effects of selective activation of cholinergic input within the terminal fields of the BLA *per se*. To examine the effects of increased cholinergic signaling on inputs to BLA, I optogenetically stimulated endogenous cholinergic fibers while recording EPSCs evoked by internal capsule (thalamic) vs. external capsule (cortical) stimulation. Briefly, I found that optogenetic stimulation of ACh release potentiates cortico-BLA synapses while depressing thalamo-BLA synapses. These opposite effects on the cortical and thalamic inputs demonstrate input specificity of this system.

Finally, I applied optogenetic methods for both stimulating and inhibiting cholinergic axons in the BLA *in vivo* to assess the role of this input in a conditioned fear paradigm. Specifically, I examined the effect of both stimulation and inhibition of ACh release at the time of fear learning on subsequent memory and extinction learning. Previous work has shown that ACh is elevated in the BLA for up to two hours after training. Pharmacological inhibition or activation of ACh receptors either globally or specifically in the BLA has been shown to modulate fear conditioning and other aversive learning paradigms. However, the results of these pharmacological studies are mixed, with effects heavily dependent on drug type, dosage and timing of drug delivery (Tinsley, Quinn, & Fanselow, 2004). These mixed results underscore a major limitation of pharmacological techniques; namely, the difficulty with precise spatial and temporal control of drugs as they can diffuse far from the injection site and can remain active over a long period of time. Moreover, it is difficult to know if effects of agonists are due to

activation or desensitization because they act over long time-courses. While pharmacological studies have been of great value, using optogenetics to specifically stimulate the endogenous cholinergic system is a natural extension of this work. My work shows that selective, brief stimulation of endogenous ACh release enhanced fear learning, slowing the rate of fear extinction. In contrast selective inhibition of ACh release diminished fear learning with profound effects on the acquisition of the fear learning task during training. Overall, my work is consistent with the idea that normal levels of cholinergic activity lie somewhere in the middle of a wide dynamic range thus allowing this system to tune circuit activity in a bidirectional and state-dependant manner. These results are consistent with my findings in the slice preparation, where I show that both inhibition of AChRs and activation of endogenous cholinergic activity induces changes in synaptic transmission.

Fig 1.1 - Synaptic organization of acetylcholine receptors in basolateral amygdala

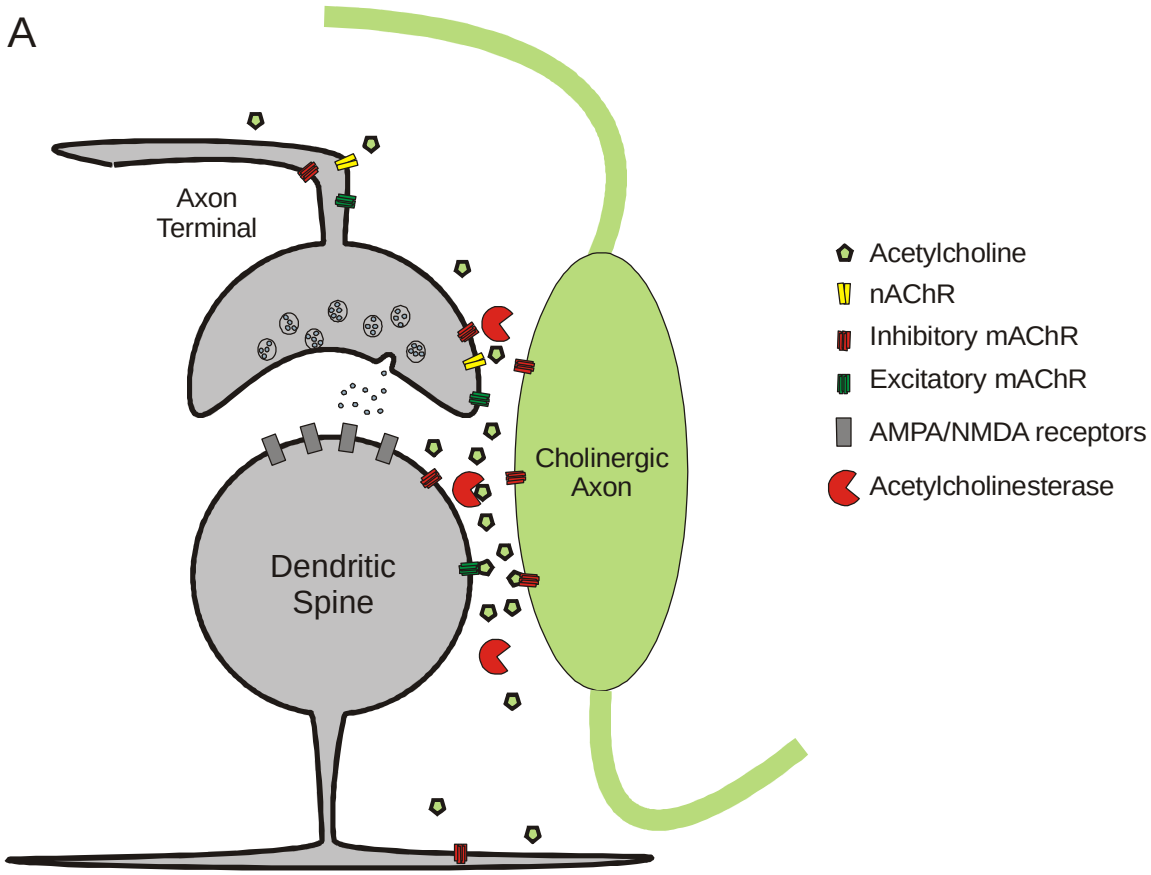

Figure 1.1 - Synaptic organization of acetylcholine receptors in basolateral amygdala. (A) Cholinergic axons typically form release sites in close proximity to glutamatergic synapses on dendritic spines. Acetylcholine released here (green hex) can interact with both pre- and post-synaptic cholinergic receptors. Presynaptic receptors include α7-containing and α4β2 nicotinic receptors (yellow), and excitatory (M_1, M_3) shown in green and inhibitory (M_2), shown in red, muscarinic receptors. Evidence suggests that nicotinic receptors here increase intracellular calcium concentrations, facilitating synaptic vesicle release, a calcium-dependent process. Post-synaptic receptors are limited to muscarinic receptors, although functional nicotinic receptors are present on cell bodies. The synaptic function of muscarinic receptors is not well understood. Acetylcholinesterase (red segmented circle) is present in high concentrations in the extracellular space, likely limiting the extent to which acetylcholine can diffuse. However, muscarinic receptors can be found along dendrites and axons far from cholinergic release sites, though it is not know if these are functional or not.

Chapter 2 - Synaptic transmission and plasticity of cortical and thalamic inputs to BLA

Introduction

A common theme that has emerged from studies of the amygdala is that it serves as a gateway between sensory stimuli and emotion (J. E. LeDoux, 2000). The amygdala receives inputs from all sensory modalities including low-level inputs from thalamus and other subcortical areas containing information about basic sensory features as well as high-level inputs from sensory, polymodal, and higher order association cortices (McGaugh, 2004). These inputs converge in the lateral and basolateral nuclei of the amygdala where they ultimately give rise to outputs of the amygdala that stimulate cognitive, physiological, and motor/behavioral activity collectively comprising an emotional response (McGaugh, 2004). Particularly important to my dissertation work is the fact that cortical and thalamic inputs to the BLA project through anatomically distinct and spatially separate pathways. Specifically, inputs from sensory thalamic areas project through the internal capsule while cortical inputs project through the external capsule. Once in the BLA these projections form synapses on the dendritic trees of pyramidal neurons that comprise 90% of the cells in the BLA. Synaptic plasticity here is renowned for its role in learning and memory, particularly in regards to emotionally salient stimuli.

Ample evidence exists that the convergence of inputs to the lateral and basolateral nuclei are an essential element of the neural circuitry underlying many

aspects of cognition, especially associative and extinction learning (Davis, 1992; J. E. LeDoux, 2000; Maren & Quirk, 2004; Sigurdsson et al., 2007). The synapses in the BLA are potentiated after fear conditioning and interfering with neural transmission here profoundly affects learning, recall and memory consolidation (Sigurdsson et al., 2007). While specific behaviors that rely on amygdala nuclei and their connectivity are well documented, amygdalar circuitry and synaptic mechanisms underlying these behaviors is not well understood. Studies of immediate early gene activation show that pyramidal cells here are specifically activated by learning cues such as tones during cued fear conditioning, and by aversive stimuli such as electrical shocks, establishing that neural activity arising from these sensory stimuli does indeed converge onto these cells during learning (Barot, Chung, Kim, & Bernstein, 2009). At the synaptic level, spines on pyramidal cells in the lateral amygdala receiving thalamic inputs differ at both a molecular and functional level from those receiving cortical inputs. In particular, spines that receive thalamic input are larger, express a greater number of R-type voltage-dependent calcium channels, and allow greater calcium flux upon activation (Shin et al., 2006). In the lateral amygdala, Bolshakov and colleagues showed that low frequency co-activation of cortical and thalamic inputs can induce synaptic plasticity not otherwise induced by the same stimulation of either pathway alone (Cho et al., 2012), suggesting that these cells are arranged to respond to coincident converging signals.

While these and other studies give a general idea of what to expect from the circuitry of the lateral/basolateral complex, they have several shortcomings insofar as providing a starting point for understanding cholinergic modulation of this circuit. For

one, they have mostly focused on juvenile rats. All the experiments done in this project used adult mice in order to avoid confounding results due to the substantial developmental changes in amygdala function that continue to occur prior to adulthood (Pan, Ito, & Morozov, 2009), and for the genetic power of the mouse. In addition, most prior studies have examined the inputs to the lateral nucleus, while the inputs to the basolateral nucleus have received less attention. Ultimately, this project seeks to examine cholinergic modulation of the cortical and thalamic excitatory inputs to the basolateral nucleus.

The patch-clamp experiments presented here compare and contrast properties of excitatory synaptic transmission to pyramidal cells in the BLA arising from cortical and thalamic inputs. To do this I recorded from BLA pyramidal neurons in brain slices acutely prepared from adult mice. To isolate excitatory currents, all experiments were conducted under conditions of continuous exposure to bicuculine, a GABA-A receptor antagonist. In order to examine the properties and plasticity of the cortical and thalamic inputs specifically, I used a concentric bipolar electrode to stimulate the internal or external capsules, the white-matter tracts that carry projections from thalamic and cortical brain areas, which are easily visualized in the acute slice preparation. I begin my dissertation work by examining basic properties and plasticity of these synapses. I find that thalamo-BLA synapses have a unit amplitude response best fit by a normal distribution centered around 12 pA. Cortico-BLA synapses, on the other hand, are best fit by a log-normal distribution with a peak near 7 pA. In addition, they differ greatly in their plastic responses to patterns of stimulation including theta-burst and 100 Hz

tetanus. I also find that low frequency coactivation of both inputs can induce plasticity at both inputs.

Methods

Slice preparation

Coronal brain slices were prepared from C57/BL6 mice at postnatal day 42-80. Animals were intraperitoneally injected with a mixture of ketamine and xylazine (100 mg ketamine and 11 mg xylazine/kg body weight). After decapitation, the brain was rapidly dissected (60 to 90 seconds), mounted with cyanoacrylate glue, and transferred to the chamber of a vibratome (Leica VT1000S) containing an ice-cold high-sucrose solution (in mM: sucrose 230; KCl 2.5; $MgSO_4$ 10; $CaCl_2$ 0.5; NaH_2PO_4 1.25; $NaHCO_3$ 26; glucose 10; pyruvate 1.5) bubbled with 95% O_2/5% CO_2. Coronal slices (300 µm) were made with the vibratome, then transferred to a 50/50 mix of the cutting solution and aCSF (in mM: NaCl 126; KCl 2.5; NaH_2PO_4 1.25; $NaHCO_3$ 26; $CaCl_2$ 2; $MgCl_2$ 2; glucose 10) bubbled with 95% O_2/5% CO_2 where they were allowed to equilibrate at room temperature (24-26ºC) for at least 1 hour. After this period, slices were transferred to the recording chamber and continuously superfused at a rate of 2 ml/min with aCSF bubbled with 95% O_2/5% CO_2.

Electrophysiological recordings

BLA pyramidal neurons were visualized on an Olympus BX51WI upright microscope (Olympus Optical) equipped with differential inference contrast (DIC) optics. Patch electrodes with a resistance of 4–6 MΩ were pulled with a P-97 Brown Flaming electrode puller (Sutter Instrument). Signals were recorded with an AxoPatch 200B amplifier (Molecular Devices). The pipette solution contained (in mM: 130 K-gluconate;

2 KCl; 2 $MgCl_2$; 10 HEPES; 0.5 EGTA; 1 ATP; 0.2 GTP; QX314 5 (pH 7.3). Visually-identified pyramidal neurons were patched in the BLA and held at -60 mV. In all experiments, the slice was bathed in 50 µM bicuculine to block GABA-A receptor-mediated currents.

The criteria applied for inclusion of recorded cells in the final analysis were as follows: *1*) seal resistances maintained throughout the recording period at >1 GΩ; *2*) holding current in whole cell clamp configuration remained within 10% of the initial value and was ≤100 pA; and *3*) series resistance (R_s), measured at least once every 10 min throughout the course of the experiment, remained stable (<20% change from initial value).

To examine miniature EPSCs, 1 µM tetrodotoxin (TTX) was added to the aCSF superfusate. To examine transmission at cortico–BLA and thalamo-BLA inputs, excitatory postsynaptic currents (EPSCs) were evoked by field stimulation with a concentric bipolar stimulation electrode (FHC) placed on the external capsule or internal capsule, respectively. The input of interest was stimulated at a rate of 0.1 Hz. Depending on the experiment, stimulation strength was adjusted to either "minimal stimulation", defined as the stimulus intensity required to evoke EPSCs on approximately 50% of trials, or "robust stimulation" defined as the lowest stimulus intensity required to evoke an EPSC in 100% of trials. As specified in plasticity experiments, either one of two patterns of stimulation were used, either theta-burst or tetanus. The theta-burst pattern used was a series of 50 Hz, 4 pulse bursts delivered 10

times at a 5 Hz inter-burst interval. The tetanus pattern was a 100 Hz, 100 pulse train of stimuli. In all experiments, the intensity of the patterned stimulus was unchanged from the stimulus used in the control period.

Data analysis and statistics

EPSC peak amplitudes were measured by subtracting peak deflection of the current trace to a baseline established by taking the mean of the baseline 1 ms prior to the stimulus. Criteria for inclusion of evoked EPSCs in analysis were: rapid (<3 ms) 10% - 90% rise time, time-locked to stimulus (+/- 1 ms) and low latency (<15 ms) to stimulus.

Data were analyzed using Clampfit 10.0. Statistics and plotting was done using OriginPro 9.0 and Prism 6 statistical software packages. In plasticity experiments, data were binned in 5 minute bins immediately prior to, immediately after, and 15 to 20 minutes after patterned stimulus delivery. These bins were compared by one-way ANOVA with Tukey *post-hoc* comparisons. Calculation of probability of success (P_s) was done by dividing number of evoked EPSCs that passed criteria over total of evoked EPSC and failure events. P_s for each 5 minute bin was compared pairwise to the control period 5 minutes prior to patterned stimulus delivery using Pearson's X^2 statistic.

Results

I first examined miniature EPSCs, synaptic currents that occur in the absence of presynaptic action potentials. Action potentials were blocked by blocking voltage gated sodium channels using tetrodotoxin. Under these conditions, synaptic transmission, therefore, occurs only when vesicles spontaneously fuse in the presynaptic terminal. Thus, each miniEPSC can be presumed to arise from the fusion of a single vesicle at a single synapse (Fig 2.1). I conducted this experiment in a total of 8 cells that passed criteria for evaluation (Fig. 2.2). The population of miniEPSCs from all 8 cells were fit by a log-normal distribution with the peak at approximately 6 pA (*M* = 5.93, *SE* = 0.28) and the average frequency of events was 7 Hz (*M* = 6.93, *SD* = 8.70) (fig 2.3).

To distinguish cortical from thalamic inputs, I used an evoked EPSC paradigm in which I placed a concentric bipolar stimulation electrode on either the internal or external capsule to specifically stimulate and measure thalamic or cortical inputs, respectively. Using minimal stimulation intensity (intensity required to evoke an EPSC in ~50% of trials), I evoked unitary EPSCs from either the internal (Fig. 2.4) or external (Fig. 2.7) capsules. In the thalamic pathway I conducted this experiment in 8 cells that passed criteria for evaluation (Fig. 2.5). In the cortical pathway I conducted this experiment in 6 cells that passed criteria for evaluation (Fig. 2.8). I found that the mean peak amplitude of unitary EPSCs from the thalamic input to BLA was 13.4 pA (*M* = 13.40, *SD* = 3.39). The pooled, normalized distribution of thalamo-BLA unitary EPSCs was fit by a Gaussian distribution with the peak at 11.57 pA (*xc* = 11.57, *SE* = 0.30, R^2 =

0.91) (Fig. 2.6). Unitary EPSCs from cortical inputs had a mean amplitude of approximately 12 pA (*M* = 11.93, *SD* = 1.19). The pooled, normalized distribution of cortico-BLA unitary EPSCs was fit by a log-normal distribution with the peak at 8.28 pA (*xc* = 8.28, *SE* = 0.24, R^2 = 0.95) (fig. 2.9).

I next examined the input/output relationship of these pathways by eliciting EPSCs at a range of stimulus intensities. In the thalamo-BLA pathway, increasing the stimulus intensity resulted in a step-wise increases in EPSCs amplitudes (fig. 2.10). A maximum EPSC amplitude of approximately 200-300 pA was achieved in 2 of 3 cells tested (fig. 2.10 A (*M* = 201.89, *SD* = 26.61), B (*M* = 207.49, *SD* = 33.17)), and 600 pA in 1 of 3 cells tested (fig. 2.10 C (*M* = 617.40, *SD* = 69.93)). In the cortico-BLA pathway, increasing the stimulus intensity resulted in a smooth increase in EPSC amplitude that reached a maximum plateau (fig. 2.11). In 1 of 3 cells tested, this maximum was approximately 100 pA (fig. 2.11 A (*M* = 109.68, *SD* = 25.25)). In a second cell tested, this maximum was 350-400 pA (fig. 2.11 B (*M* = 375.86, *SD* = 31.28)), and in a third cell it was approximately 500 pA (fig. 2.11 C (*M* = 510.58, *SD* = 15.12)).

To compare synaptic plasticity in thalamic vs. cortical inputs, I first examined the effect of theta-burst stimulation at minimal intensity on these pathways. I found that in thalamo-BLA synapses, theta-burst induces either potentiation (*N* = 1/7) (Fig. 2.12) or depression (*N* = 2/7) (Fig. 2.13) and in about half of cells has no effect (*N* = 4/7). Moreover, the change in synaptic efficacy was typically manifested as a change in the failure rate, which most likely reflects a change in the probability of release at the

presynaptic terminal. In the cortico-BLA pathway, however, theta-burst stimulation elicits potentiation, and was never observed to elicit depression. Moreover, potentiation in these synapses manifests as a reduction in failure rate concomitant with an increase in EPSC amplitude. Given the variability and unreliability of the plasticity in the thalamic pathway, I next tested whether a stronger pattern of stimulation would change the reliability or direction of the response in these synapses. Using a super-minimal (??) stimulation intensity such that it reliably elicited an EPSC in 100% of trials, I compared the evoked EPSC amplitude before and after administering 100 Hz tetanus to the internal capsule. I found that this stimulation paradigm had very similar effects to the theta-bust paradigm in that 3 out of 7 cells tested demonstrated plasticity. Of those, 1 showed clear potentiation (Fig. 2.14) while 2 showed depression (Fig. 2.15). This same paradigm administered to the cortical pathway to BLA elicited LTP in both of two cells recorded from (Fig. 2.17). In addition to these 2 examples, this pathway has been extensively studied previously by others in our laboratory, who has also found that it reliably potentiates in response to tetanic and theta-burst stimulation; my work replicates this result.

Finally, I tested whether there is plasticity that arises from an interaction between these two pathways. I used stimulation electrodes on both the internal and external capsules and recorded the EPSCs evoked by alternately stimulating the two inputs every 10 seconds. After a baseline control period, I then stimulated both pathways with an 8 ms delay between first the thalamic, then the cortical pathway. Stimulating these

pathways in this manner at 1 Hz induced plasticity in either or both pathways in 3 cells tested, an example of which is shown in figure 2.16.

Discussion

In these experiments, I compared excitatory transmission and plasticity at cortical and thalamic inputs to the basolateral amygdala, and plasticity induced by patterned electrical stimulation. Comparing the unit amplitudes of these pathways to the miniEPSC amplitudes reveals that cortical inputs to BLA are better represented by the miniEPSC population than thalamic inputs. The typical miniEPSC has a peak amplitude of approximately 8 pA, while the peak of the distribution of the cortical units is around 7 pA. In addition, the cortical unit distribution is similar (log-normal) to miniEPSC distribution. This suggests that these synapses have a higher probability of spontaneous release that thalamo-BLA synapses under miniature EPSC recording conditions. This is consistent with finding that spines connecting to thalamic inputs are physically larger than spines connecting to cortical inputs (Humeau et al., 2005). However, miniEPSCs can also arise from several other sources, so it is unknown precisely what proportion of minis arise from any particular input. Other sources of input that likely contribute to the miniEPSC population include the lateral amygdala, which in fact accounts for a large number of the inputs to BLA. It is also possible that, while miniEPSCs arise from a single synapse, single fibers in the internal and external capsules might bifurcate and form multiple connections onto a single cell in the BLA. When minimal stimulation is used to stimulate a single fiber, it may in fact trigger more than one synapse. However, this seems a less likely explanation as if this were the case, given that these synapses have a relatively low probability of release, one would expect to see a multimodal distribution of the units, which there is not.

The input-output relationship of these 2 pathways is different as well. As stimulation intensity increases in the thalamo-BLA pathway, the EPSC amplitude increases in a stepwise manner. Meanwhile, the increasing stimulation intensity of the cortico-BLA increases EPSC amplitude smoothly to a maximum. The EPSC amplitudes achieved at maximum intensity were somewhat different from cell to cell, ranging from about 100 to 600 pA, but no difference was apparent between pathways. The stepwise I/O relationship of the thalamic pathway is likely due to the diffuse and striated manner in which axons traverse the internal capsule. As stimulation intensity increases, small fiber bundles are stimulated further and further from the tip of the stimulation electrode, resulting in large jumps in EPSC amplitude. In the external capsule carrying cortical inputs, the axons are tightly arranged. Thus, as stimulation intensity increases, the number of axons recruited will increase linearly. In both the thalamic and cortical pathways, maximum EPSC amplitudes of several hundred pA were attained. Given the typical unit amplitude of 8 pA in the cortical pathway and 12 pA in the thalamic pathway, this implies that the total number of synapses triggered at maximum stimulation intensity is on the order of 10 to 100.

The cortical-BLA pathway reliably potentiates to both tonic stimulation at 100 Hz over 1 second and to theta-burst patterned stimulation consisting of 5, 20 Hz bursts at a 5 Hz inter-burst rate. The thalamo-BLA pathway is much more variable in its response. When plasticity is induced in this pathway, it is typically depression, manifested as a reduction in the probability of release. However, a somewhat smaller proportion of the

time these synapses potentiate in response to patterned stimulation. Finally, this pathway was generally less responsive than the cortico-BLA pathway, in that only approximately half of cells receiving patterned stimulation of the internal capsule had no significant change in EPSC amplitude while the cortical inputs respond nearly 100% of the time, both in my experiments and in similar experiments conducted by Dr. Jiang in our laboratory (Jiang, Emmetsberger, Talmage, & Role, 2013; Jiang & Role, 2008).

The variability of the plasticity in the thalamic pathway might imply that subsets of pyramidal neurons synapse with thalamic inputs in different ways, while synapses to cortical inputs are more uniform. Alternatively, it may be the case that these sets of synapses have similar molecular machinery but that the initial state of the thalamic inputs varies more widely than that of the cortical inputs . Thus, synapses already potentiated or otherwise altered in the animal might be more likely to depress, and vice versa. This state can be affected by experience hours, days, or longer prior to examination. Future experiments might utilize stricter controls on animals' environment and stimuli in the days prior to recording to minimize variability. The thalamic inputs that do not respond to patterned stimulation might mean that there are many "hardwired" inputs from thalamic areas, while cortical inputs are typically more plastic.

Finally, that co-activation of both inputs can induce plasticity implies that there is a synergistic relationship between these two pathways. These experiments were the most technically challenging, limiting the number of examples to only 4 cells. Given the variability of the response, there is no clear pattern of plasticity induced this way. This

result supports the idea of the basolateral amygdala as a coincidence detector. Only one study shows the same effect in lateral amygdala (Cho et al., 2012). Studying the effects induced by patterned stimulation of a single pathway is informative of the dynamic range and direction of plasticity these synapses are prone to exhibit. However, a more physiologically realistic scenario is one in which many input pathways are constantly being activated at synapses distributed along the entire dendritic arbor. If these cells are arranged to detect and remember coincident activation of pairs of inputs, as suggested by various studies of the basolateral complex in associative learning paradigms, then an input-timing dependent plasticity of nearby pairs of dendritic spines seems a likely mechanism allowing them to do so. Moreover, evidence suggests that the amygdala entrains to hippocampal and cortical theta rhythms (Likhtik, Stujenske, Topiwala, Harris, & Gordon, 2014). Activity arising from a sensory stimulus induces cascades of activity at this rhythm over long periods of time. Thus, it may be the case that these cortical rhythms "prime" pyramidal cells to potentiate to thalamic input.

Fig 2.1 - mEPSCs in a BLA pyramidal neuron

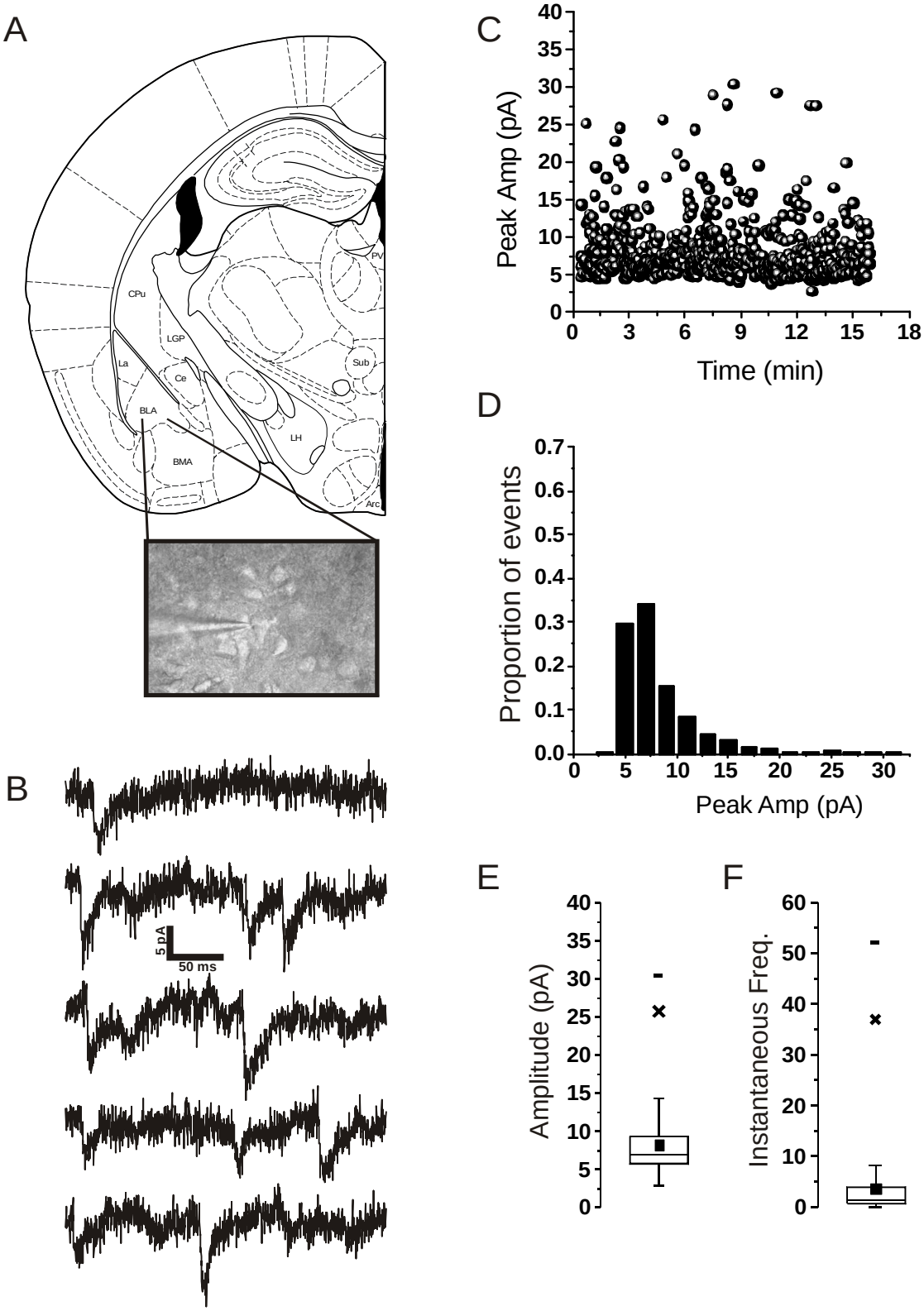

Figure 2.1 - Miniature EPSCs in a BLA pyramidal neuron. (A) Drawing of coronal section (Paxinos Mouse Brain Atlas) indicating recording area in BLA. Image shows a patched pyramidal neuron. (B) Examples of miniEPSC recordings (Noise RMS = 1.52 pA). (C) Plot of miniEPSC peak amplitudes over time. (D) Histogram of miniEPSCs over entire timecourse of the experiment. Bins were normalized by dividing by the total number of events. (E) Box plot of mini EPSC peak amplitudes. Box encloses middle 2 quartiles; mean is represented by square; median by horizontal line; whiskers mark outlier range; x represents 99th percentile; small horizontal line marks largest event. Events had a mean amplitude of 8.20 pA (*SD* = 3.91, *SEM* = 0.15). (F) Box plot of instantaneous frequency of each miniEPSC. Symbols are same as in E. Events had a mean instantaneous frequency of 2.69 Hz (*SD* = 4.84, *SEM* = 0.18).

Fig 2.2 - Population histograms for mEPSCs in BLA

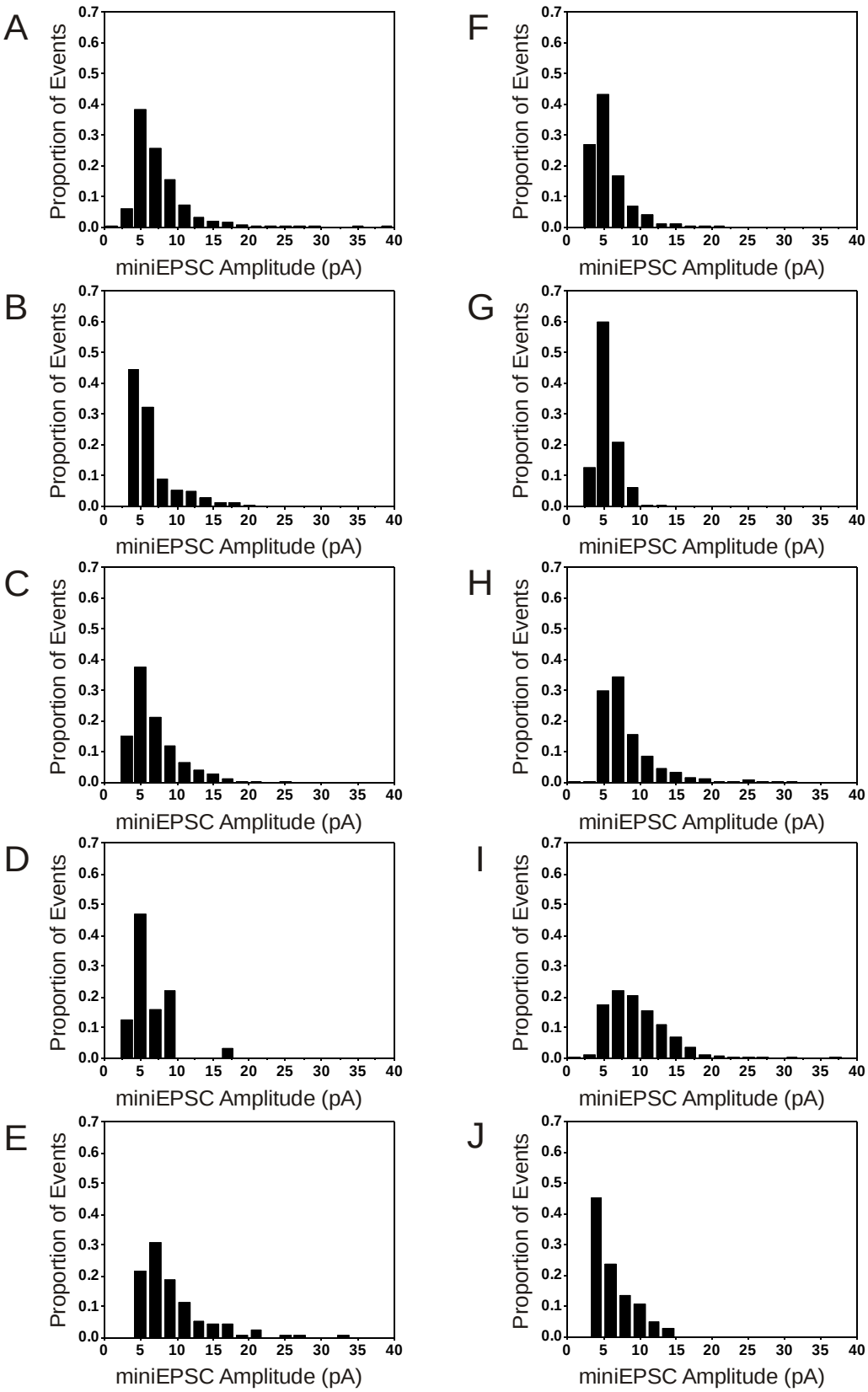

Figure 2.2 - Histograms of miniature EPSC amplitudes for all 10 cells included in analysis.

Fig 2.3 - BLA mEPSCs pooled data

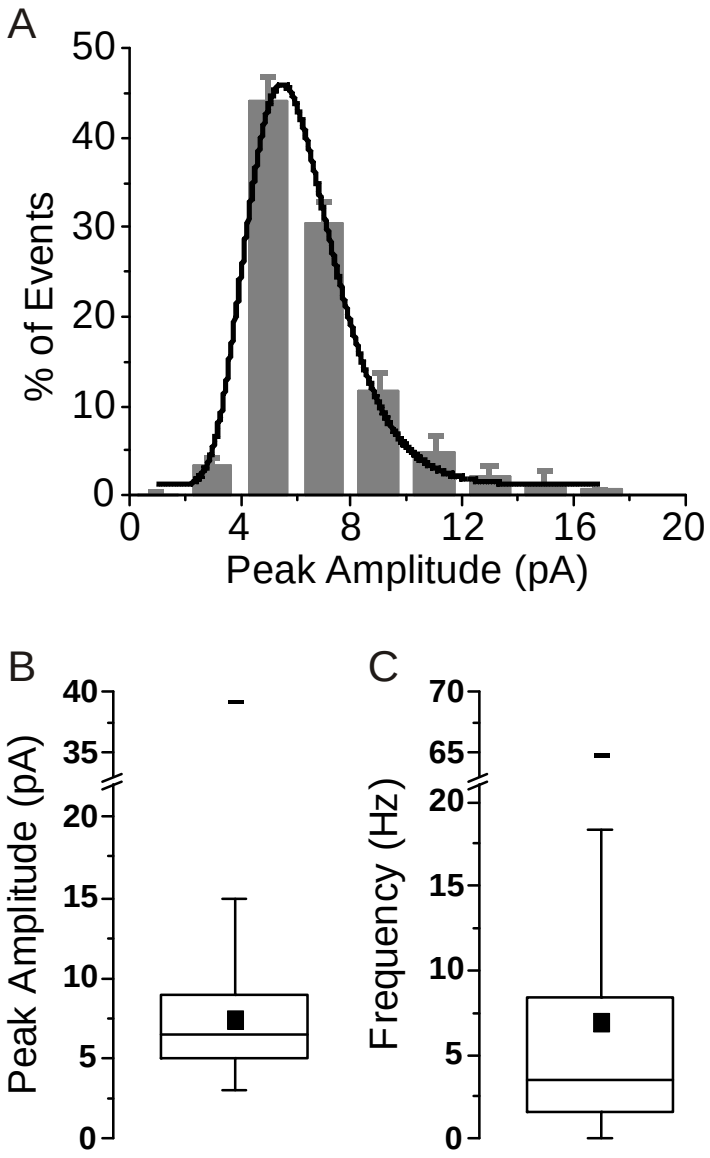

Figure 2.3 - Pooled miniature EPSC data. (A) Normalized histograms from 10 cells that passed criteria for evaluation (Fig. 2.2) were pooled by plotting the mean of each bin across cells. Whiskers indicate standard error. The histogram was fit by a log-normal distribution (r^2 = 0.93). (B) Box plot of peak amplitude of all miniEPSCs analyzed (*N* = 9765). Box encloses middle 2 quartiles; mean is represented by square; median by horizontal line; whiskers mark outlier range; x represents 99th percentile. Events had a mean amplitude of 7.47 pA (*SD* = 3.64, *SEM* = 0.04). (C) Box plot of instantaneous frequency of each miniEPSC. Symbols are same as in B. Events had a mean instantaneous frequency of 6.93 Hz (*SD* = 8.70, *SEM* = 0.09).

Fig 2.4 - Thalamo-BLA unitary EPSCs evoked by internal capsule stimulation

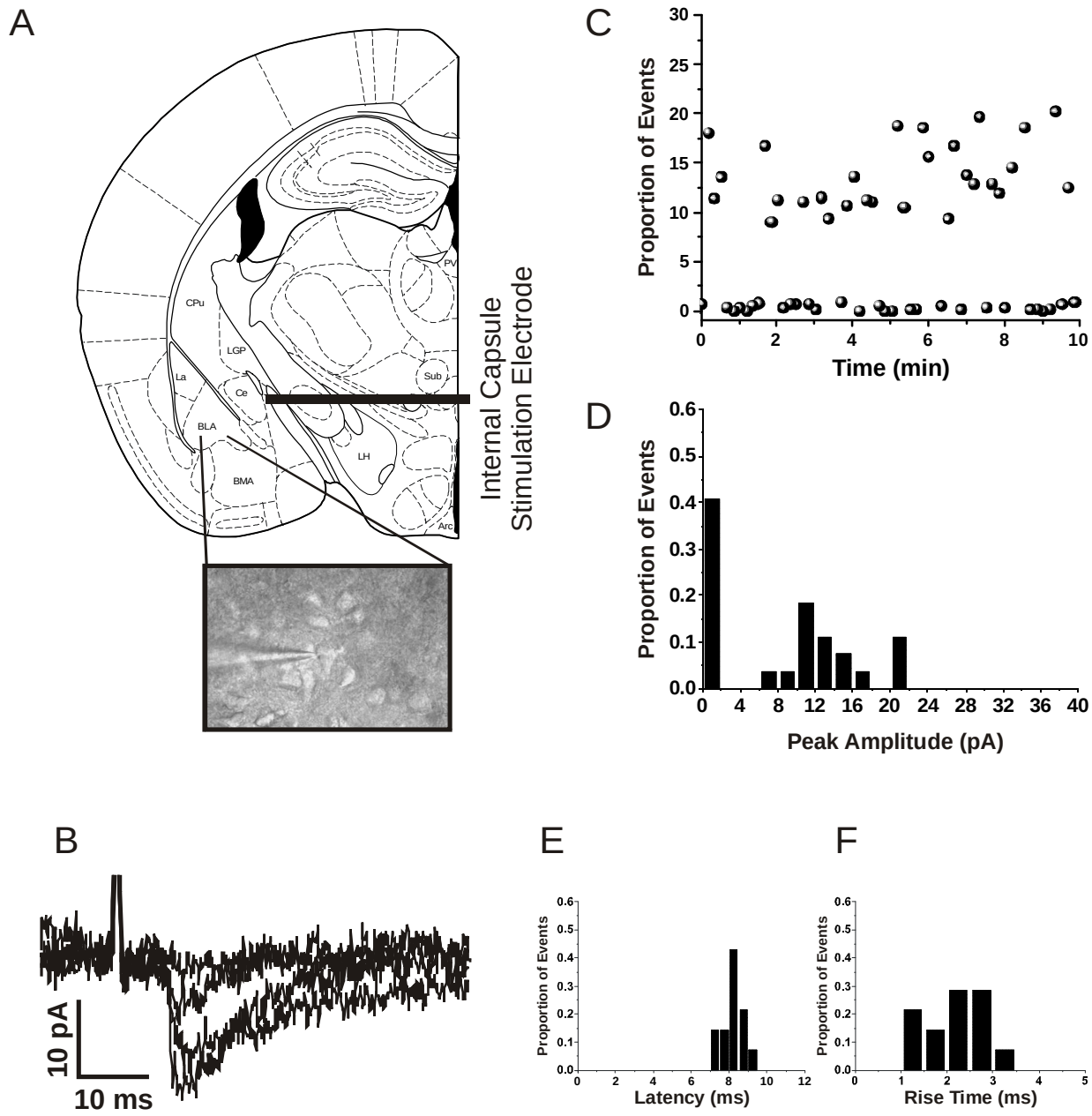

Figure 2.4 - Thalamo-BLA unitary EPSCs evoked by internal capsule stimulation. (A) Diagram of mouse brain coronal section (Paxinos Mouse Brain Atlas) illustrating recording area in BLA and stimulation electrode position. (B) Overlay of 4 example recording traces including 1 failure and 3 evoked EPSCs (Noise RMS = 1.32). Truncated stimulation artifact marked by 's'. (C) Evoked EPSC peak amplitudes and failures (represented as points near 0 pA) plotted over time. (D) Histogram of all events and failures. Mean peak amplitude was 13.99 pA (*SD* = 4.31, *SE* = 1.08). Distribution suggests a mode at 10 pA and a second mode at 20 pA. (E) Histogram of event latencies. Mean latency was 8.16 ms (*SD* = 0.52). (F) Histogram of event rise times. Mean rise time was 2.09 ms (*SD* = 0.60).

Fig 2.5

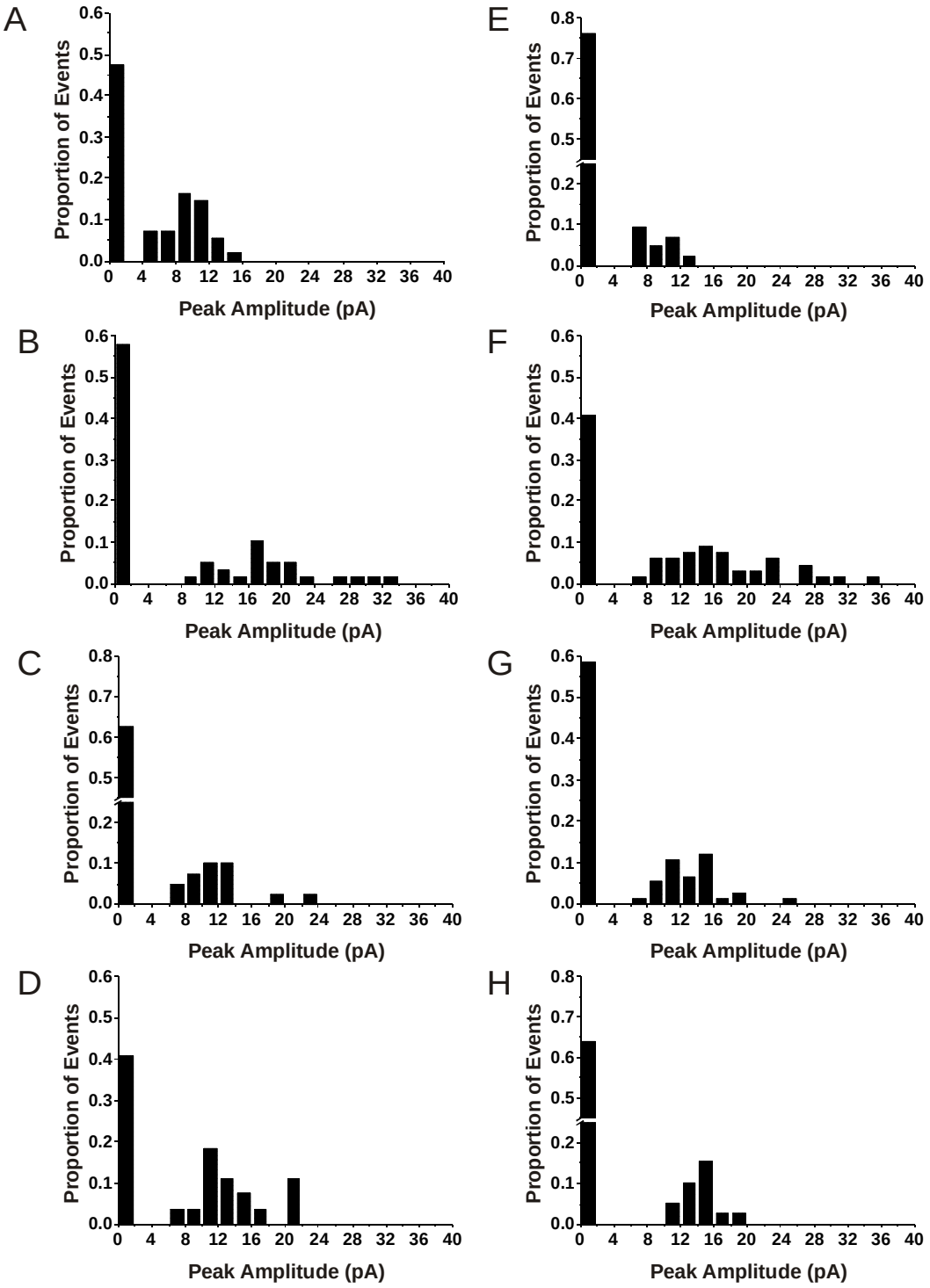

Figure 2.5 - Histograms of thalamo-BLA unitary EPSCs evoked by stimulation of the internal capsule from 8 cells that passed criteria for evaluation.

Fig 2.6 - Pooled thalamo-BLA unitary EPSC data

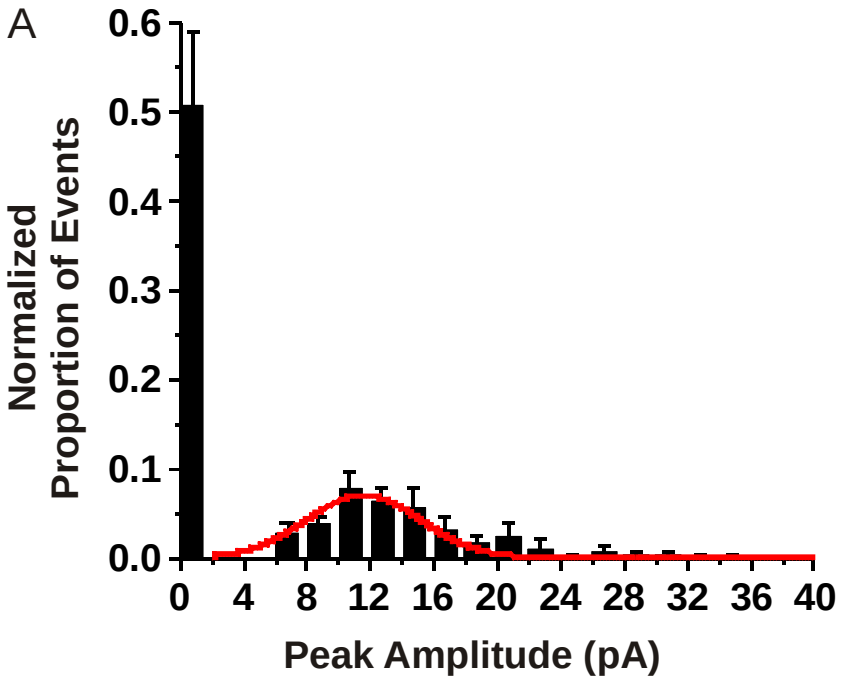

Figure 2.6 - Pooled Thalamo-BLA unitary EPSC data. (A) Normalized histograms from 8 cells that passed criteria for evaluation (Fig. 2.5) were pooled by plotting the mean of each bin across cells. Whiskers indicate standard error. Events (not including failures) were fit by Gaussian distribution (r^2 = 0.91).

Fig 2.7 - Cortico-BLA Unitary EPSCs

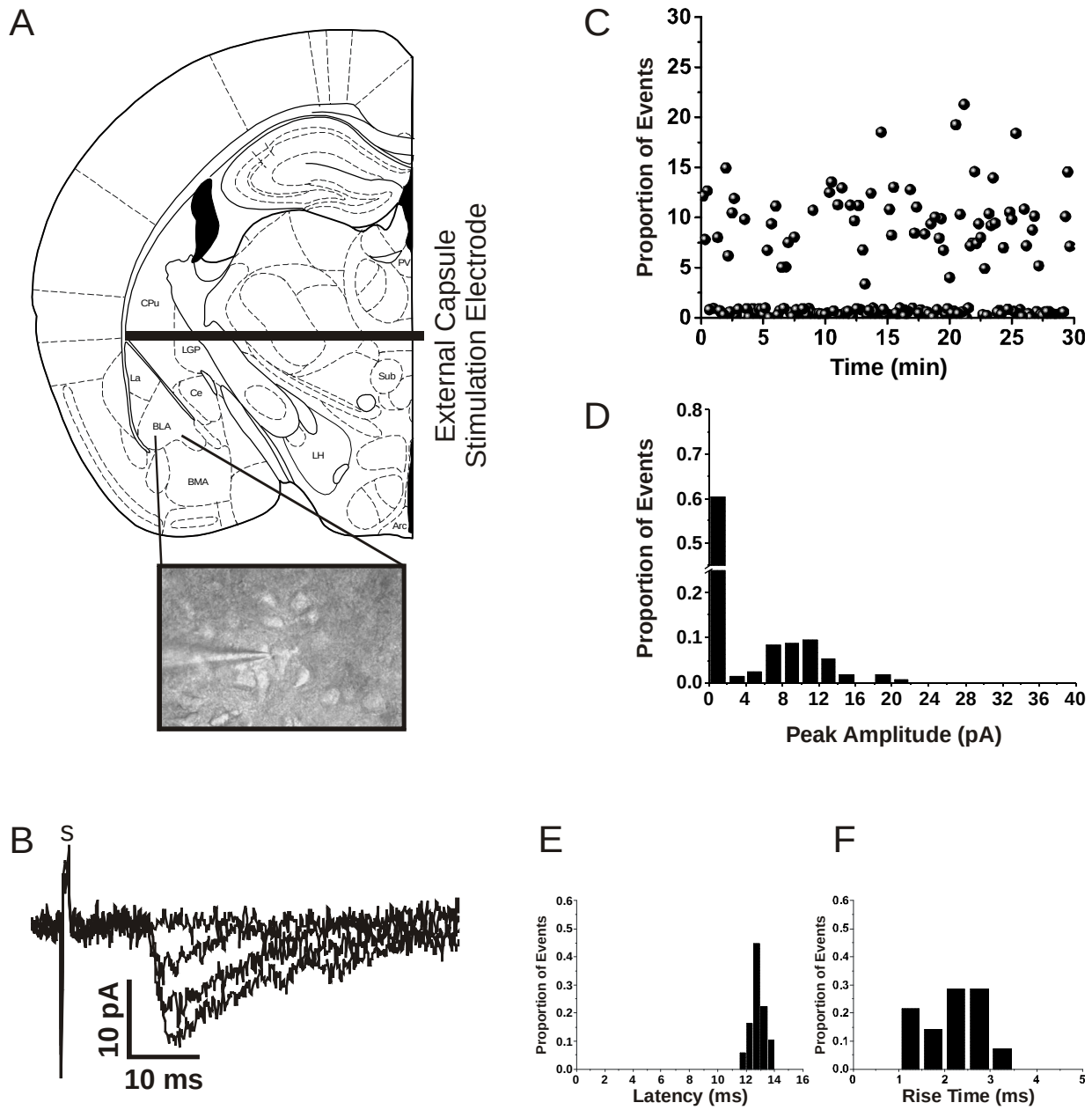

Figure 2.7 - Cortical-BLA unitary EPSCs evoked by external capsule stimulation. (A) Diagram of mouse brain coronal section (Paxinos Mouse Brain Atlas) illustrating recording area in BLA and stimulation electrode position. The external capsule is highlighted in blue. (B) Overlay of 4 example recording traces including 1 failure and 3 evoked EPSCs (Noise RMS = 0.86 pA). Stimulation artifact marked by 's'. (C) Evoked EPSC peak amplitudes and failures (represented as points near 0 pA) plotted over time. (D) Histogram of all events and failures. Mean peak amplitude was 10.06 pA (*SD* = 3.53, *SE* = 0.43). (E) Histogram of event latencies. Mean latency was 12.79 ms (*SD* = 0.46). (F) Histogram of event rise times. Mean rise time was 1.79 ms (*SD* = 0.47).

Fig 2.8 - Cortico-BLA Unit Histograms

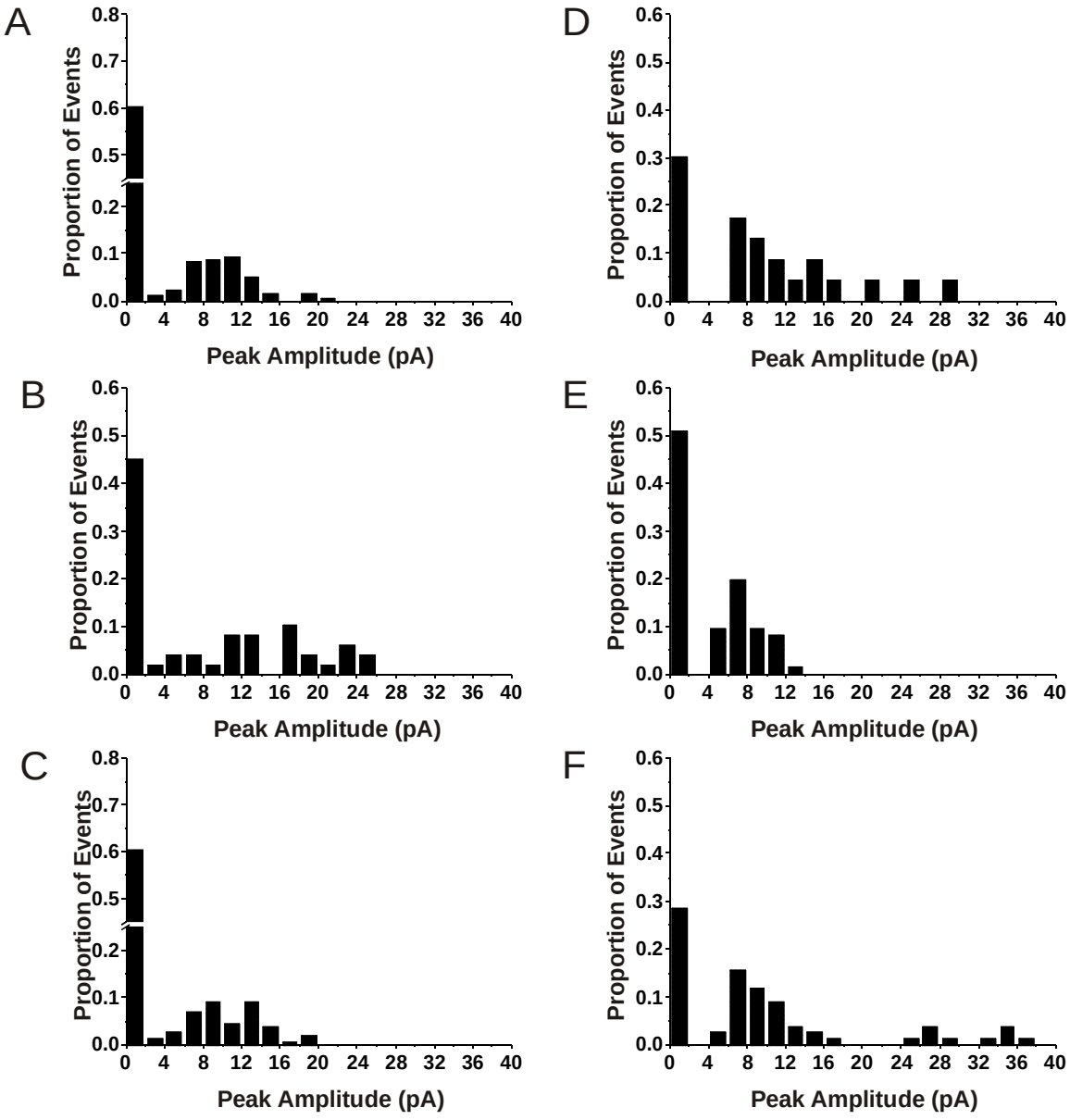

Figure 2.8 - Histograms of cortico-BLA unitary EPSCs evoked by stimulation of the external capsule from all 6 cells that passed criteria for evaluation.

Fig 2.9 - Pooled cortico-BLA unitary EPSC data

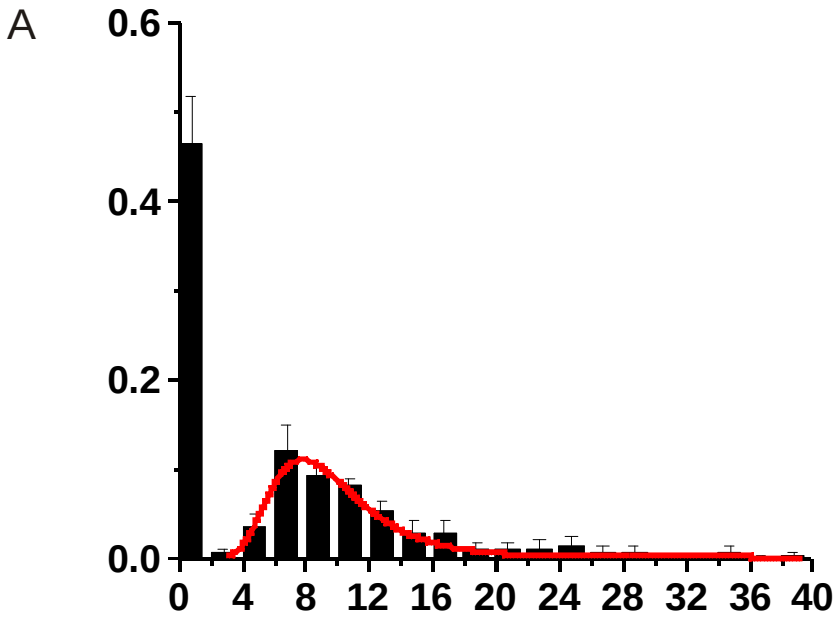

Figure 2.9 - Pooled Cortico-BLA unitary EPSC data. (A) Normalized histograms from 6 cells that passed criteria for evaluation (Fig. 2.8) were pooled by plotting the mean of each bin across cells. Whiskers indicate standard error. Events (not including failures) were fit by log-normal distribution (r^2 = 0.95).

Fig 2.10 - Input/Output relationship of the thalamo-BLA pathway

A

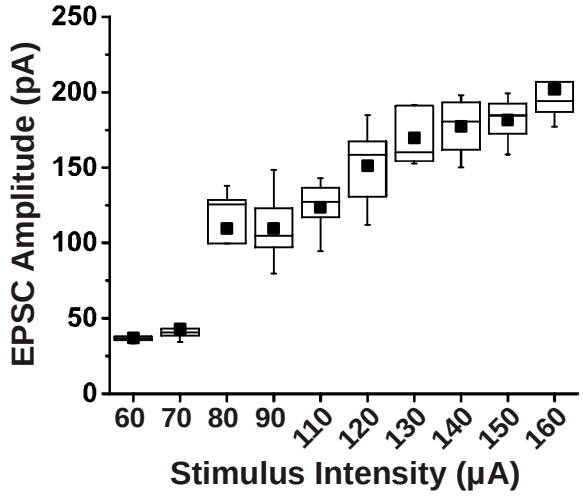

B

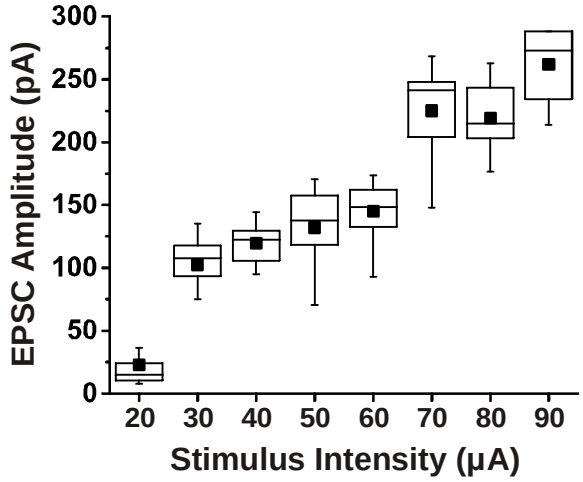

C

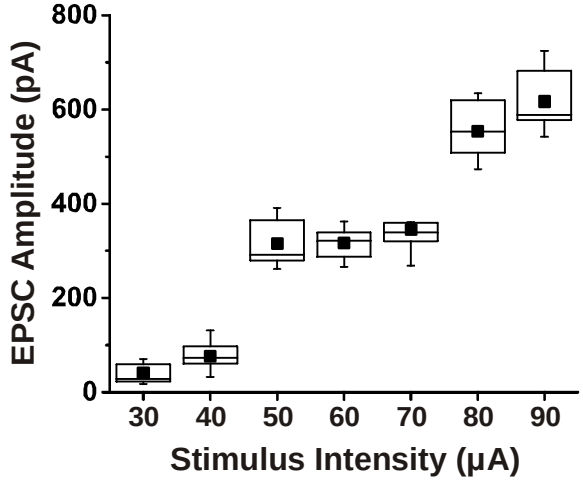

Figure 2.10 - Input/Output relationship of the thalamo-BLA pathway. Stimulation intensity of the internal capsule was adjusted to the minimum required to evoked EPSCs in BLA pyramidal cells. After recording for 1 to 3 minutes, stimulation intensity was incremented by 10 μA. This was repeated until EPSC amplitude reached a stable maximum. In the thalamo-BLA input, EPSC amplitude increased in a stepwise manner, with little or no increase in amplitude over several incremental increases in stimulation intensity followed by a large jump in amplitude. This suggests recruitment of additional groups of fiber bundles near the stimulation site.

Fig 2.11 - Input/Output relationship of the cortico-BLA pathway

A

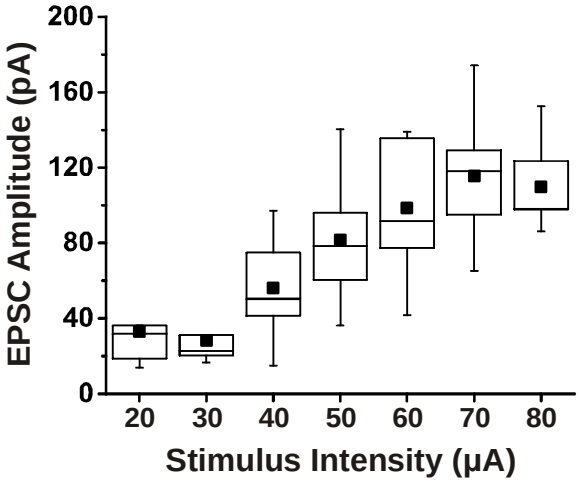

B

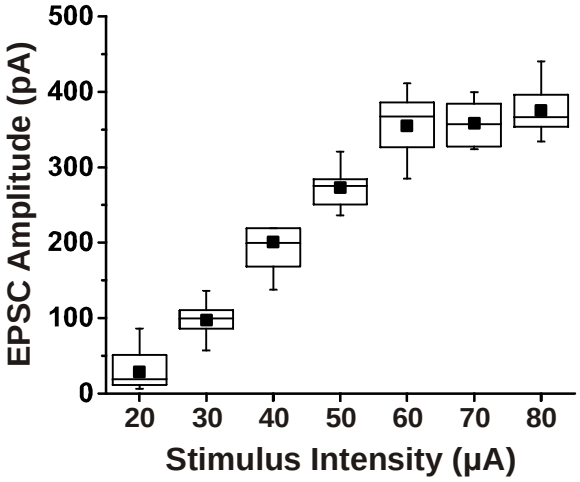

C

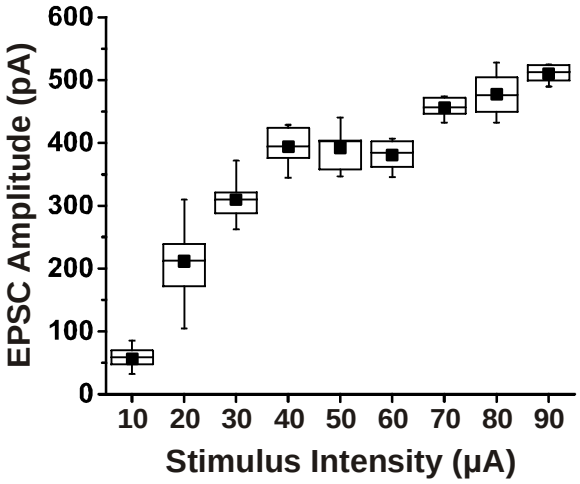

Figure 2.11 - Input/Output relationship of the cortico-BLA pathway. Stimulation intensity of the internal capsule was adjusted to the minimum required to evoked EPSCs in BLA pyramidal cells. After recording for 1 to 3 minutes, stimulation intensity was incremented by 10 µA. This was repeated until EPSC amplitude reached a stable maximum. In the cortico-BLA pathway, EPSC amplitude generally increased linearly with incremental increases in stimulation intensity before reaching a maximal plateau.

Fig 2.12 - TBS can elicit LTP at subcortico-BLA synapses

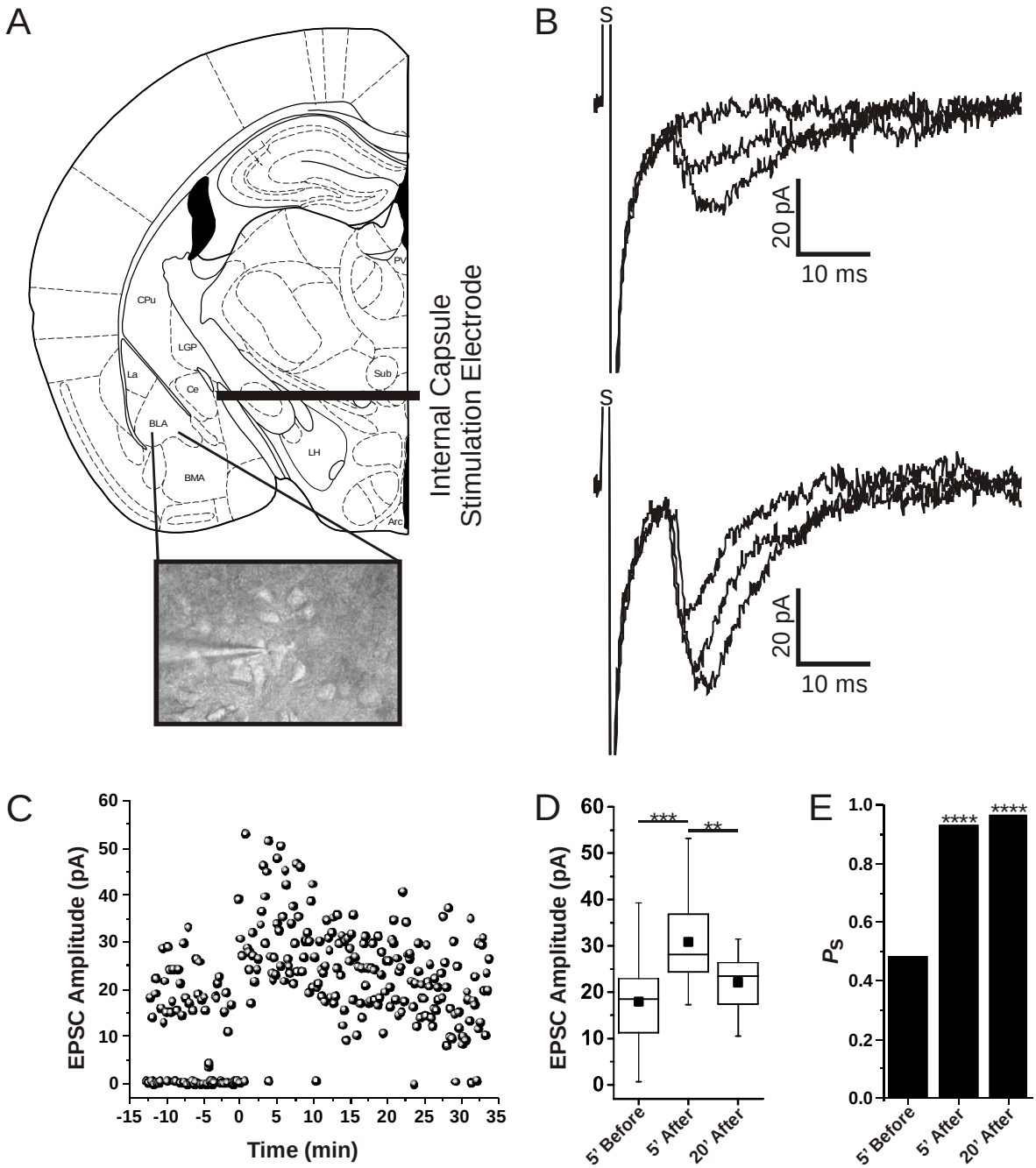

Figure 2.12 - Theta-burst stimulation can elicit long-lasting potentiation at thalamo-BLA synapses. (A) Diagram of mouse brain coronal section (Paxinos Mouse Brain Atlas) illustrating recording area in BLA and stimulation electrode position. (B) Overlaid example recording traces before (top) and after (bottom) theta-burst stimulation. Stimulus artifacts marked with 's' (Noise RMS = 1.73). (C) Evoked EPSC amplitudes plotted over time. Theta-burst stimulation was delivered at time 0. (D) EPSC amplitudes were binned in 5 minute bins immediately before, immediately after, and 15-20 minutes after theta-burst stimulation. These bins were compared by one-way ANOVA and found to be significantly different ($F(2,65) = 10.43$, $p < 0.001$). A Tukey *post-hoc* comparison showed a significant increase in amplitude in the 5 minutes after TBS compared to 5 minutes before (***$p < 0.001$), but no significant difference 20 minutes after TBS ($p = 0.37$). (E) Probability of successfully evoking an EPSC (P_s) was compared using Pearson's X^2 statistic between 5 minute time bins immediately before, immediately after, and 15-20 minutes after TBS. P_s was greatly elevated 5 minutes after TBS ($X^2(57) = 16.36$, ****$p < 0.0001$), and remained elevated at 20 minutes post-TBS ($X^2(56) = 19.07$, ****$p < 0.0001$).

Fig 2.13 - Theta-burst stimulation can elicit depression at thalamo-BLA synapses

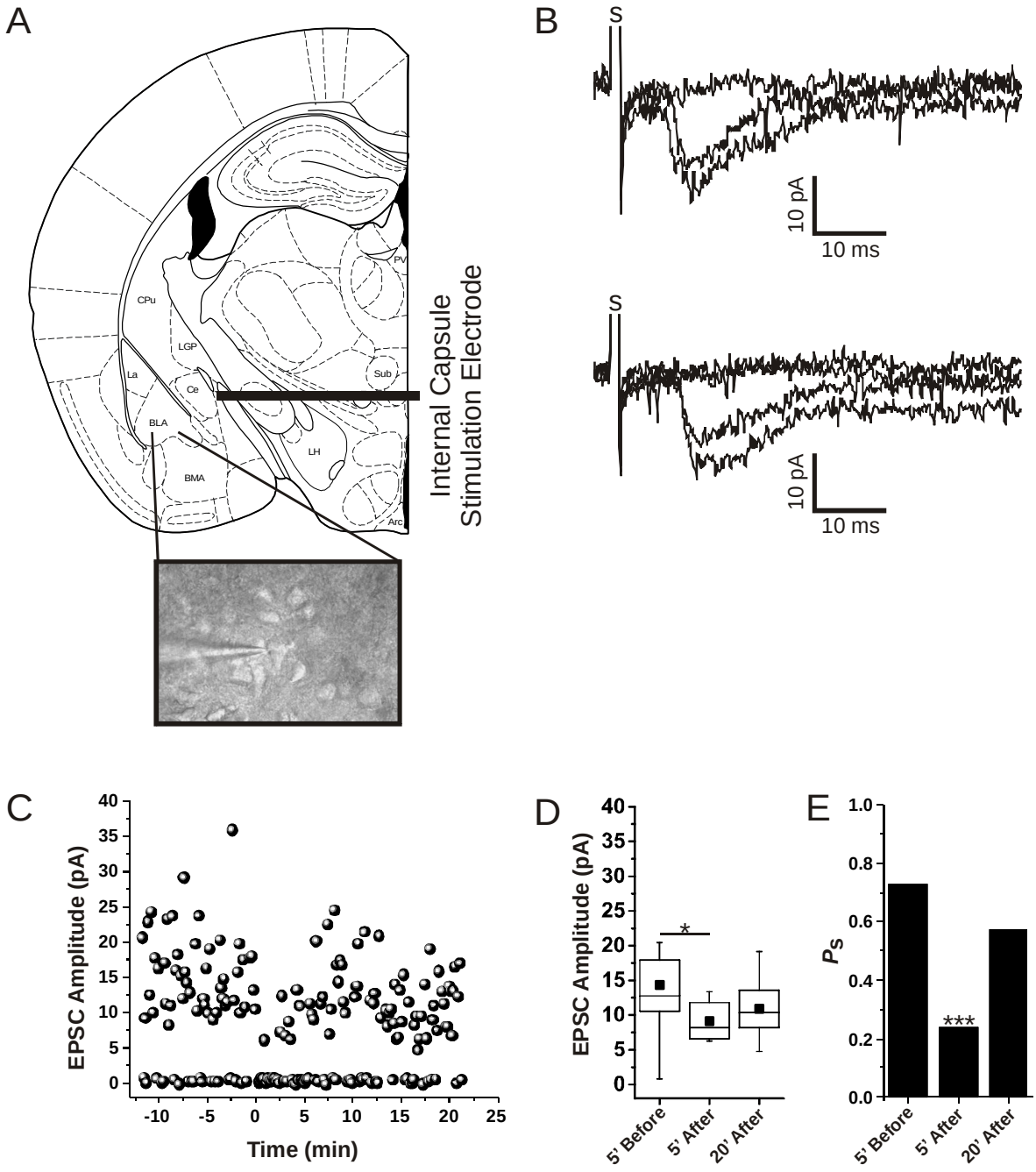

Figure 2.13 - Theta-burst stimulation can elicit short-term depression at thalamo-BLA synapses. (A) Diagram of mouse brain coronal section (Paxinos Mouse Brain Atlas) illustrating recording area in BLA and stimulation electrode position. (B) Overlaid example recording traces before (top) and after (bottom) theta-burst stimulation. Truncated stimulus artifact marked with 's'. (C) Evoked EPSC amplitude plotted over time. Failures represented as points near 0 pA. Theta-bust stimulation delivered at time 0. (D) EPSC amplitudes were binned 5 minutes before, 5 minutes after and 15-20 minutes after TBS. A significant difference between bins was found by one-way ANOVA ($F(2, 47) = 4.01$, $p = 0.02$). A *post-hoc* Tukey test showed a significant difference 5 minutes after TBS compared to before ($*p = 0.04$), but not 20 minutes after ($p = 0.69$). (E) Probability of evoking an EPSC (*P*s) was measured by dividing number of failures over total measurable events in 5 minutes bins before, after, and 15-20 minutes after TBS. The time bins after TBS were compared pairwise to control using Pearson's X^2 statistic. *P*s was significantly different 5 minutes after TBS ($X^2(1, 59) = 14.28$, $***p < 0.001$) but not 20 minutes after TBS ($X^2(1, 58) = 0.35$, $p = 0.56$).

Fig 2.14 - 100 Hz can elicit LTP at subcortico-BLA synapses

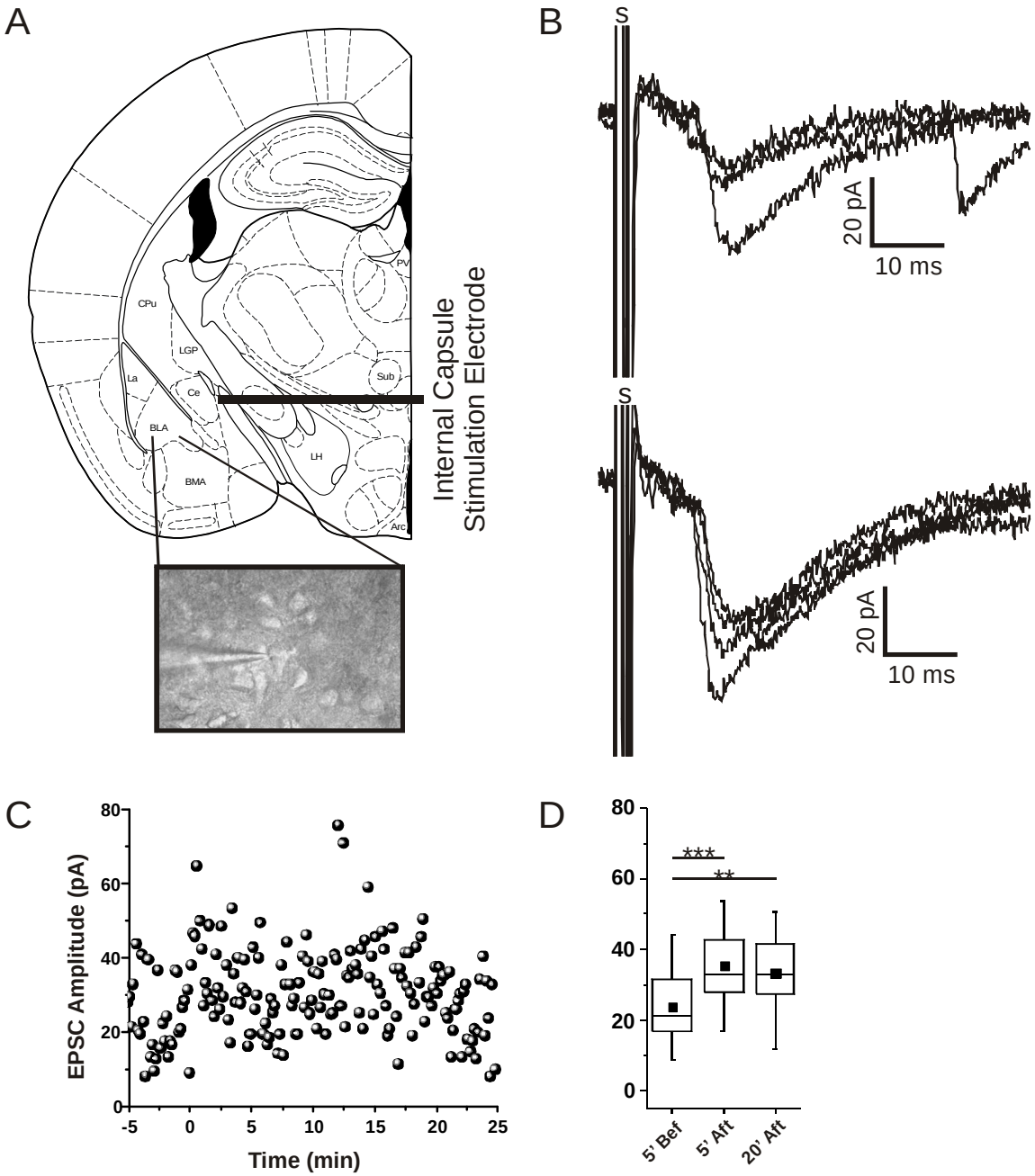

Figure 2.14 - Tetanic stimulation can elicit long-lasting depression at thalamo-BLA synapses. (A) Diagram of mouse brain coronal section (Paxinos Mouse Brain Atlas) illustrating recording area in BLA and stimulation electrode position. (B) Overlaid example recording traces before (top) and after (bottom) 100 Hz tetanic stimulation. Truncated stimulus artifact marked with 's'. (C) Evoked EPSC amplitude plotted over time. A 1 s,100 Hz tetanus was delivered at time 0. (D) EPSC amplitudes were binned 5 minutes before, 5 minutes after and 15-20 minutes after 100 Hz tetanus. A significant difference between bins was found by one-way ANOVA ($F(2, 87) = 14.07$, $p < 0.0001$). A *post-hoc* Tukey test showed a significant difference 20 minutes after tetanus compared to before (****$p < 0.0001$), but not 5 minutes after ($p = 0.99$). However, this appears to be due to the averaging of post-tetanic potentiation followed by depression, supported by the significant difference in variance before and after tetanic stimulation ($F(29) = 0.12$, $p < 0.0001$).

Fig 2.15 - 100 Hz can elicit LTD at subcortico-BLA synapses

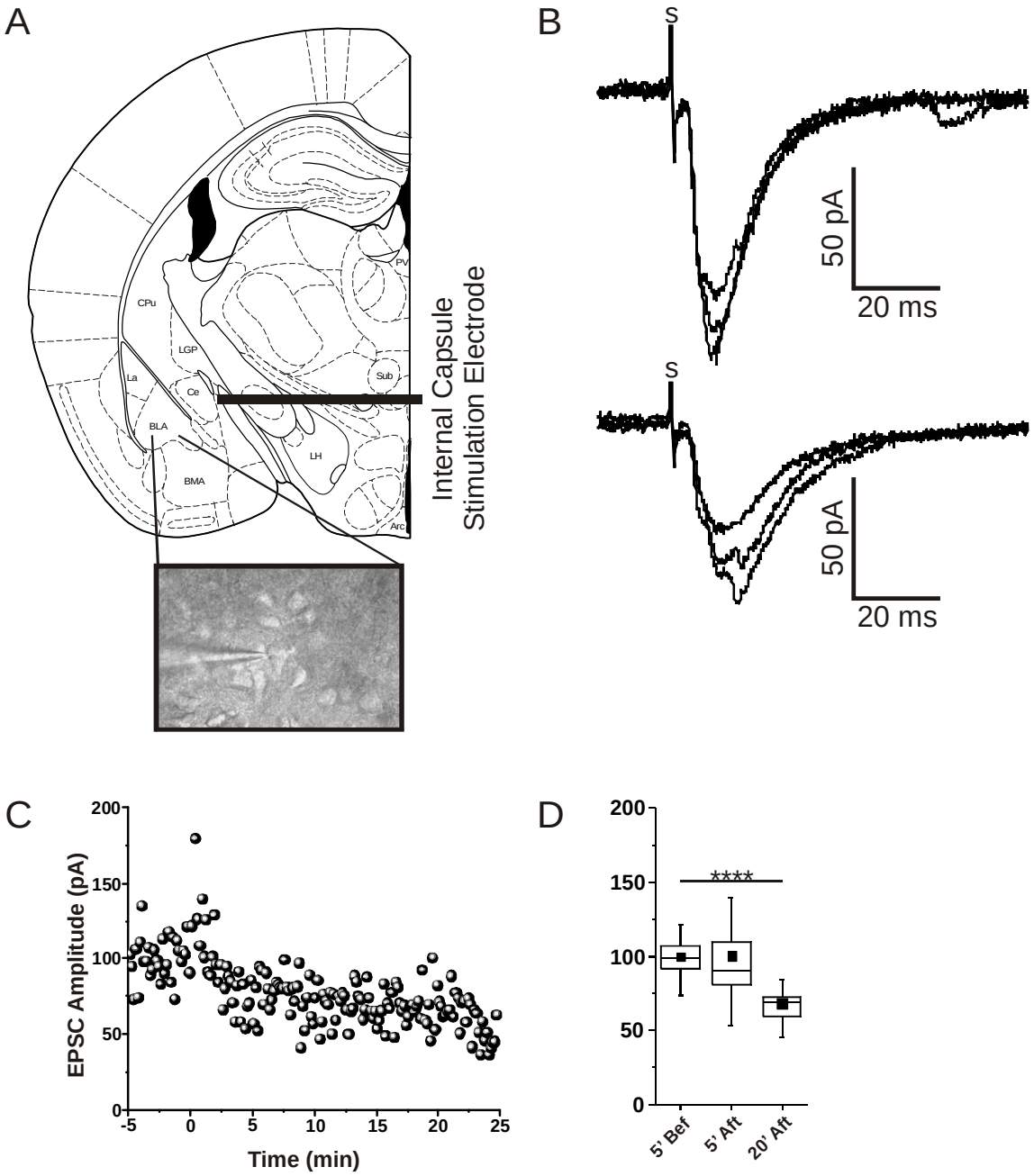

Figure 2.15 - Tetanic stimulation can elicit LTP at thalamo-BLA synapses. (A) Diagram of mouse brain coronal section (Paxinos Mouse Brain Atlas) illustrating recording area in BLA and stimulation electrode position. (B) Overlaid example recording traces before (top) and after (bottom) tetanic stimulation. Truncated stimulus artifact marked with 's'. (C) Evoked EPSC amplitude plotted over time. A 1 s,100 Hz tetanus was delivered at time 0. (D) EPSC amplitudes were binned 5 minutes before, 5 minutes after and 15-20 minutes after 100 Hz tetanus. A significant difference between bins was found by one-way ANOVA ($F(2, 87) = 11.06$, $p < 0.0001$). A *post-hoc* Tukey test showed a significant difference 5 minutes after tetanus compared to before (****$p < 0.0001$), and 20 minutes after (**$p < 0.01$).

Fig 2.16 - 100 Hz Subcortico-BLA pooled data

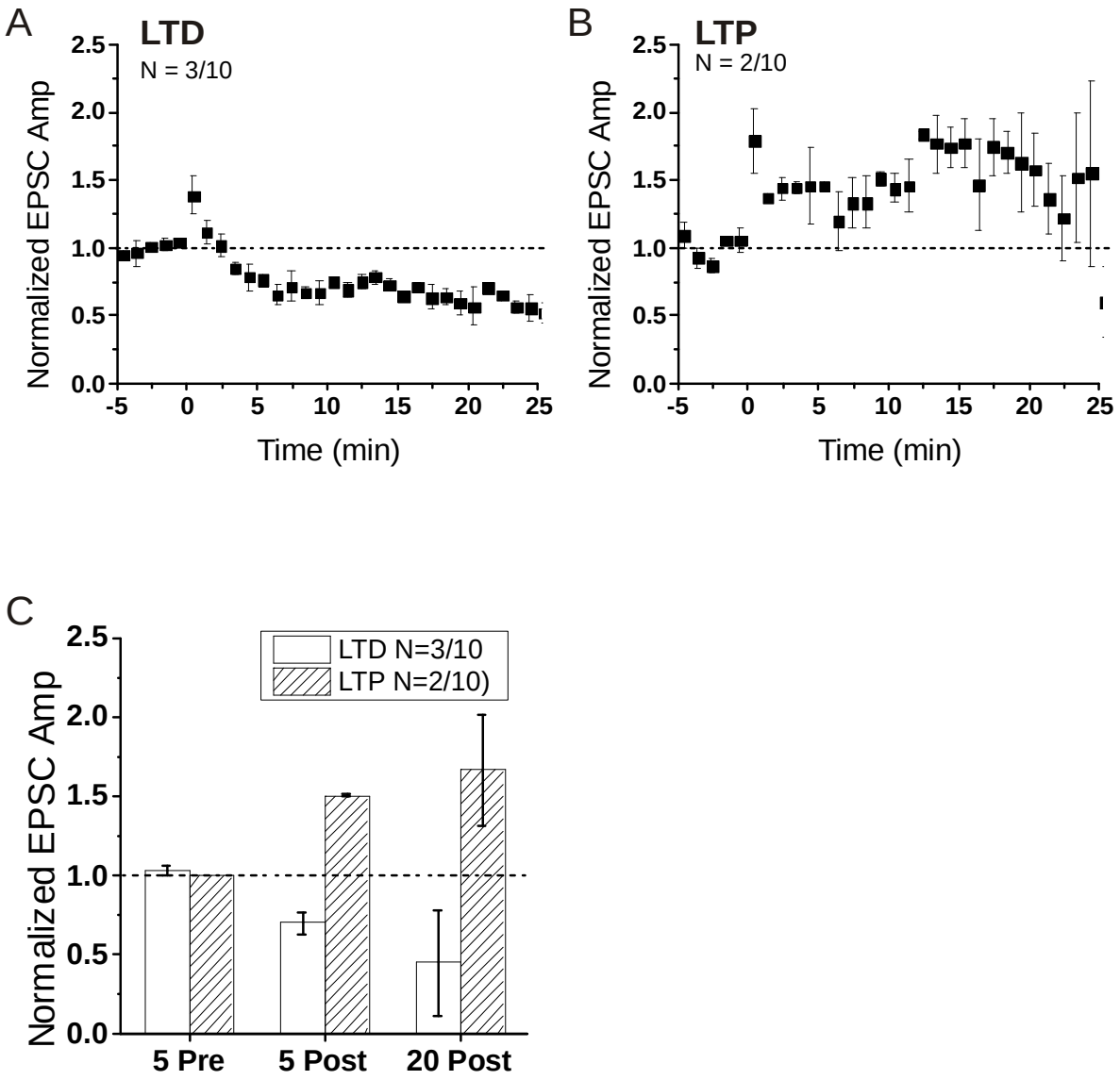

Figure 2.16 - Thalamo-BLA tetanic stimulation pooled data. (A) Evoked EPSC peak amplitude data from 3 of 10 cells that showed statistically significant depression after 100 Hz tetanus was normalized to the 5 minute control period and averaged in 1 minute bins. (B) Evoked EPSC peak amplitude data from 2 of 10 cells that showed statistically significant potentiation after 100 Hz tetanus was normalized to the 5 minute control period and averaged in 1 minute bins. (C) Data from plots A and B was averaged in 5 minute bins before, after, and 15-20 minutes after tetanic stimulation. Whiskers denote standard error.

Fig 2.17 - 100 Hz elicits LTP at Cortico-BLA synapses

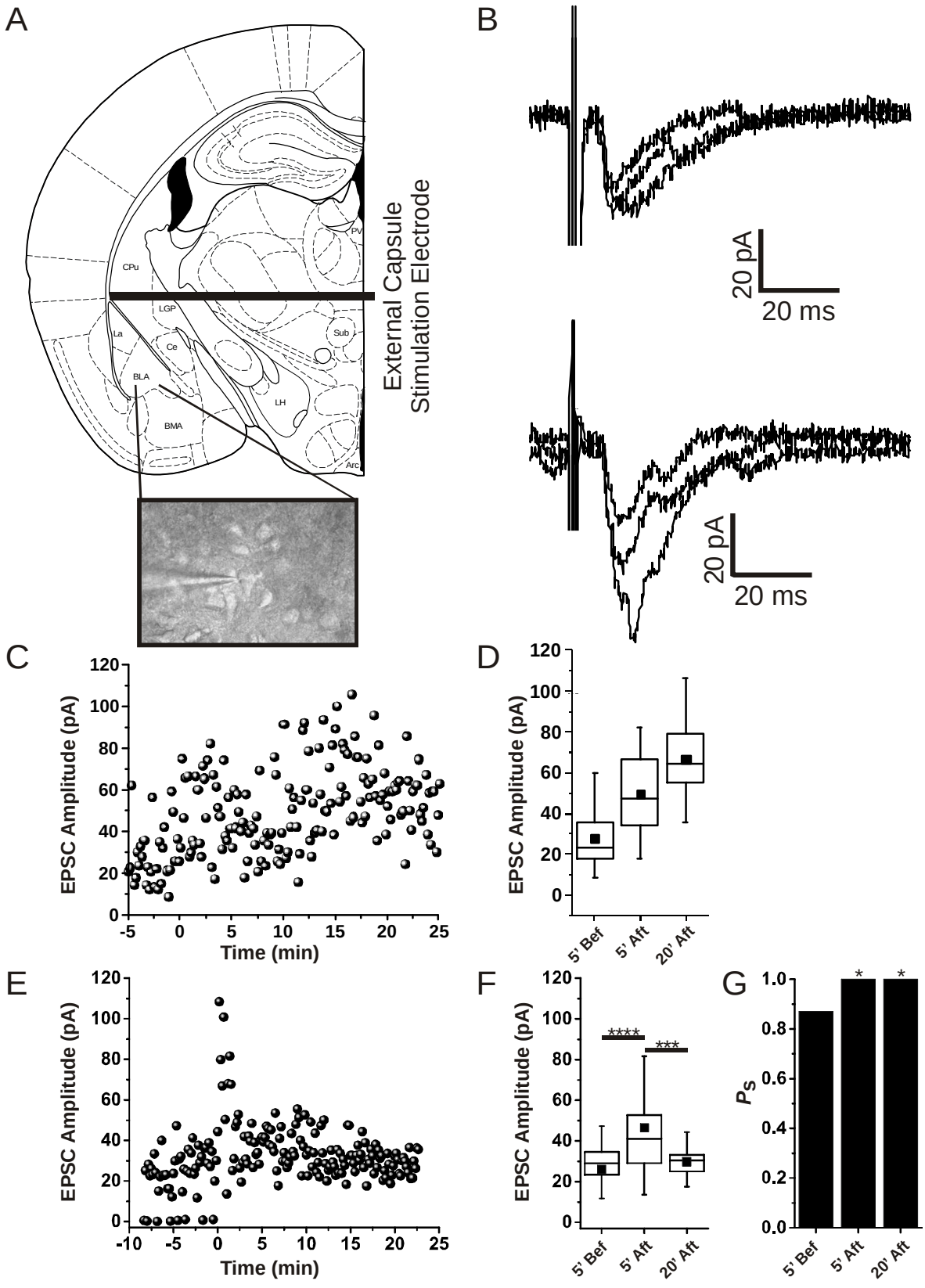

Figure 2.17 - Tetanic stimulation induces LTP at cortico-BLA synapses. (A) Diagram of mouse brain coronal section (Paxinos Mouse Brain Atlas) illustrating recording area in BLA and stimulation electrode position. (B) Overlaid example recording traces before (top) and after (bottom) tetanic stimulation. Truncated stimulus artifact marked with 's'. (C) Evoked EPSC amplitude plotted over time. A 1 s,100 Hz tetanus was delivered at time 0. (D) EPSC amplitudes were binned 5 minutes before, 5 minutes after and 15-20 minutes after 100 Hz tetanus. A significant difference between bins was found by one-way ANOVA ($F(2, 87) = 38.73$, $p < 0.0001$). A *post-hoc* Tukey test showed a significant difference 5 minutes after tetanus compared to before (****$p < 0.0001$), and 20 minutes after (****$p < 0.0001$). There was also a significant difference between the 20 minute after and 5 minutes after bins (***$p < 0.001$). (E) Second example cell, evoked EPSC amplitude plotted over time. A 1 s,100 Hz tetanus was delivered at time 0. (F) Binned EPSC amplitudes as in D. (G) For data in E, F, probability of evoking an EPSC (*P*s) was measured by dividing number of failures over total measurable events in 5 minutes bins before, after, and 15-20 minutes after 100 Hz tetanus. The time bins after TBS were compared pairwise to control using Pearson's X^2 statistic. *P*s was significantly different 5 minutes after TBS ($X^2(1, 60) = 4.29$, *$p = 0.04$) and 20 minutes after TBS ($X^2(1, 59) = 4.15$, *$p = 0.04$).

Fig 2.18 - Coactivation of thalamic and cortical inputs induces plasticity

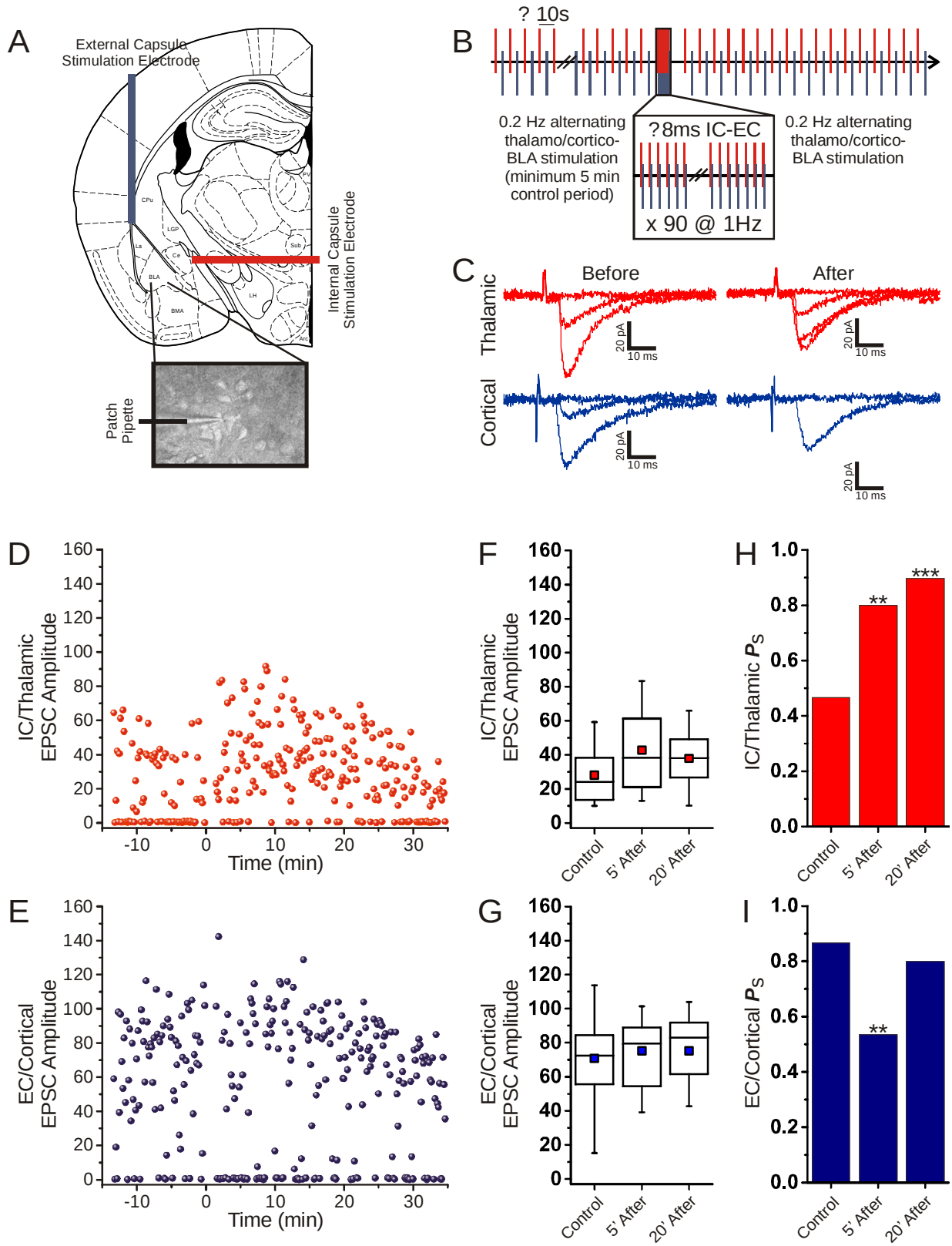

Figure 2.18 - Coactivation of thalamo- and cortico-BLA pathways induces synaptic plasticity. (A) Diagram of mouse brain coronal section (Paxinos Mouse Brain Atlas) illustrating recording area in BLA and stimulation electrode positions. (B) Timeline of experimental protocol. Internal and external capsules were alternately stimulated at an interval of 5s (rate of 0.2 Hz) to establish a control period. Then 90 pairings of internal capsule stimulation followed by external capsule stimulation with a delay of 8 ms was given at a rate of 1 Hz. Alternating stimulation of each input was resumed at a rate of 0.2 Hz. (C) Example traces of thalamo-BLA failures and evoked EPSCs (top) and cortico-BLA failures and evoked EPSCs (bottom) before (left) and after (right) the train of Δ8 ms pairings was delivered. (D) Timecourse of thalamo-BLA failures and evoked EPSCs. Δ8 ms train was delivered at time 0. Failures are represented as points near 0 pA. (E) Plot of cortico-BLA failures and evoked EPSCs as in D. (F) Thalamo-BLA evoked EPSCs were binned in 5 minute bins before, immediately after, and 15-20 minutes after Δ8 ms stimulus train was delivered. One-way ANOVA found no significant difference between bins ($F(2, 61) = 2.48$, $p = 0.09$). (G) Cortico-BLA evoked EPSCs were binned as in F. One-way ANOVA found no significant difference between bins ($F(2, 61) = 0.23$, $p = 0.80$). (H) Thalamo-BLA P_s was calculated by dividing number of evoked EPSCs by total number of events for each bin. Post- Δ8 ms stimulus bins were compared pairwise to control using Pearson's X^2 statistic. P_s was significantly different 5 minutes after ($X^2(1, 60) = 7.18$ (**$p < 0.01$)), and 20 minutes after ($X^2(1, 59) = 12.48$ (***$p < 0.001$). (I) Cortico-BLA P_s was calculated and binned as in H. P_s was significantly different 5 minutes after ($X^2(1, 60) = 7.94$ (**$p < 0.001$)), but not 20 minutes after ($X^2(1, 60) = 0.48$ ($p = 0.49$)).

Chapter 3 - Optogenetic stimulation of cholinergic afferents in BLA induces plasticity at cortico- and thalamo-BLA synapses

Introduction

The overall goal of my dissertation is to understand how pyramidal neurons in the BLA integrate diverse inputs from distant brain regions, and how acetylcholine might influence this integration and shape the behaviorally adaptive response. In the previous chapter I examined some basic properties of cortico- and thalamo-BLA transmission to the BLA, as well as the plasticity of these pathways in response to patterned stimulation and coactivation. Another aspect of integration in the BLA is the role of neuromodulators, which the BLA hosts in an abundance. Particularly relevant to the sensory integration aspect of my thesis project is the role acetylcholine (ACh). ACh is well known to contribute to attention, learning and memory, especially during emotional arousal and stress response. The role of modulation by ACh on cortico- and thalamo-BLA transmission is the focus of this chapter.

The BLA is densely enmeshed in afferents from cholinergic neurons in the nucleus basalis (NBM), one of several cholinergic nuclei in the basal forebrain (Fig 3.1). Direct cholinergic synapses onto neurons in the BLA are thought to be rare. Rather, they typically form *en passant* release sites at peri-synaptic zones including axons, dendrites, and spine necks (Sarter, 2009, 2014; Jones 1999; Huh and Fuhrer 2002;

Dunant 2010). Thus, acetylcholine released by these fibers modulates the activity of the closely associated glutamatergic and GABAergic synapses. These synapses express both nicotinic and muscarinic receptors and these cholinergic receptors are localized to both pre- and post-synaptic sites. For this reason, the action of ACh is complex and varies greatly by brain region and cell type. The experiments in this chapter will examine the effects of cholinergic signaling on cortico- and thalamo-BLA glutamatergic transmission to BLA pyramidal neurons, primarily using an optogenetic technique to stimulate the endogenous cholinergic afferents from NBM.

Optogenetics is a technology recently developed that enables both temporal and spatial precision in the control of neuronal activity and the cell type specificity afforded by genetic targeting with engineered variants of channelrhodopsins. Channelrhodopsins are transmembrane, light-activated ion channels found naturally in unicellular organisms. When channelrhodopsins are activated by specific wavelengths of light, they allow ions to pass, depolarizing or hyperpolarizing the membrane, depending on the type of channel, and thus activate or inhibit the cell. Channelrhodopsin genes have been optimized for improved activation and decay kinetics, and coupled with a variety of promoters allowing for expression in specific classes of mammalian neuronal cells. These constructs are typically virally transfected. An additional level of specificity is achieved in the spatial control of virus delivery. In this project, I inject the NBM of ChAT-Cre mice with adeno-associated virus (AAV) containing a double-inverted floxed version of channelrhodopsin2 (ChR2), optimized by genetic engineering for temporal precision and minimal desensitization in the face of

repeated stimulation, called oChIEF (Lin et al., 2009). Since, in ChAT-cre mice, cre-recombinase is under the control of the ChAT promoter, only cells that normally express ChAT, the defining feature of cholinergic cells, will express the channel rhodopsin since cre-mediated recombination is required to convert the DiO construct from its antisense to its sense configuration. Expression in the cell membrane extends throughout the axonal arborization (fig. 3.1). Hence, the afferents of cholinergic cells in BLA, far removed from their cell bodies in NBM, become subject to control by light, otherwise impossible by any other stimulation method. Experiments done by others in the Role laboratory demonstrate that transfected cholinergic cell bodies in the NBM fire action potentials in response to optical stimulation, and that they can entrain with 100% fidelity up to a rate of 10 Hz (fig. 3.2).

Experiments presented here will first examine the effects of pharmacological blockade of cholinergic receptors on excitatory synaptic transmission of thalamic inputs to BLA. Since cholinergic afferents from NBM to BLA pass through the internal capsule, but not the external capsule, I questioned whether stimulation of the internal capsule to evoke EPSCs concomitantly stimulated cholinergic fibers, confounding any comparison between the properties of the two inputs. Finally, I will examine the effect of optogenetic stimulation of endogenous cholinergic afferents on thalamo-BLA excitatory synaptic transmission.

Methods

Viral delivery of optogenetic construct

Cholinergic neurons in the NBM were selectively targeted for expression of a channel rhodopsin construct using a ChAT-cre transgenic mouse line (Jackson Labs). The construct used was a double-inverted open reading frame floxed (DIO) version of channelrhodopsin2 called oChIEF. This construct was engineered using single point mutations by the Deisseroth laboratory for increased activation speed, reduced inactivation time, and reduced activation fatigue in the face of repeated stimulation (Lin et al., 2009). At post-natal day 28-30, the NBM of ChAT-Cre positive mice was stereotaxically injected with AAV serotype 9 packaged with (DIO-oChIEF-tdtomato). After allowing 3 weeks for recovery and viral expression, mice were sacrificed for experiments.

Slice Preparation

Slice preparation procedures were conducted under dark-room (red) illumination from the time of decapitation to the end of the experiment so as not to stimulate channelrhodopsin-expressing tissue with ambient room light. Coronal brain slices were prepared from C57/BL6 mice at postnatal day 42-84. Animals were intraperitoneally injected with a mixture of ketamine and xylazine (100 mg ketamine and 11 mg xylazine/kg body weight). After decapitation, the brain was rapidly dissected (60 to 90 seconds), mounted with cyanoacrylate glue, and transferred to the chamber of a vibratome (Leica VT1000S) containing an ice-cold high-sucrose solution (in mM:

sucrose 230; KCl 2.5; $MgSO_4$ 10; $CaCl_2$ 0.5; NaH_2PO_4 1.25; $NaHCO_3$ 26; glucose 10; pyruvate 1.5) bubbled with 95% O_2/5% CO_2. Coronal slices (300 µm) were made with the vibratome, then transferred to a 50/50 mix of the cutting solution and aCSF (in mM: NaCl 126; KCl 2.5; NaH_2PO_4 1.25; $NaHCO_3$ 26; $CaCl_2$ 2; $MgCl_2$ 2; glucose 10) bubbled with 95% O_2/5% CO_2 where they were allowed to equilibrate at room temperature (24-26ºC) for at least 1 hour. After this period, slices were transferred to the recording chamber and continuously superfused at a rate of 2 ml/min with aCSF bubbled with 95% O_2/5% CO_2.

Electrophysiology

BLA pyramidal neurons were visualized on an Olympus BX51WI upright microscope (Olympus Optical) equipped with differential inference contrast (DIC) optics. Patch electrodes with a resistance of 4–6 MΩ were pulled with a P-97 Brown Flaming electrode puller (Sutter Instrument). Signals were recorded with an AxoPatch 200B amplifier (Molecular Devices). The pipette solution contained (in mM: 130 K-gluconate; 2 KCl; 2 $MgCl_2$; 10 HEPES; 0.5 EGTA; 1 ATP; 0.2 GTP; QX314 5 (pH 7.3). Visually-identified pyramidal neurons were patched in the BLA and held at -60 mV. In all experiments, 50 µM bicuculine was used in the aCSF bath solution.

The criteria applied for inclusion of recorded cells in the final analysis were as follows: *1*) seal resistances maintained throughout the recording period at >1 GΩ; *2*) holding current in whole cell clamp configuration remained within 10% of the initial value and was ≤100 pA; and *3*) series resistance (R_s), measured at least once every 10 min

throughout the course of the experiment, remained stable (<20% change from initial value).

To examine the effects of optogenetic stimulation of cholinergic terminal fields on transmission at cortico–BLA and thalamo-BLA inputs, excitatory postsynaptic currents (EPSCs) were evoked by field stimulation with a 200 μm platinum/iridium concentric bipolar stimulation electrode (FHC) placed on the external capsule or internal capsule, respectively. The input of interest was stimulated at a rate of 0.1 Hz. Depending on the experiment, stimulation strength was adjusted to either "minimal stimulation", defined as the stimulus intensity required to evoke EPSCs on approximately 50% of trials, or "robust stimulation" defined as the lowest stimulus intensity required to evoke an EPSC in 100% of trials. In experiments examining the effect of AChR blockers, a cocktail of 1 μM atropine and 10 μM mecamylamine was used. Optical stimulation was delivered through the high power (40X) objective supplied by a mercury lamp with a 480nm bandpass filter (Chroma HQ480/40x). Total power of light exiting the objective was measured to be 6.6 mW. The illuminated spot size was approximately 1 mm in diameter. This yields a power density of approximately 8.4 mW/m^2. This stimulation light was controlled by an electronic shutter (Uniblitz) to deliver 8 ms pulses of light at 10 Hz for 10s in all optogenetic experiments.

Results

Bath application of cholinergic blockers (1 μM Atropine, 10 μM Mecamylamine) greatly decreased the probability of evoking an EPSC by internal capsule stimulation. (fig 3.3, 3.4). A 100 Hz tetanus administered while cholinergic antagonists were applied induced a post-tetanic potentiation, manifested as both an increase in EPSC amplitude and an increased probability of evoking an event. After about 2 minutes the P_S returned to the pre-tetanus level (fig. 3.3). In 2 cells, AChR antagonists had no effect on thalamo-BLA transmission (fig. 3.5).

To assess the role of optogenetically stimulated ACh release in the BLA on thalamo-BLA transmission, I recorded EPSCs evoked by stimulating the internal capsule at a rate of 0.1 Hz for at least 5 minutes to establish a baseline control. After this control period, I optically stimulated the area around the BLA neuron (see methods) at a frequency of 10 Hz. Following this optical stimulation, I resumed evoking EPSCs by electrically stimulating the internal capsule (fig. 3.7). This experiment was performed in 9 cells that met criteria for evaluation. In 5 of these cells optogenetic stimulation significantly reduced P_S (fig. 3.8). In 4 cells there was no effect of optogenetic stimulation. Finally, I conducted this experiment in 1 cell under bath application of 1 μM Atropine. The effect of optogenetic stimulation was robust depression (fig. 3.8)

Discussion

In 3 of 5 cells tested, blockade of AChRs caused a significant reduction in the probability of evoking an EPSCs by internal capsule stimulation. This suggests that endogenous cholinergic activity contributes to synaptic transmission, even in the slice preparation where cholinergic afferents are severed from their cell bodies. Nicotine has long been known to increase activity in various brain areas. Moreover, previous findings in our laboratory and by others have implicated presynaptic nicotinic AChRs in facilitating synaptic transmission by increasing presynaptic calcium levels. It's probable that there is a baseline level of activation of these receptors for synaptic transmission to occur. The brief facilitation of transmission after tetanic stimulation likely increased presynaptic calcium levels temporarily, briefly allowing transmission to occur normally. However, that I recorded from cells with intact synaptic transmission despite the presence of AChR antagonists implies that these synapses vary in their dependence on cholinergic activity to function, perhaps with a subset of synapses functioning without ACh signaling all together.

Experiments in which I optogenetically stimulated cholinergic fibers in BLA reveal that thalamic connections to BLA pyramidal neurons depress in response to increased ACh release. While this may seem surprising, given that AChR blockade also induced synaptic depression, it is important to consider the mixed composition of AChRs, both pre- and post-synaptically, and that effects of ACh signaling are usually highly dose-dependent. Likely, some level of nicotinic AChR activation is necessary to facilitate

release under normal conditions in the slice preparation. When AChR activation is increased by driving excess ACh release, it may activate pre- or postsynaptic muscarinic AChRs, many of which have inhibitory effects on synaptic release (Sugita, Uchimura, Jiang, & North, 1991; Washburn & Moises, 1992). It is also possible that excess ACh desensitizes nAChRs, although given the transient time-course of ACh stimulation and the long lasting effects of the depression, this seems a less likely explanation. Further experiments using selective pharmacological blockers of nicotinic and muscarinic receptor subtypes would be necessary to dissect the role of each receptor class.

The predominant effect of optogenetic stimulation of cholinergic terminal fields on thalamo-BLA transmission was a reduction in the P_s, suggesting a presynaptic mechanism underlying the plasticity in most of these synapses. In some experiments, however, changes in EPSC amplitude were also observed, suggesting that post-synaptic mechanisms may contribute to cholinergic-input induced depression at some thalamo-BLA synapses. The results of similar experiments examining the effects of cholinergic modulation of the cortico-BLA pathway show consistent potentiation, both in terms of an increase in P_s and EPSC amplitude (Fig. 3.9) (Jiang et al., 2014 (in prep)). Akin to the results of experiments in Chapter 2, the thalamo- and cortico-BLA pathways respond in opposite ways to optogenetic stimulation of cholinergic terminals.

The experiments in this chapter examined aspects of the role of cholinergic modulation at cortico- and thalamo-BLA synapses and allowed me to draw several

conclusions. First, there is some endogenous cholinergic activity in the slice preparation evidenced by the dramatic effect of cholinergic receptor blockade on thalamo-BLA transmission. This is consistent with findings by others that ACh signaling occurs at a baseline level under normal conditions *in vivo* and that baseline BLA firing is significantly depressed following infusion of cholinergic receptor antagonists into the BLA (Jiang et al., 2014 (in prep)) Additional studies also indicate that optogenetic stimulation of ACh release from NBM can be both up- and down-regulated depending on an animal's arousal state.

Second, the effects of ACh on thalamo-BLA transmission are described by an "inverted U" curve in that too little ACh signaling (*i.e.* in the presence of cholinergic blockers) depresses synaptic function, while overdriving cholinergic release (optogenetically stimulated ACh fibers) also depresses synaptic transmission.

Finally, thalamo- and cortico-BLA transmission are very different in the way ACh modulates transmission. In the following chapter I will present experiments demonstrating the effects of optogenetic stimulation *in vivo* on a behavioral task to examine how cholinergic modulation of signals in the BLA contributes to generating an adaptive behavioral response.

Fig 3.1 - Labeling of cholinergic fibers in ChAT-GFP mice by oChIEF-tdtomato optogenetic construct

A

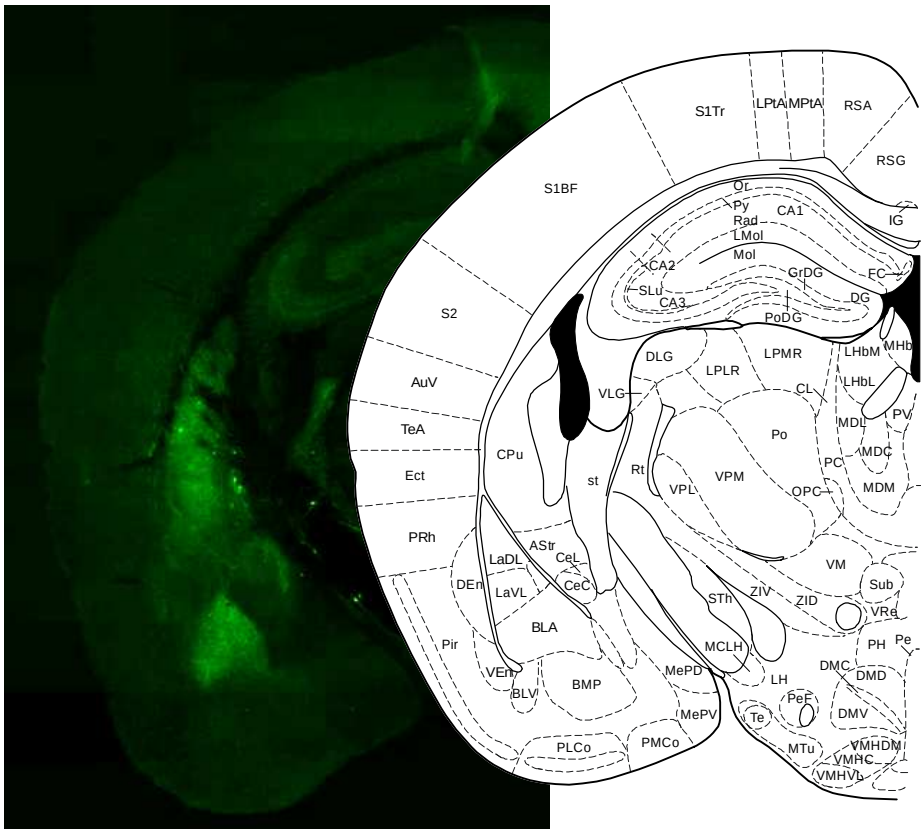

B

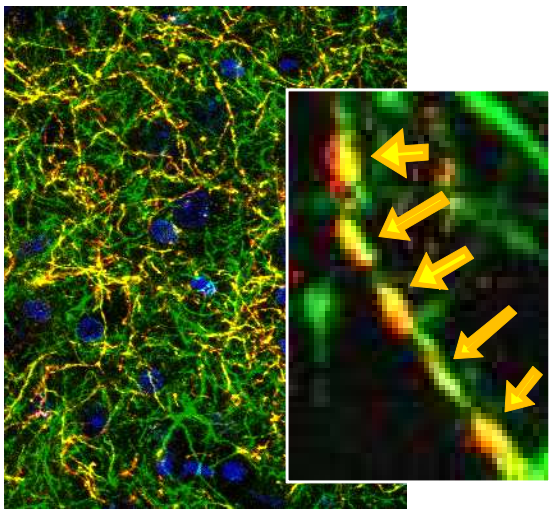

Figure 3.1 - ChAT-GFP coronal section and opto labeling of fibers in BLA. (A) ChAT-GFP slice and Mouse Brain Atlas diagram (B) High power view of GFP and mCherry channels showing overlapped labeling of ACh afferents

Fig 3.2 - Action potentials evoked by optical stimulation of oChIEF-labeled cell bodies in NBM

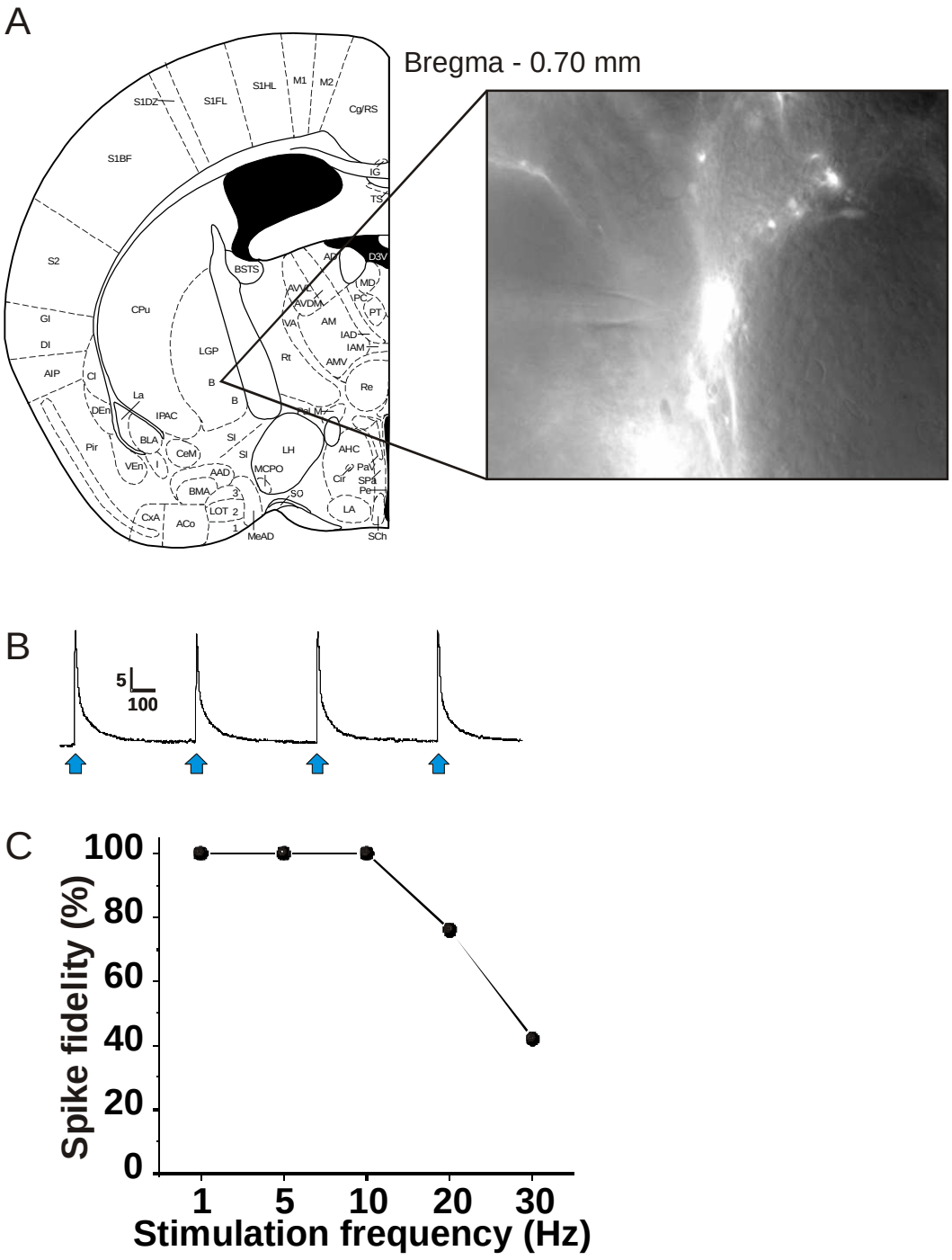

Figure 3.2 - Action potentials evoked by optical stimulation of oChIEF-labeled cell bodies in NBM. (A) Traces showing evoked APs in response to pulses of 473 nm light (blue arrows). (B) Plot of spike fidelity vs. stimulation frequency. Cells are able to fire with 100% fidelity up to 10 Hz. Cholinergic terminal fields in BLA were stimulated at 10 Hz in all experiments in this chapter.

Fig 3.3 - Cholinergic receptor antagonists impair thalamo-BLA transmission

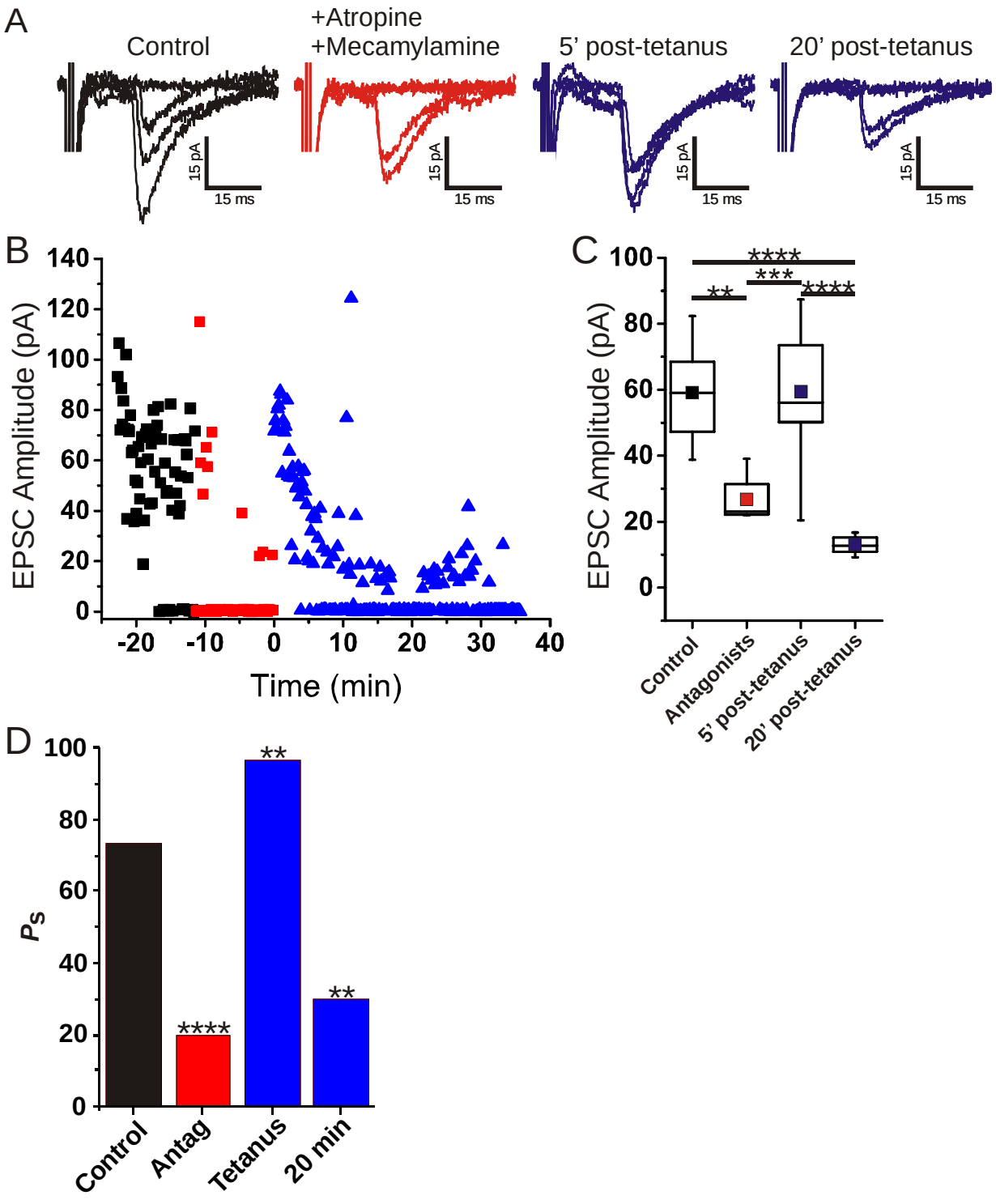

Figure 3.3 - Cholinergic receptor antagonists impair thalamo-BLA transmission. (A) Example traces before and after AChR antagonists, 5 minutes and 20 minutes after 100 Hz tetanus (B) Timeline of experiment showing evoked EPSC amplitude before (black) and after (red) AChR antagonists, and after 100 Hz tetanic stimulation (blue). (C) EPSC amplitude of events, not including failures, at 5 minutes before antagonists were applied, 5 minutes before 100 Hz tetanus, and 20 minutes after 100 Hz tetanus, in 5 minute bins. Bins were compared using one-way ANOVA ($F(3,57) = 27.57$, $p < 0.0001$) and Tukey *post-hoc* comparison (**$p < 0.01$, ***$p < 0.001$, ****$p < 0.0001$). (D) Probability of successfully evoking an EPSC (P_s) at 5 minutes before antagonists were applied, 5 minutes before 100 Hz tetanus, and 20 minutes after 100 Hz tetanus, in 5 minute bins. Bins were compared pairwise to control, 5 min pre-tetanus (+antagonists): $\chi^2(1, N = 60) = 19.82$ (****$p < 0.0001$), washout-5 min: $\chi^2(1, N = 60) = 7.68$ (**$p < 0.01$), washout-20 min: $\chi^2(1, N = 60) = 9.60$ (**$p < 0.01$). Comparison of 5 min post-tetanus to 5 minutes pre-tetanus: $\chi^2(1, N = 60) = 42.09$ (****$p < 0.0001$).

Fig 3.4 - Cholinergic receptor antagonists impair thalamo-BLA transmission - collected examples

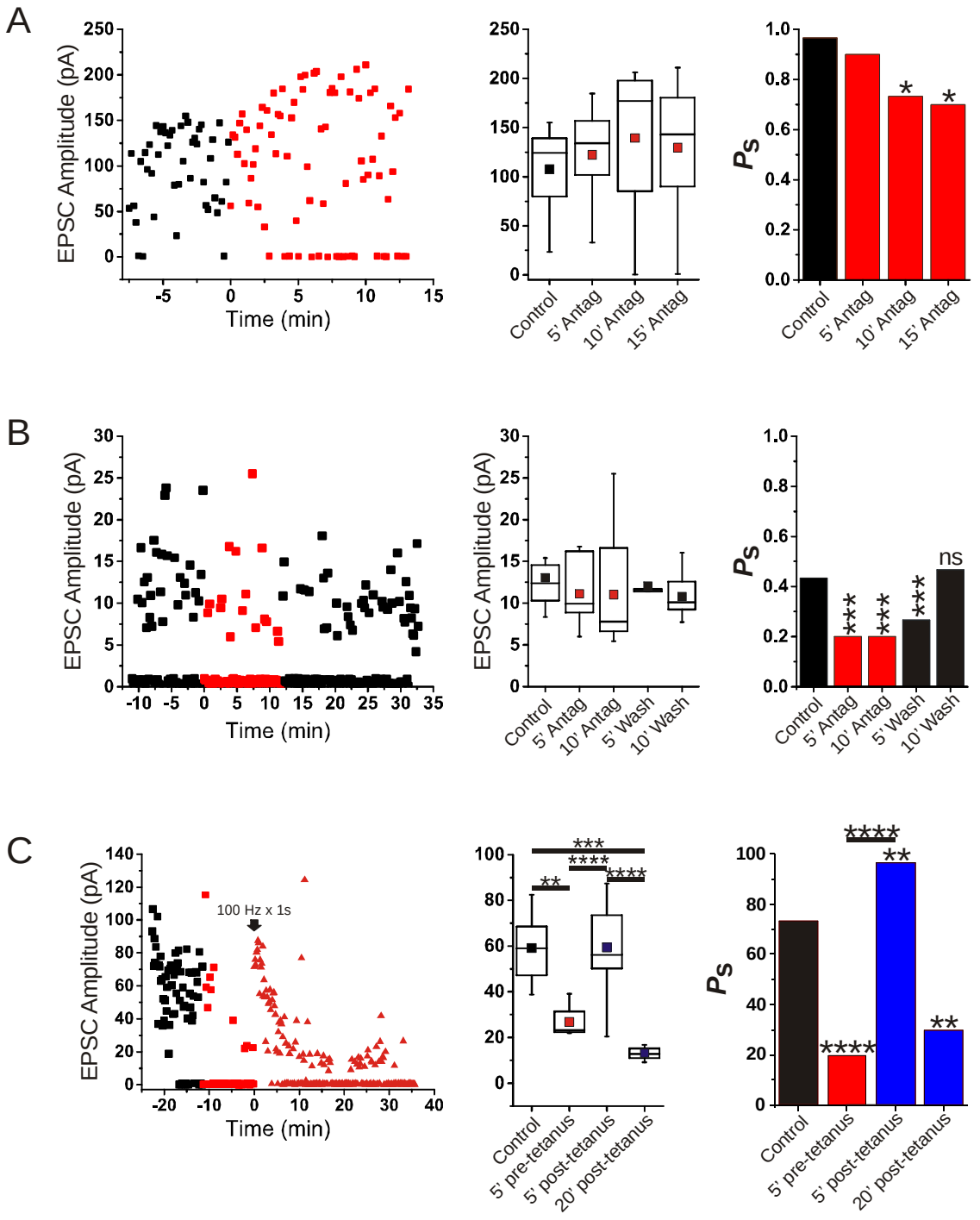

Figure 3.4 - Cholinergic receptor antagonists impair thalamo-BLA transmission - collected examples. (A) Left - Amplitude of EPSCs evoked from electrical stimulation of the internal capsule. Center - EPSC amplitude was binned in 5-minute bins. Comparison by one-way ANOVA found no significant difference ($F(3,37) = 2.07$, $p = 0.11$). Right - *P*s was calculated as number of failures divided by total measurable events in 5-minute bins. Bins were compared pairwise to control, antagonists-5 min: $\chi^2(1, N = 60) = 1.07$ ($p = 0.30$), antagonists-10 min: $\chi^2(1, N = 60) = 6.41$(*$p = 0.014$), antagonists-15 min: $\chi^2(1, N = 60) = 4.04$ (*$p = 0.04$). (B) Left - Amplitude of EPSCs evoked from electrical stimulation of the internal capsule. Center - EPSC amplitude was binned in 5-minute bins and analyzed by one-way ANOVA finding no significant difference ($F(4,37) = 0.16$, $p = 0.95$). Right - *P*s was calculated as number of failures divided by total measurable events in 5-minute bins. Bins were compared pairwise to control, antagonists-5 min: $\chi^2(1, N = 134) = 15.12$(***$p < 0.001$), antagonists-10 min: $\chi^2(1, N = 60) = 15.12$(***$p < 0.001$), antagonists-5 min: $\chi^2(1, N = 134) = 12.75$ (***$p < 0.001$), washout-20 min: $\chi^2(1, N = 60) = 12.75$ ($p = 0.12$). (C) See fig. 3.4 B, C, D.

Fig 3.5 - AChR antagonists can have no effect on Thalamo-BLA transmission

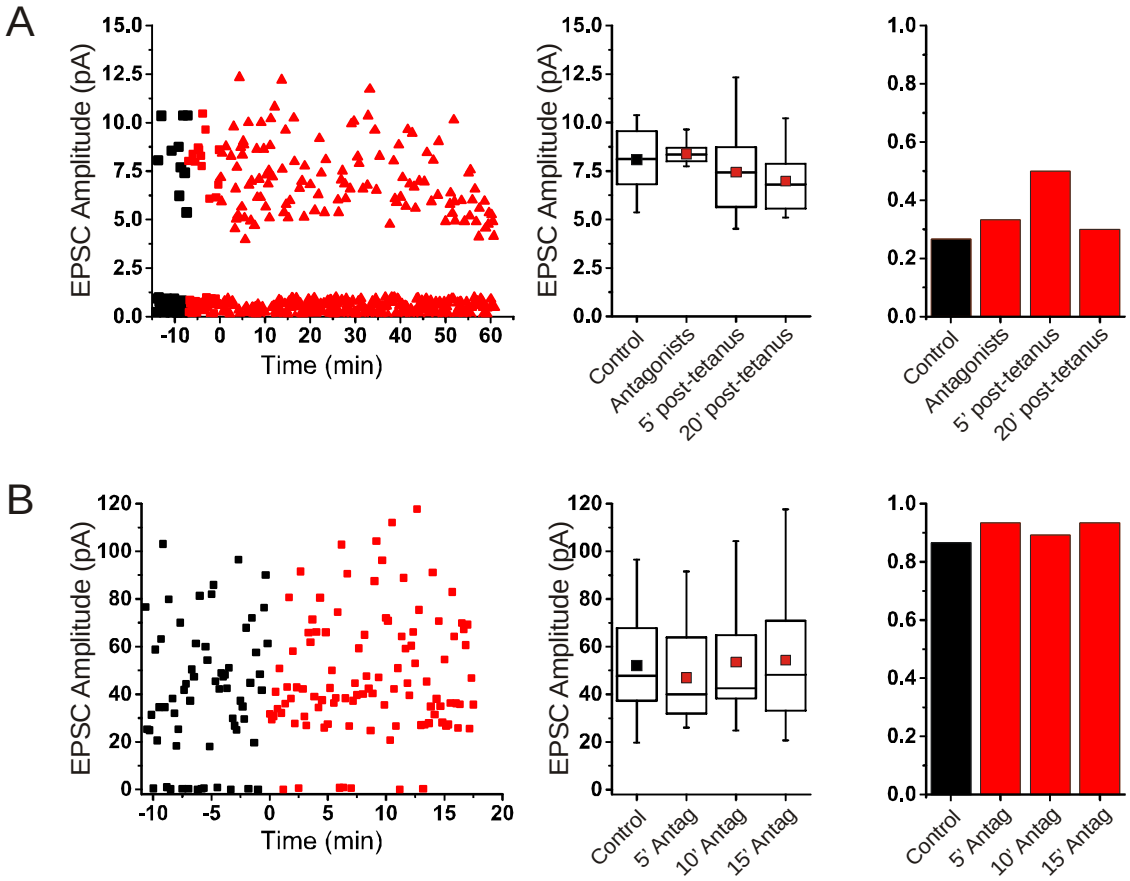

Figure 3.5 - Cholinergic receptor blockade can have no effect on thalamo-BLA transmission. (A) EPSCs were evoked by electrical stimulation of the internal capsule at a rate of 0.1 Hz for 5 minutes to establish control period before bath application of 0.2 µM atropine and 1 µM mecamylamine. After recording EPSCs for 5 more minutes, a 100 Hz, 1 s duration tetanus was delivered via the same stimulation electrode, then stimulation at 0.1 Hz was resumed. Left - peak EPSC amplitude v. time (black, control; red, antagonists, triangle, post-tetanus) Center - Peak EPSC amplitudes were binned in 5-minute bins. Comparison by one-way ANOVA found no significant difference ($F(3,36) = 1.18$, $p = 0.33$). Right - *P*s was calculated as number of failures divided by total measurable events in 5-minute bins. Bins were compared pairwise to control, 5 minutes pre-tetanus (+antagonists): $\chi^2(1, N = 60) = 0.32$ ($p = 0.57$), 5 minutes post-tetanus: $\chi^2(1, N = 60) = 2.58$ ($p = 0.11$), 20 min post-tetanus: $\chi^2(1, N = 60) = 0.00$ ($p = 1.00$). (B) Left - Peak amplitude of EPSCs evoked from electrical stimulation of the internal capsule at a rate of 0.1 Hz. Center - EPSC amplitude was binned in 5-minute bins and analyzed by one-way ANOVA finding no significant difference ($F(3,103) = 0.57$, $p = 0.63$). Right - *P*s was calculated as number of failures divided by total measurable events in 5-minute bins.

Fig 3.6 - Optogenetic stimulation of ACh release induces depression at thalamo-BLA synapses

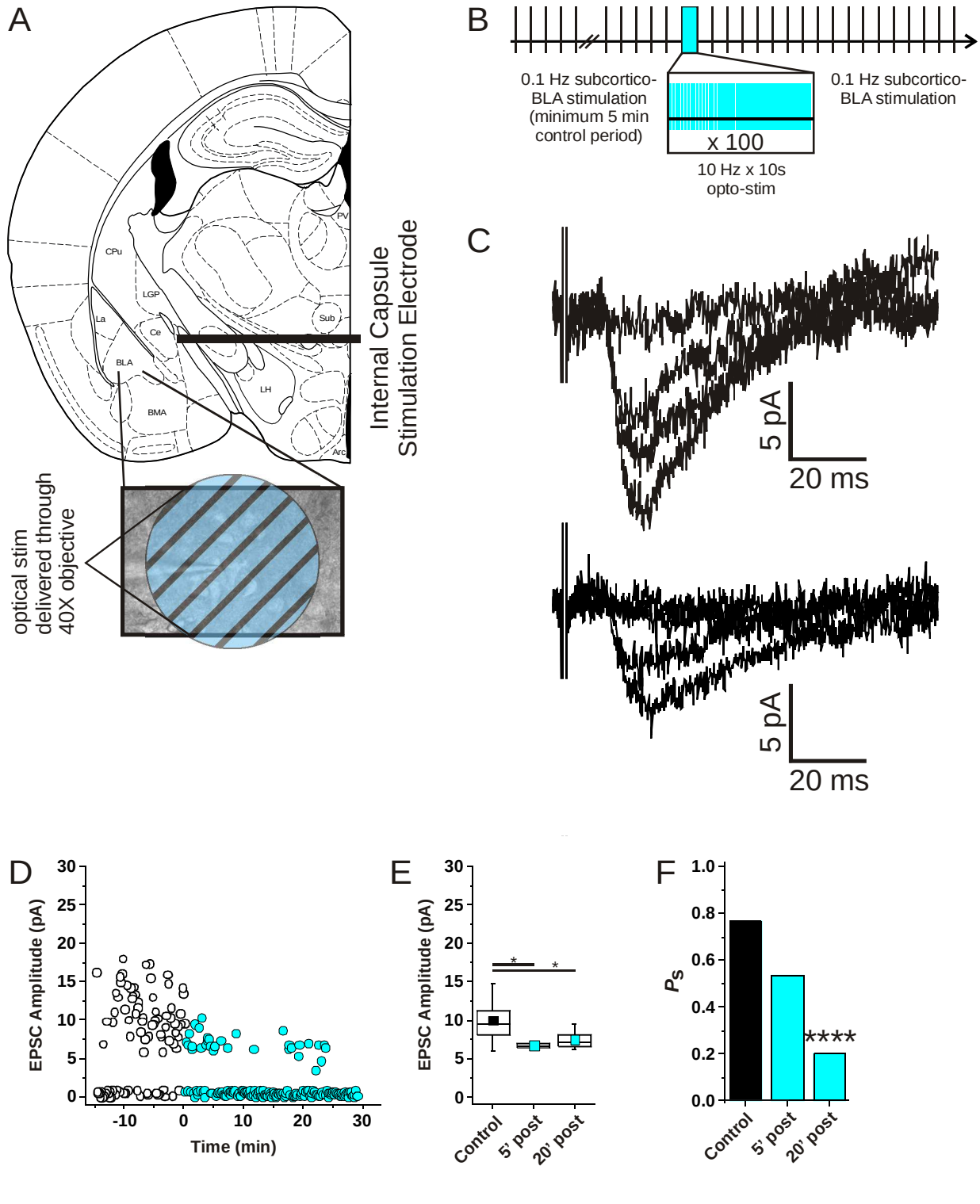

Figure 3.6 - Optogenetic stimulation of cholinergic afferents in BLA induces depression in thalamo-BLA synapses. EPSCs were evoked in BLA pyramidal neurons at a rate of 0.1 Hz by electrical stimulation of the internal capsule for a minimum of 5 minutes to establish a control period before administering a 10 s, 10 Hz train of optical stimulation. Electrical stimulation was immediately resumed at a rate of 0.1 Hz. For A-E, left plots show peak EPSC amplitude plotted over time (control, open circles; post-optical stimulation, blue circles), with failures represented as points near 0 pA. Center shows data binned from 5 minutes pre-stimulation period, 0-5 minutes and 15-20 minutes post-stimulation. Data were compared using one-way ANOVA with Tukey *post-hoc* comparison of means, except in E, where data was only available for 2 bins, student's t-test was used. Right panels show P_s, calculated as number of evoked EPSCs divided by total measurable events, binned as in center panels. Post-stimulation bins were compared pairwise to control using Pearson's χ^2. Statistical results: (A) EPSC amplitude, a significant difference was found by ANOVA ($F(2, 42) = 9.55$, $p < 0.0001$) Tukey (***p.< 0.001). $P_{s;}$ 5 minutes post-stimulus, difference was not significant $\chi^2(1, N = 60) = 3.59$ ($p = 0.06$), 20 minutes post-stimulus, difference was significant $\chi^2(1, N = 60) = 19.29$ ($p < 0.0001$). (B) EPSC amplitude, a significant difference was found by ANOVA ($F(2, 67) = 44.95$, $p < 0.001$), Tukey (*$p < 0.05$, ****$p < .0001$) (. $P_{s;}$ 5 minutes post-stimulus, difference was not significant $\chi^2(1, N = 60) = 0.80$ ($p = 0.37$), 20 minutes post-stimulus, difference was not significant $\chi^2(1, N = 60) = 1.49$ ($p = 0.22$). (C) EPSC amplitude, a significant difference was found by ANOVA ($F(2, 52) = 0.18$, $p = 0.83$). $P_{s;}$ 5 minutes post-stimulus, difference was not significant $\chi^2(1, N = 58) = 2.90$ ($p = 0.09$),

20 minutes post-stimulus, difference was significant $\chi^2(1, N = 44) = 15.73$ ($p < 0.0001$). (D) EPSC amplitude, a significant difference was found between post-stimulation periods by ANOVA ($F(2, 72) = 5.36$, $p < 0.01$) Tukey (**$p < 0.01$). P_s, 5 minutes post-stimulus, difference was not significant $\chi^2(1, N = 60) = 3.16$ ($p = 0.08$), 20 minutes post-stimulus, difference was significant $\chi^2(1, N = 60) =$ (***$p < 0.001$). (E) EPSC amplitude, no significant difference was found by student's t-test $t(22) = 1.17$ ($p = 0.25$). P_s, 5 minutes post-stimulus, difference was significant $\chi^2(1, N = 60) = 10.00$ ($p < .01$).

Fig 3.7 - Optogenetic stimulation of ACh release induces synaptic depression at thalamo-BLA synapses

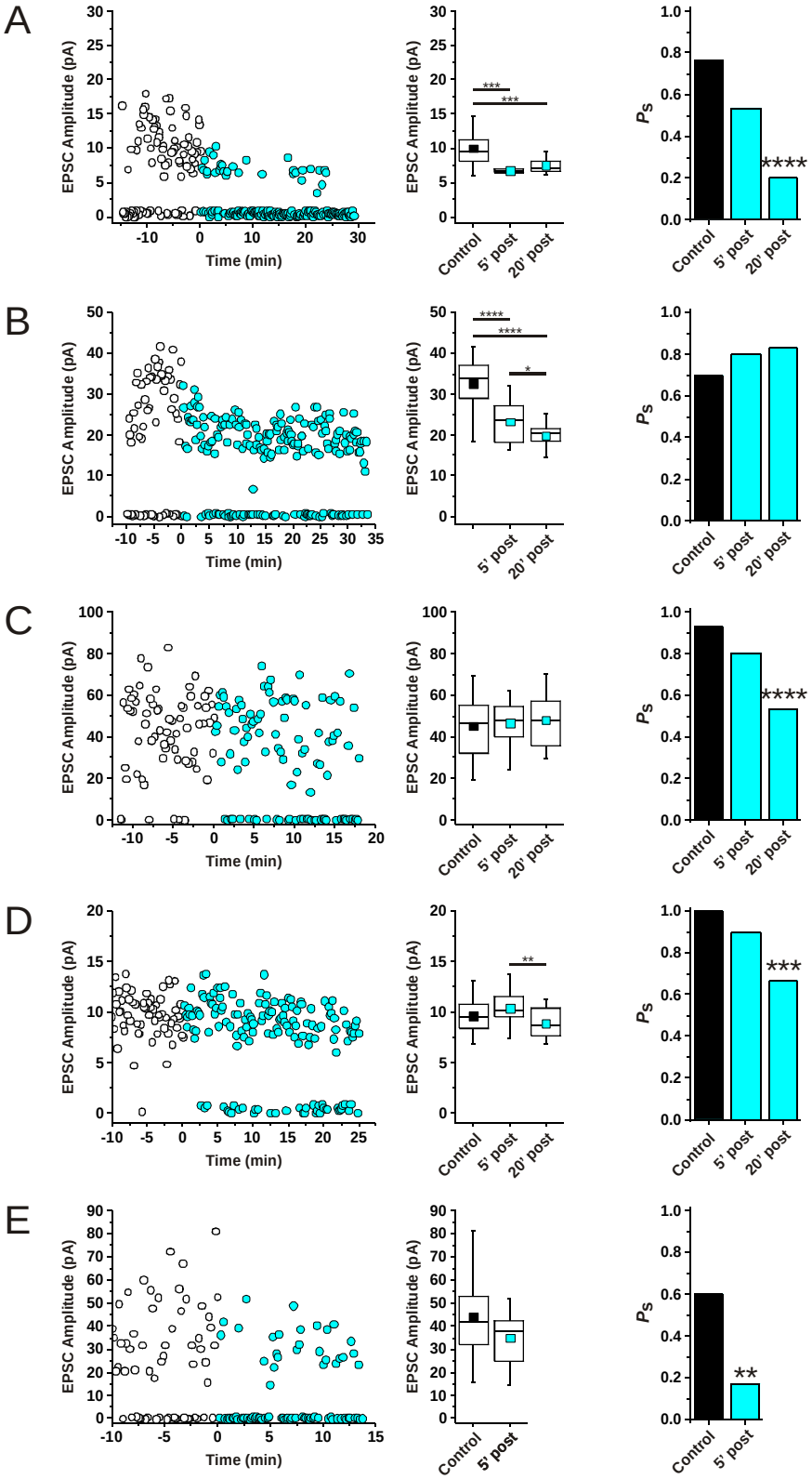

Figure 3.7 - Timelines of thalamo-BLA evoked EPSCs and failure rate change from 5 cells showing synaptic depression.

Fig 3.8 - Thalamo-BLA synaptic depression induced by optogenetic stimulation of Ach release is not blocked by Atropine

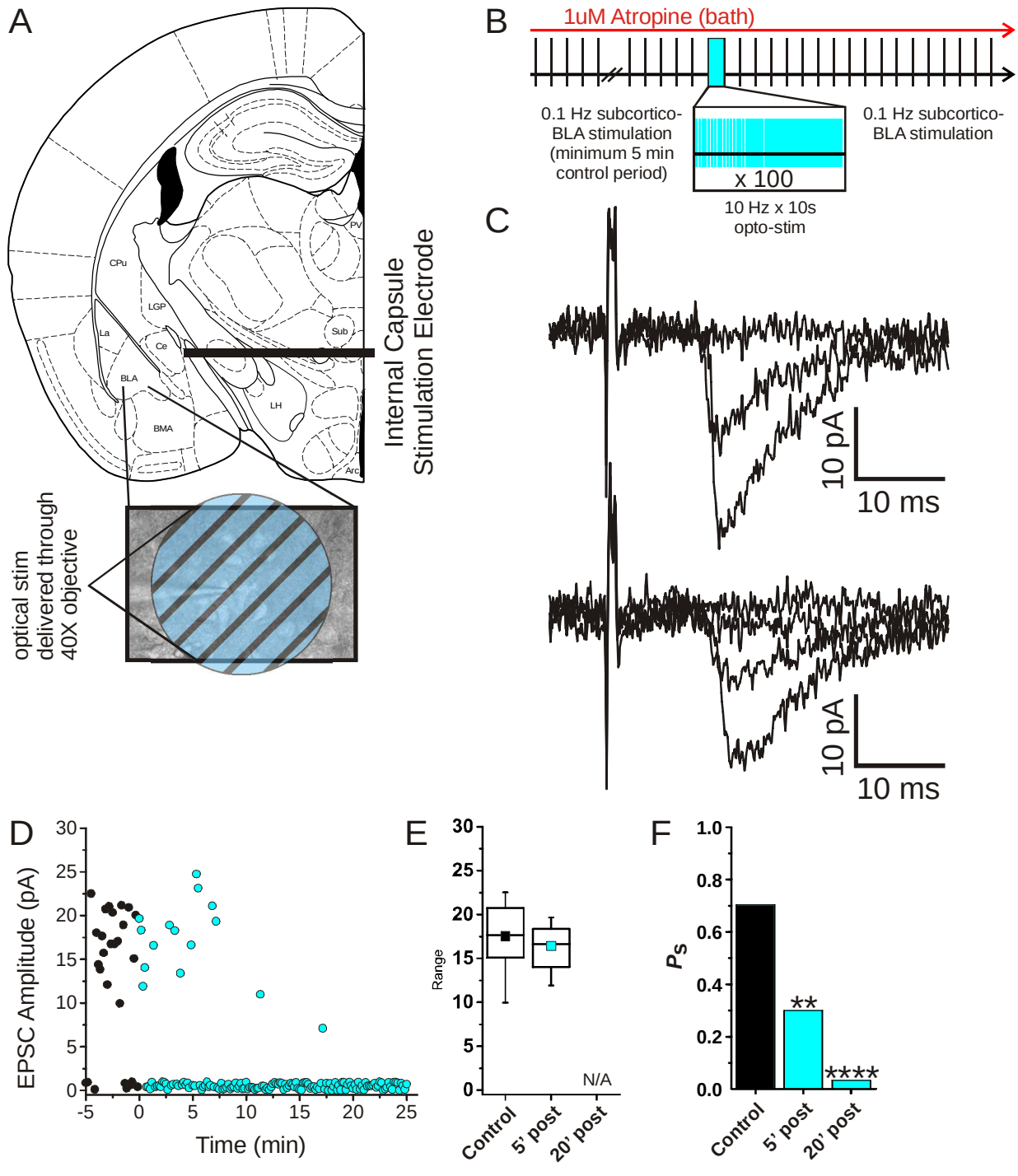

Figure 3.8 - LTD of thalamo-BLA synapses induced by optogenetic stimulation of cholinergic terminal fields is not blocked by atropine. (A) With 0.2 µM in the ACSF bath solution, the internal capsule was stimulated a rate of 0.1 Hz at minimal stimulus intensity. EPSCs or failures were recorded from a patch-clamped BLA pyramidal neuron. After establishing a control period, the area surrounding the patched cell was stimulated with a 1 s duration, 10Hz train of 460-500 nm light delivered through the high power objective. Electrical stimulation was immediately resumed as before. (B) Timeline illustrating experiment protocol. (C) Example traces before (top) and after (bottom) optical stimulation. (D) EPSC peak amplitude, or failures, plotted over time. Failures are represented as points near 0 pA. (E) EPSCs peak amplitudes from control and 5 minutes post-stimulus, were binned and means were compared using student's *t*-test, finding no significant difference ($t(26) = 0.86$, $p = 0.40$). A 20-minute bin was not used as there were 0 events between 15 and 20 minutes. P_s, measured as number of failures divided by total measurable events, were binned in 5 minute periods for control, 5 minutes post-stimulus and 20 minutes post-stimulus. Bins were compared pair-wise to control using Pearson's χ^2 statistic. 5 minutes post-stimulus, difference was significant $\chi^2(1, N = 57) = 9.27$ (**$p < 0.01$); 20 minutes post-stimulus, difference was significant $\chi^2(1, N = 57) = 31.67$ (****$p < 0.0001$).

Fig 3.9 - Optogenetic stimulation of endogenous acetylcholine induces potentiation at cortico-BLA syanpses.

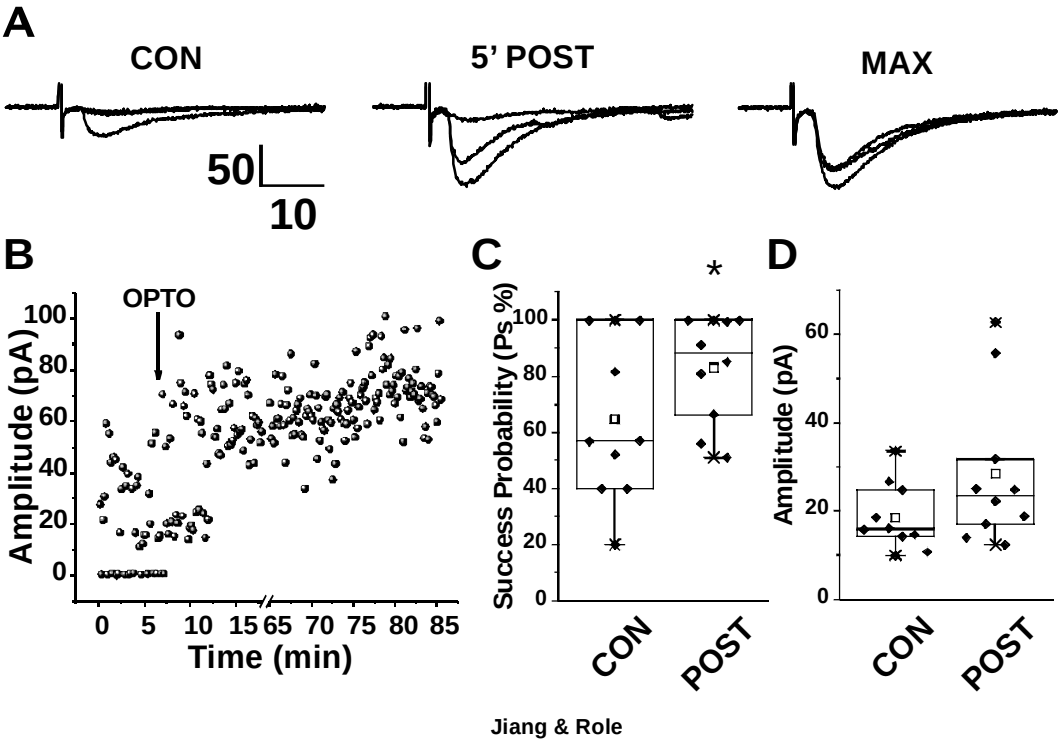

Figure 3.9 - Optogenetic stimulation of cholinergic afferents in BLA induces potentiation in cortico-BLA synapses. (A) Example traces of EPSCs evoked by stimulation of the external capsule. (B) EPSC peak amplitude plotted over time. A 10 Hz, 10 s train of optical stimulation was delivered where indicated. (C) Box plots of probability of successfully evoking an EPSC before (CON) and after (POST) optical stimulation in 10 cells examined. (D) Box plots of peak evoked EPSC amplitude before (CON) and after (POST) optical stimulation in 10 cells examined. Data collected and analyzed by Li Jiang.

Chapter 4 - Optogenetic manipulation of endogenous acetylcholine activity in the basolateral amygdala bidirectionally modulates learned fear

Introduction

In the previous chapter I presented data consistent with the idea that cholinergic signaling in the BLA is input-specific. Here, I ask whether this modulation contributes to the amygdala's well known role in effecting adaptive behavioral responses. To this end, I will assess the effects of optogenetic stimulation and inhibition of ACh release in the BLA during a cued fear conditioning paradigm. The amygdala is especially sensitive to fear-related stimuli. It is necessary for the acquisition, storage, and retrieval of emotionally salient memories, particularly fearful ones.

Links between cholinergic signaling, the amygdala, and anxiety disorders are well-documented, yet complex and poorly understood. The amygdala, along with the ventro-medial prefrontal cortex (vmPFC) and hippocampus, are the most notable brain areas involved in post-traumatic stress disorder (PTSD) . In patients with PTSD, vmPFC activity is decreased while amygdala activity is increased, especially during symptom provocation. Meanwhile, cholinergic activity, and acetylcholine-related gene expression are increased in the disorder. Additionally, increasing cholinergic activity with anti-acetylcholinesterase (the enzyme that rapidly breaks down acetylcholine after it is released) drugs induces a psychosis reminiscent of PTSD, and smokers are more likely than non-smokers to develop PTSD after a traumatic event. Finally, adding to the

complex relationship between this disorder and neurotransmitter is the fact that while PTSD patient often turn to smoking (whether or not they were smokers before developing PTSD) to mitigate symptoms acutely, smoking exacerbates symptoms in the long-term. Thus, investigation of the cholinergic circuitry, particularly in the BLA, will hopefully shed light on the pathogenesis and treatment possibilities for this disorder.

Classical fear conditioning and subsequent fear extinction learning, often used in animals as a model for PTSD (Quirk & Milad, 2010), is a behavioral paradigm in which an animal learns to associate a typically innocuous stimulus, such as a audible tone, called the conditioned stimulus (CS) with an aversive stimulus, such a foot shock, called the unconditioned stimulus (US). When these stimuli are paired in time such that the CS precedes the US, the animal will learn to express fear, *i.e*. the "fight or flight" response, when the CS is later presented alone. This type of learning is especially potent, in many cases requiring only a single trial, and especially robust, persisting for months or years after training.

Once the memory of the fearful association is formed, the fear response to the US can be diminished by extinction training. During extinction, the CS (tone) is presented repeatedly in the absence of the US (foot shock). Over the course of many trials (tens to hundreds or more), the animal learns to inhibit its fear response to the CS. Unlike the initial conditioning, extinction learning is slow and often does not persist over time. If extinction training is not regularly performed, then the fear memory may spontaneously recover. Extinction is not an erasure of the fearful association, but rather

a learned inhibition of it, mediated primarily by the prefrontal cortical inhibition of the amygdala.

In PTSD, fearful associations are formed between environmental and discrete cues and the physical or emotional pain of the event, as in classical fear conditioning. What distinguishes PTSD from normal learning, however, is that the fear and anxiety may arise *in the absence of cues*, or in response to generalized cues, and that the learned fear is highly resistant to extinction learning. Nevertheless, extinction training is currently the most widely utilized treatment for PTSD. Whether or not the actual incidence of PTSD is increasing or the escalation in the number of cases of PTSD is simply due to a more widely accepted recognition of the disorder, it is an ever increasing problem and more effective interventions are desperately needed.

Neuromodulators such as ACh play a critical role at the synaptic level to tune the synaptic plasticity underlying integration of sensory signals and alter the output of the amygdala. During fear conditioning, some cells respond to the presentation of the cue, some respond to the aversive stimulus, and some respond to both (Barot et al., 2009). It is the convergence and subsequent synaptic plasticity in these cells that is thought to be a key event underlying associative learning. Neuromodulators, such as ACh, act on the synapses where this convergent integration occurs. Previous pharmacological studies have implicated cholinergic signaling as a key regulator of aversive conditioning. However, most of these studies have focused on extinction learning, and pharmacology in general cannot examine the temporally precise window of the pairing between the

conditioned and unconditioned stimuli. In these experiments I will use optogenetic control of cholinergic transmission in the BLA to assess how ACh in the BLA contributes to the formation of fearful memories, specifically at the time the tone and shock pairing occurs. Based on my results in patch-clamp experiments, and findings from others, I believe that the amount of ACh present at synapses in the BLA will have a profound effect on the integration of signals arising from the CS and US, and hence alter the behavioral output of the amygdala.

Methods

Viral Constructs

For optogenetic excitation of cholinergic afferents, an EF1a-DIO-oChIEF-tdtomato construct (provided by Dr. Shaoyu Ge, Stony Brook University, produced by the UNC Vector Core), packaged in AAV serotype 9 was used.

For optogenetic inhibition of cholinergic afferents, an EF1a-DIO-eNpHR3.0-EYFP construct (Deisseroth, produced by the UNC Vector Core), packaged in AAV serotype 9 was used.

Viral delivery and fiber-optic cannula implantation

Adult ChAT-Cre (Jackson Labs) mice, matched for age (+/- 2 days) underwent viral injection and fiber optic implantation surgery at post-natal day 42-48. Mice were anesthetized with isoflurane (4% induction, 2% maintenance) and placed in a stereotaxic apparatus (Kopf Instruments). Body temperature was monitored using a rectal thermometer and heat pad. Ophthalmic gel was applied to the eyes to prevent drying. After the scalp was shaved and prepped with Betadine solution, an incision was made, exposing the skull. After removing the meninges membrane, 3% hydrogen peroxide solution (Sigma) was applied to sterilize the site and visualize the suture lines of the skull. Bregma and lambda were leveled. The skull was then prepped with etchant and activator gel for acrylic dental cement (Metabond). Using the stereotaxic arm, holes were then drilled bilaterally for viral delivery to NBM, and fiber optic cannula

implantation. Again using a stereotaxic arm, 0.5 µl of virus was injected to each site using a 26 gauge, 1 µl syringe (Hamilton) at a rate of 0.05 µl per 20 seconds, over a period of 3 minutes. Two minutes were then allowed for virus to diffuse before retracting the syringe. After viral injection, fiber optic cannulas (Doric Lenses) were positioned at their target coordinate with a stereotaxic arm, and dental cement (Metabond) was mixed and applied to adhere the cannula to the skull. After allowing 5 minutes for the cement to set up, the wound was closed using Vetbond tissue adhesive. Mice were injected with 0.1 mg/kg Ketorolac for analgesia and returned to their home cage. Mice were monitored for signs of distress for 2 subsequent days and additional analgesia was administered if deemed necessary. Mice typically showed no signs of distress within hours following surgery.

Behavior

After allowing 2 weeks for recovery, mice were handled daily for 5 days. Handling included being connected to a dummy fiber-optic connected to a rotary joint and allowed to freely explore a housing cage (not the behavioral chamber). After handling, mice were connected bilaterally via their fiber-optic implants to 2 100um fiber-optics, connected to a 2-channel optical rotary joint, connected to a fiber-coupled laser, which was adjusted to produce 10-12mW total power at each fiber tip, and were place in a fear conditioning chamber (Coulbourn Instruments). In mice transfected with oChIEF, a 473nm laser was used, in mice transfected with Halo3.0, a 590nm laser was used. After being allowed to freely explore the chamber, a 30s, 80dB, 5kHz tone was played, which co-terminated with a 2-second foot shock (oChIEF mice, 0.8mA; Halo mice, 0.5mA).

Two behavioral groups, counterbalanced by littermates, were comprised of a control group, which received no laser stimulation, and an opto-stimulated group which received laser light stimulation. In oChIEF mice, this stimulation consisted of 5 seconds of laser-light, pulsed at 20Hz with a 5ms pulse-width, co-terminating with the tone/shock pairing. In oChIEF mice, this pairing was repeated 3 times, with 1.5 minutes between the end of the pairing and the onset of the next tone/shock/laser pairing. In Halo mice, the laser-light stimulation was not pulsed, but steady on, and began at the onset of the tone, persisted for 2.5 minutes, and terminated at the end of the experiment protocol. All mice were allowed 2 minutes to freely explore the chamber after the termination of the final tone/shock pairing, then removed to their home cage. Chambers were thoroughly cleaned with 70% ethanol, and chamber floors were cleaned with 70% ethanol and rinsed with water and dried before each trial.

On the following day, extinction training was administered. The extinction paradigm was the same for all mice, in all experiments. For extinction training, the contextual cues of the chambers were altered, including changing the floors from thick metal bars to a finer metal grid, broad black stripes were added to the sides of the chambers, and a mild vinegar-based cleaning solution (7th Generation, Fresh Scent) was used instead of ethanol. Mice were placed in the chambers (not connected to optical fibers) and allowed 2 minutes to freely explore the chamber. After 2 minutes, a series of 10 tones, identical to the tone used on the training day, were played over 17 minutes in a pseudo-random order with a minimum of 30s and maximum of 2 minutes between tones. This order was shuffled on each extinction day. After the series of 10

tones, mice were allowed 2 minutes to freely explore before being removed to their homecages. Cages were thoroughly cleaned with cleaning solution and chamber floors were cleaned with cleaning solution, rinsed with water, and dried before each trial.

Freezing, defined as no movement except for breathing for a bout of at least 1 second, was measured using an automated video-based system (Actimetrics FreezeFrame). Experiments were binned in 30s intervals. Freezing on extinction days was measured during the first tone only. The automated video analysis was cross-checked visually and in some cases on the training days, artifacts due to the optical fibers in front of the camera lens were manually corrected for.

Statistics

For training days, freezing data was binned in 30 second increments. In oChIEF mice, a two-way ANOVA was used to compare differences in freezing between groups and across time. In halo mice, a two-way ANOVA was used to compare differences in freezing between groups and across time bins before (opto light off) the tone/shock pairing, and after (opto light on) the tone/shock pairing.

For extinction days in both oChIEF and Halo experiments, mixed-model two-way ANOVA was used with Sidak *post-hoc* multiple comparisons.

Results

On training days, when the labeled cholinergic fibers in the BLA were depolarized concurrently with tone/shock pairing, freezing in both groups increased over time ($F(17, 594) = 5.54$, $p < 0.0001$). There was no difference in the extent of freezing between the control and the optogenetically stimulated groups ($F(1, 594) = 0.56$, $p = 0.45$) over the course of the training protocol (figure 4.2 A). In contrast, optogenetic inhibition during training acutely reduced freezing to nearly 0% of the time (fig. 4.3 A). This difference was highly significant between groups ($F(1,120) = 56.38$, $p < 0.0001$).

On the first day of extinction training, mice that received optogenetic stimulation of cholinergic afferents to BLA and controls froze approximately 60% of the time during the first tone presentation (fig 4.2 B). Over the course of 8 days of extinction training, the ACh opto-stimulated group did not demonstrate extinction, assessed as a significant reduction in the amount of time spent freezing to the cue, until day 6. This is in sharp contrast the profile of extinction learning displayed by the control: controls achieved a significantly lower level of freezing from pre extinction levels by day 4. The difference between groups was significant as compared by mixed-model two-way ANOVA ($F(1, 245) = 28.16$, $p < 0.0001$. The difference on day 4 was significant as compared by Sidak *post-hoc* multiple comparison test ($t(245) = 3.704$, $p < 0.001$).

Mice that received optogenetic inhibition of cholinergic afferents to BLA during training froze approximately 25% of the time during the first presentation of the cue on

the first day, decreasing to approximately 15% by day 3. Controls froze approximately 40% of time during the first cue presentation on day 1, decreasing to approximately 25% by day 3. The difference between groups was significant as compared by mixed-model two-way ANOVA ($F(1, 72) = 5.57$, $p = 0.02$).

Post-hoc histological verification was used to confirm cannula placements and virus expression in the BLA (fig. 4.4). Mice in which the cannula was not dorso-ventrally aligned with, and within 0.5 mm from the BLA in both hemispheres were excluded from analysis. Mice with no visible virus expression in either BLA were excluded from analysis.

Discussion

In these experiments I successfully transfected mice expressing cre-recombinase under the ChAT promoter with optogenetic constructs to specifically label cholinergic cells in the NBM, and in the same surgery implanted fiber optic cannulas targeted to the dorsal surface of the BLA to allow for stimulation *in vivo*. Optogenetic stimulation of cholinergic afferents to BLA made learned fear more resistant to extinction training while optogenetic inhibition of the same afferents interferes with fear learning, yet has no effect on the rate of extinction when normalized for the initial freezing level. Optogenetic stimulation of ACh afferents in BLA on the training day had no effect on freezing during the training. On the following day, there was no significant difference in freezing to the first tone in the extinction regimen. However, over the course of 8 days of extinction trials, the opto group froze significantly more than controls as measured by repeated-measures ANOVA. The opto-stimulated group did not significantly change until day 6, and by day 8 they were freezing at the same level as controls. Hence, the learned fear is resistant to extinction, but not immune to it. Increased ACh signaling may strengthen the synaptic plasticity that occurs when activity arising from the CS and US converge in BLA, plasticity that underlies the learned association, and thus strengthens the association making it more difficult to inhibit by extinction learning. Given my patch clamp experiments and data from others, this seems a likely scenario. However, increased ACh may also alter the output of the BLA during learning, having effects on downstream circuits that may also contribute to the impaired extinction learning.

The first finding in optogenetically inhibiting ACh release during conditioning was that while inhibiting the cholinergic fibers during training, mice nearly cease to freeze. Recent work by the Tye, *et. al.* shows that optogenetic stimulation of BLA pyramidal neurons is acutely anxiolytic (Tye et al., 2011). Upon optogenetic stimulation of the BLA, mice show increased locomotor activity and a greater propensity to explore the open arms of an elevated plus maze. Likewise, optogenetic inhibition of pyramidal neurons in the BLA is anxiogenic, having the opposite effect in the elevated plus maze (Tye et al., 2011). Based on these findings, one might propose that the anxiolytic effects I observed when inhibiting ACh release in the BLA may be due to an overall increase in BLA pyramidal neuron activity. This net increase may depend in part on effects of ACh on pyramidal neurons themselves vs. effects on inhibitory interneurons, both of which express cholinergic receptors. Preliminary results from *in vivo* recordings of BLA neuronal firing done in our laboratory before and after local infusion of cholinergic antagonists suggest that decreases BLA firing. Further experiments combing *in vivo* electrical recordings with optogenetic stimulation or inhibition of ACh release are necessary, and currently ongoing in our laboratory, to address these competing hypotheses. Moreover, whether this net effect on BLA output neurons is direct or mediated by the significant population of interneurons in the BLA remains to be determined, but might also be investigated using a combination of optogenetic and pharmacological methods concomitant with *in vivo* electrophysiological monitoring.

Clearly, the BLA has a multifaceted role in fear-related behaviors. It both acutely modulates the fear response, while also contributing to the formation of long lasting

memories about fearful stimuli. In other words, interfering with freezing *per se* may or may not interfere with acquisition of fear memory (Ribeiro et al., 2011). In my experiments, however, fear memory, as measured by the amount of time spent freezing to the cue on the day following training, is significantly impaired. This suggests that the impaired freezing on the training day is not merely a "short circuited" freezing pathway, but that the normal long term changes to the circuit are also impaired by lack of ACh signaling. Future experiments examining the acute effects of cholinergic inhibition on locomotor activity and anxiety should clarify which components of the behavior and circuitry are most affected.

Fig 4.1 - Schematic of fear conditioning experiments with optogenetic manipulation of ACh release

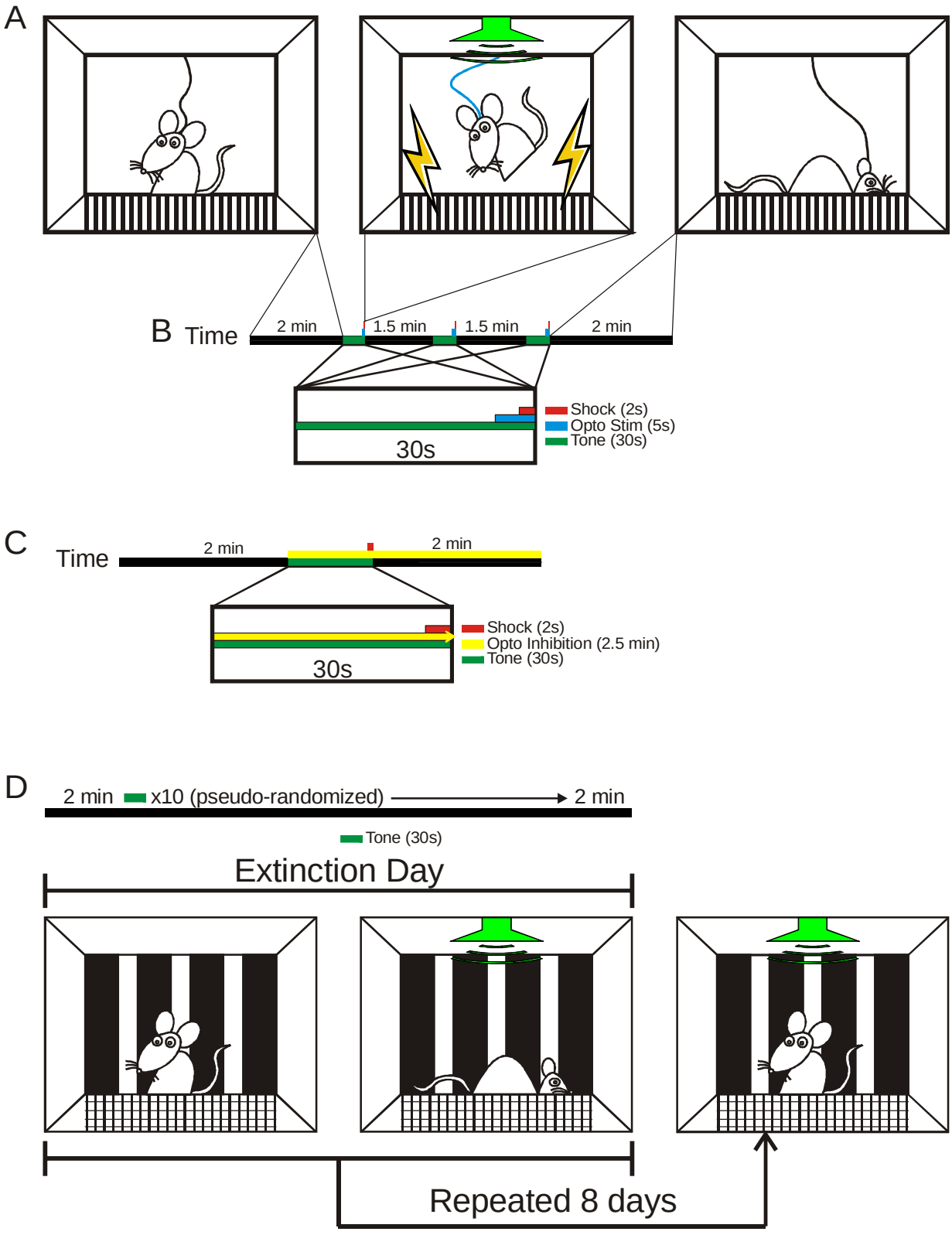

Figure 4.1 - Experiment design for optogenetic manipulation of ACh release during fear conditioning. (A) On the training day, mice are connected to optical fibers and placed in a fear conditioning chamber. Mice are allowed to freely explore for 2 minutes before the onset of the first tone (left panel). The 30s, 80dB, 5kHz tone plays for 30s and co-terminates with a 2s footshock (center panel). The opto-stimulated group also receives laser-light stimulation during this period. The mice are allowed 2 minutes to freely explore the chamber after the termination of the final tone/shock pairing (right panel). They typically freeze for much of this time. (B) The timeline for mice transfected with oChIEF for optogenetic stimulation of ACh release. Mice receive 3 tone/shock pairings. Experiment duration is 8.5 minutes. (C) The timeline for mice transfected with Halo3.0 for optogenetic inhibition of ACh release. Mice receive 1 tone/shock pairing. Experiment duration is 4.5 minutes. (D) On the extinction day, mice are placed in the conditioning chamber with an altered context (see methods). Mice are allowed 2 minutes to freely explore the chamber (left panel). After this period, ten 30s tones, identical to the tone played on the training day, play over 17 minutes, in a pseudo-random order (center panel). Following the final tone, mice are allowed 2 minutes to freely explore the chamber. This paradigm is repeated daily for 8 days. Successful extinction training is demonstrated by lack of freezing (typically mice groom, rear, and explore) (right panel).

Fig 4.2 - Optogenetic stimulation of ACh release in BLA enhances fear learning

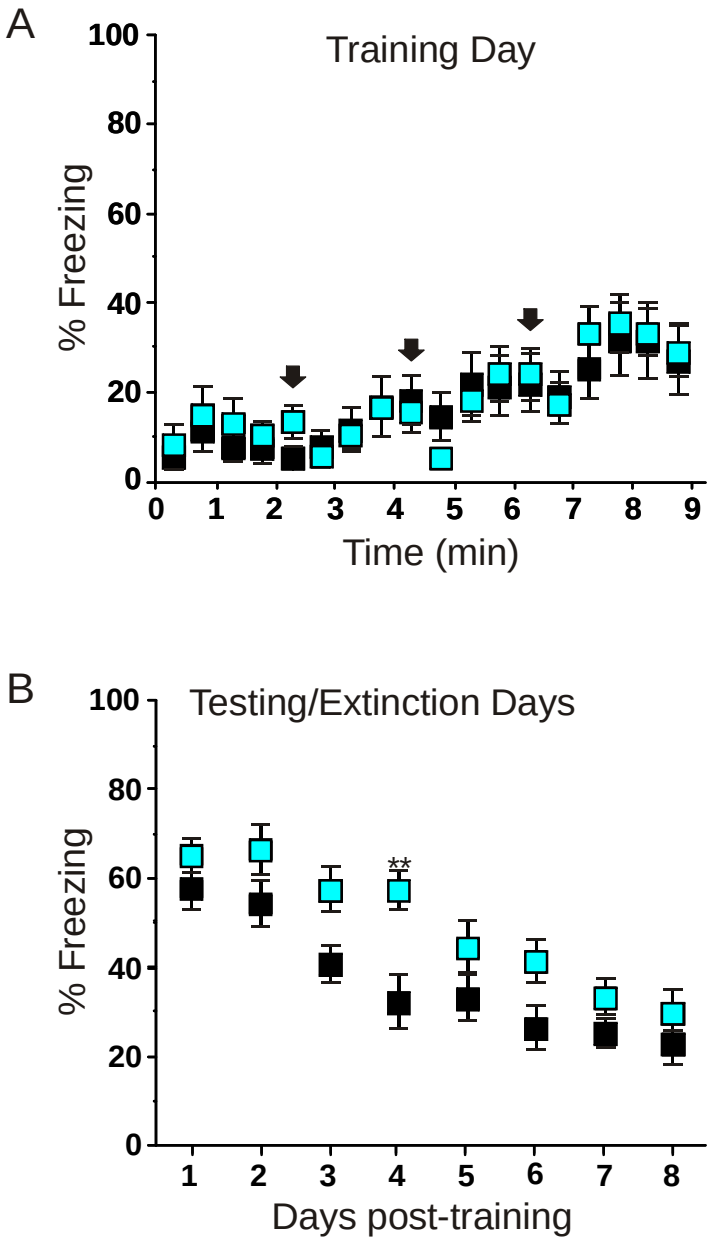

Figure 4.2 - Optogenetic stimulation of ACh release in BLA enhances fear learning. Data is pooled from 2 repetitions of the experiment (A) On the training day, the percentage of time spent freezing was measured in 30s bins over the course of the protocol. Arrows mark bins during which the tone/shock pairing occurred. Time bins were compared by 2-way ANOVA, finding a significant effect of time, $F(17, 594) = 5.54$, $p < 0.0001$; no significant effect of group, $F(1, 594) = 0.56$, $p = 0.45$; and no significant interaction between group and time, $F(17, 594) = 0.3173$, $p = 0.10$. (B) Extinction training began on the first day following conditioning. Percentage of time spent freezing during the first tone on each day was compared using mixed-model two-way ANOVA, finding a significant effect of group, $F(1, 245) = 28.16$, $p < 0.0001$; a significant effect of day, $F(7, 245) = 15.04$, $p < 0.0001$; and no significant interaction between group and day, $F(7, 245) = 0.79$, $p = 0.60$. A Sidak *post-hoc* multiple comparison test showed a significant difference between groups on day 4, $t(245) = 3.704$, $p < 0.001$). A comparison of linear regression lines for each group (ANCOVA) showed no significant difference between slopes, $F(1, 257) = 0.13$, $p = 0.72$, but a significant difference in elevation, $F(1, 258) = 29.62$, $p < 0.0001$.

Fig 4.3 - Optogenetic inhibition of ACh release in BLA inhibits fear learning

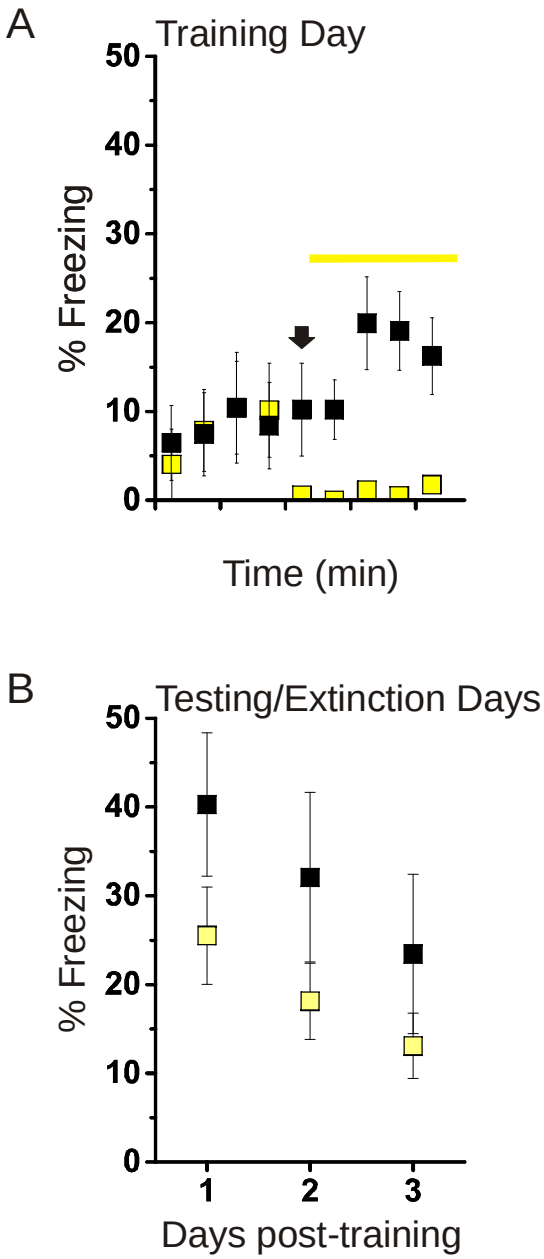

Figure 4.3 - Optogenetic inhibition of ACh release in BLA inhibits fear learning. Data is pooled from 2 repetitions of the experiment. (A) On the training day, the percentage of time spent freezing was measured in 30s bins over the course of the protocol. Arrows mark bin during which the tone/shock pairing occurred. Time bins before and after the tone/shock pairing were compared by separate 2-way ANOVAS. Before the tone/shock pairing there was no significant effect of group, $F(1, 96) < 0.01$, $p = 0.98$; no significant effect of time, $F(3, 96) = 0.63$, $p = 0.60$; and no significant interaction between group and time, $F(3, 96) = 0.10$, $p = 0.96$. After the tone/shock pairing, there was a significant effect of group, $F(1,120) = 56.38$, $p < 0.0001$; no significant effect of time, $F(4, 120) = 1.43$, $p = 0.23$; and no significant interaction between group and time, $F(4, 120) = 1.06$, $p = 0.38$. (B) Extinction training began on the first day following conditioning (see methods). Percentage of time spent freezing during the first tone on each day was compared using mixed-model two-way ANOVA, finding a significant effect of group, $F(1, 72) = 5.57$, $p = 0.02$; no significant effect of day, $F(2, 72) = 2.352$, $p < 0.10$; and no significant interaction between group and day, $F(2, 72) = 0.06$, $p = 0.94$.

Fig 4.4 - Histological verification of cannula placement and optogenetic construct expression

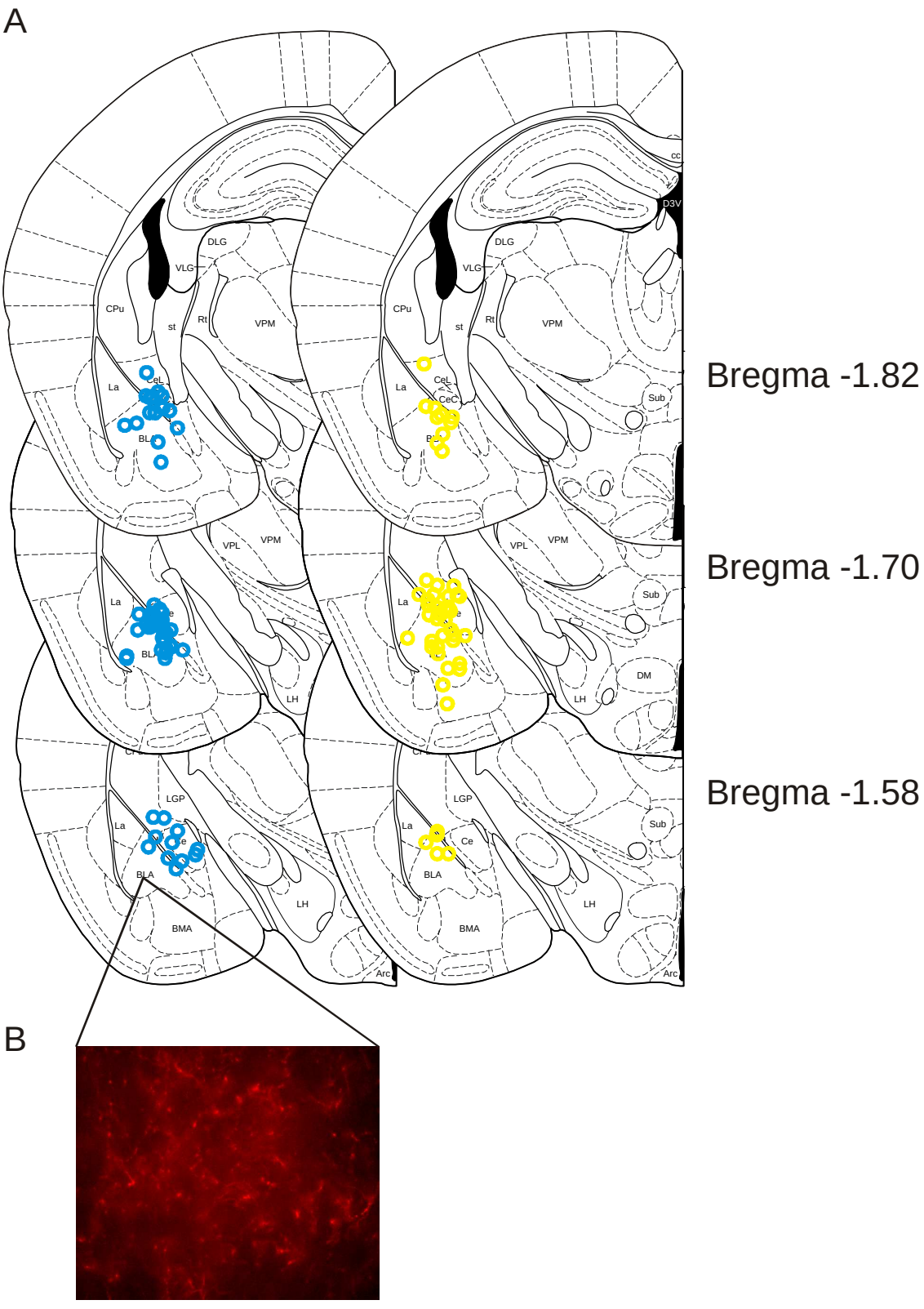

Figure 4.4 - Histological verification of cannula placement. Following the conclusion of each experiment, mice were sacrificed and perfused with 4% para-formaldehyde. Brains were removed, 100 µm sections were prepared using a vibratome and visualized under an epi-fluorescent dissecting microscope to confirm cannula placement and construct expression in the BLA. Mice with errant placement of both cannulae, or no visible construct expression were removed from analysis. (A) Diagram showing cannula locations for oChIEF (left) and Halo mice (right). (B) Example of oChIEF expression in BLA under epi-fluorescence.

Chapter 5 - Conclusion

My dissertation work reveals profound differences between thalamo- and cortico-BLA synaptic transmission, and that endogenous acetylcholine in the BLA is a potent and input-specific modulator of these connections. The work presented in Chapter 2 shows that there is potent plasticity in the long-distance inputs arising from cortical and thalamic areas. The cortico-BLA pathway nearly always potentiates in response to elevated patterns of activity. In contrast, the thalamo-BLA pathway responds to elevated patterns of activity in a variety of ways: it can potentiate, depress, or undergo no long-term change. I also showed that there is a plasticity induced by coactivation of these inputs. My work in Chapter 3 again revealed differences between the thalamic and cortical inputs to BLA; whereas cortical inputs potentiate in response to optogenetically stimulated ACh release, thalamic inputs depress. In addition, my experiments using AChR antagonists suggest that there is a baseline level of cholinergic activity, even in the slice preparation, and therefore, the cholinergic system serves to balance synaptic activity. This idea is further supported by my results in Chapter 4, where I showed that stimulation of endogenous ACh release in the BLA enhances fear learning while inhibition of ACh release diminishes fear learning, underscoring the potency and relevance of my findings in the slice preparation.

Previous studies examining synaptic transmission from cortical and thalamic afferents to the amygdala have focused primarily on the lateral nucleus in the rat. The circuitry and cellular composition of LA and BLA are very similar. Both are composed of

~80-90% pyramidal neurons and ~10-20% inhibitory interneurons, exhibit a high degree of local interconnectivity, and receive long distance inputs from similar sets of brain regions (Matyas, Lee, Shin, & Acsady, 2014; Pan et al., 2009). Long term potentiation has been studied extensively in these inputs (particularly in the cortical input) as a necessary component of fear learning. Consistent with my findings, studies report induction of robust potentiation in the cortical input by a variety of activity-dependent mechanisms (J. J. Kim & Jung, 2006; J. E. LeDoux, 1993, 2000).

The synaptic physiology of the thalamic input to LA and BLA has received considerably less attention in the literature than the cortical input, perhaps due to the greater technical difficulties in stimulating the diffusely arranged axons in the internal capsule. Nonetheless, synaptic potentiation has been reported in this pathway in slice preparations and *in vivo* (J. Kim et al., 2007; Kwon & Choi, 2009; McKernan & Shinnick-Gallagher, 1997). Activity-induced synaptic depression in naive rats was reported in one study which found that 150 seconds of 8 Hz (theta-frequency) stimulation induces long-term depression at thalamic, but not cortical inputs to LA pyramidal neurons. This effect was observed in approximately 20% of cells examined, while the remainder of cells showed either no effect or a short-term depression induced by 8 Hz stimulation (Heinbockel & Pape, 2000).

In my experiments I administered theta-burst frequency (5 Hz inter-burst rate) stimulation to the internal capsule and observed either depression or potentiation at thalamo-BLA synapses. This variability is perhaps not surprising given that axons in the

internal capsule are highly heterogeneous, arising from a collection of thalamic, and some non-thalamic subcortical areas, and include cholinergic inputs. Axons in the external capsule, on the other hand, are more homogenous, arising mainly from cortical areas and hippocampus, and are primarily glutamatergic axons from projection neurons. Thus, some of the variability observed in thalamo-BLA synapses may be due to concomitant stimulation of cholinergic inputs, which I have shown alter baseline synaptic transmission. A limitation of my experiments using electrical stimulation is the indeterminate nature of the type(s) and/or number of axons that are stimulated. An optogenetic approach could be used to examine distinct subsets of inputs by targeting specific thalamic areas or particular classes of projection neurons, then optically stimulating the labeled axonal terminal fields in the BLA. Examining plasticity and cholinergic modulation of individual inputs from specific thalamic areas would likely decrease the inter-trial variability that I observed using electrical stimulation of the internal capsule. An especially important distinction worth investigating is how thalamic areas conveying information about emotionally neutral stimuli, *i.e.* visual and auditory information from the lateral and medial geniculate nuclei, differ from those conveying innately salient stimuli such as nociceptive information, also conveyed from thalamic and other subcortical areas through the internal capsule. In the cortical pathway, optogenetic, input selective, activation of prefrontal cortical projections - known to be important for extinction learning - could be distinguished from cortical sensory inputs and hippocampal inputs. The inputs from these areas are important for different aspects of amygdala-dependent learning; understanding the synaptic physiology of each specifically is necessary for a more complete model of amygdala function.

Previous findings by our laboratory show that optogenetic stimulation of cholinergic afferents in the BLA induces synaptic potentiation at cortico-BLA synapses. It appears that the action of acetylcholine in the BLA involves both nicotinic and muscarinic receptors that are potentially located at both pre- and post-synaptic sites. Direct activation of nAChRs by nicotine in the BLA enhances glutamatergic transmission in a manner similar to the optogenetic activation of cholinergic terminal fields (Jiang et al., 2014 (in prep)). These studies and examination of the pharmacological profile of optogenetic stimulation of the cortico-BLA pathway indicates a prominent role of nAChRs in the cholinergic facilitation of cortico-BLA transmission. Unpublished results show that cortico-BLA synaptic facilitation induced by optogenetic stimulation of endogenous cholinergic afferents is blocked by mecamylamine, a nicotinic receptor antagonist but is not blocked by atropine, a muscarinic receptor antagonist. In fact, initial analyses suggest that activation of muscarinic receptors in BLA enhances inhibitory tone (Jiang et al., 2014 (in prep)).

My work presented in Chapter 3 shows that optogenetic stimulation of cholinergic afferents to BLA suppresses thalamo-BLA synaptic transmission. In half of cells tested, this stimulation had no effect, but in no case did I observe synaptic potentiation. The mechanisms underlying the depression of thalamic inputs to BLA induced by optogenetic stimulation of cholinergic afferents remain to be determined. I note that in one experiment when I used optogenetic stimulation of cholinergic inputs with thalamo- BLA activation in the presence of mAChR blockers I still saw one example

of robust depression. With only a single example in an assay where half the time there is no effect on plasticity, I cannot rule out (or rule in) a mAChR component. Nevertheless in conjunction with others work it is reasonable to expect some contribution of nAChRs to the cholinergic modulation of synaptic plasticity in the thalamo-cortical pathway.

While nicotinic receptors generally facilitate synaptic transmission in a plethora of brain areas, some evidence shows that α4β2 nicotinic receptors can presynaptically suppress synaptic transmission (Nagumo, Takeuchi, Imoto, & Miyata, 2011). Additionally, in the hippocampus there is some evidence that nicotine can induce synaptic potentiation or depression dependent on the concentration and timing of nicotine application (Maggi et al., 2004; Yun, Bazar, Lee, Gerber, & Daniel, 2005).

Muscarinic receptors remain a likely candidate for mediating (at least in part) the cholinergic stimulation-induced synaptic depression of thalamo-BLA synapses. In the cortico-BLA pathway, muscarinic receptors have been found to oppose synaptic transmission. The cholinergic agonist carbachol has been found to depress synaptic transmission at this input through the action of muscarinic receptors (Yajeya et al., 2000).This suppression of cortico-BLA transmission is partially blocked by each of several partially selective muscarinic antagonists. These include pirenzepine (M_1 and M_4), gallamine (M_2), methoctramine (M_2 and M_4) and 4-diphenylacetoxy-N-methylpiperidine (M_1 and M_3) suggesting that more than one type of muscarinic receptor opposes cortico-BLA transmission (Yajeya et al., 2000). Additional

experiments are needed to clarify which cholinergic receptors underlie the depression induced by optogenetic stimulation of cholinergic afferents on thalamo-BLA synaptic transmission. The number of examples using atropine must be increased, preferably with reagents known to be effective and more selective for mAChRs to determine if the one observed example can be repeated. Likewise, experiments using selective nicotinic agonists and antagonists need to be done to determine the role, if any, of nicotinic receptors in cholinergic depression of thalamo-BLA synapses.

It is also possible that cholinergic afferents co-release other neurotransmitters with acetylcholine. Evidence of co-release of acetylcholine with GABA or glutamate has been reported in habenula, hippocampus, and cortex (Docherty, Bradford, & Wu, 1987; El Mestikawy, Wallen-Mackenzie, Fortin, Descarries, & Trudeau, 2011; O'Malley, Sandell, & Masland, 1992; Ren et al., 2011). Thus, synaptic depression at thalamo-BLA synapses induced by stimulation of cholinergic afferents may in fact be mediated by a transmitter other than acetylcholine, though evidence of co-release of ACh with other neurotransmitters has not been demonstrated in the amygdala specifically. My experiments also showed that blockade of cholinergic receptors under baseline conditions impairs thalamo-BLA glutamatergic transmission, implying a role for acetylcholine even in the absence of stimulation. Thus, additional experiments should also examine the effects of optogenetic inhibition of acetylcholine release on both cortico- and thalamo-BLA transmission.

My results from chapters 2 and 3 suggest that cortico-BLA synapses are weaker than thalamo-BLA synapses and are dynamically altered depending on patterns of activity and levels of cholinergic signaling. Patterns of activity in either pathway, convergent coactivation of both pathways, and addition or subtraction of cholinergic signaling can alter these connections, generally shifting the weight of inputs from thalamic to cortical sources. Because the amygdala is so highly interconnected with other brain regions, it is not hard to imagine that changes to these inputs can induce broad changes in patterns of activity throughout the brain. Of particular interest is my finding, consistent with a study in the lateral amygdala (Cho et al., 2012), that co-activation of both the thalamic and cortical inputs to BLA can induce plastic changes in these inputs, otherwise known as input-timing dependent plasticity (ITDP). Given that activity arising from a sensory stimulus arrives in the BLA from thalamic sources approximately 8 ms prior to that from cortical sources (Cho et al., 2012; Li, Stutzmann, & LeDoux, 1996), one interpretation is that activation of thalamic inputs primes nearby dendritic spines to receive and react to incoming cortical inputs, thus composing a mechanism for coincidence detection. Future experiments should examine the timing window in which ITDP occurs how cholinergic activity may alter either the timing window or direction of plasticity.

In Chapter 4 I presented my findings that both stimulation and inhibition of cholinergic afferents to BLA potently modulate behavior in a learned fear paradigm. Stimulation of cholinergic afferents in BLA during fear conditioning training increased the expression of learned fear, while inhibition of cholinergic afferents in BLA diminished

fear learning. Interestingly, the effects of cholinergic stimulation did not manifest as enhanced learning *per se*, but rather as a resistance to subsequent extinction training. In the acute slice preparation, optogenetic stimulation of acetylcholine release potentiates cortico-BLA synapses. It is known that plasticity in prefrontal cortical inputs to BLA are essential for fear extinction to occur (Sierra-Mercado et al., 2011). These observations, in conjunction with my findings, suggest that additional cholinergic signaling, therefore, could interfere with subsequent extinction learning either by occluding additional plasticity from occurring, or by requiring synapses to depotentiate from a higher level than under normal conditions. Cholinergic inhibition, on the other hand, manifested as diminished learning both during training and on the first day of extinction training. These results are consistent with findings that muscarinic signaling during fear learning is essential for memory consolidation (Boccia et al., 2009; Lalumiere & McGaugh, 2005; Tinsley et al., 2004).

Very few studies have examined the effects of endogenous acetylcholine on learned fear due to the technical difficulty in selective manipulation of cholinergic signaling prior to the advent of optogenetic methods. In one study, fear conditioning was inhibited by injection of histamine receptor H3 antagonists, which indirectly inhibit acetylcholine release, in the BLA after fear training (Cecchi, Passani, Bacciottini, Mannaioni, & Blandina, 2001; Passani et al., 2001). Histamine receptor H3 agonists enhanced fear learning when injected in the BLA following training (Cangioli et al., 2002). Other studies have examined the effects of muscarinic and nicotinic agonists and antagonists on modulation of fear learning by the BLA. Acute application of either

nicotine or oxotremorine (a non-selective muscarinic agonist) in the BLA immediately before fear conditioning training enhances learning (Boccia et al., 2009; Gould, 2003; Gould & Lommock, 2003; Gould & Wehner, 1999). Administration of nicotinic antagonists, on the other hand, does not seem to impair learning (Gould & Wehner, 1999; Pavesi, Gooch, Lee, & Fletcher, 2013). Muscarinic antagonists, however, impair fear learning when administered during or immediately after training (Roldan, Cobos-Zapiain, Quirarte, & Prado-Alcala, 2001).

While cholinergic signaling in the amygdala is implicated in the modulation of fear learning, several key questions remain. First, it is unknown whether increased cholinergic tone in the BLA has a net excitatory or inhibitory effect on the amygdala. Direct optogenetic stimulation of BLA pyramidal neurons has an anxiolytic effect, so it is possible that acetylcholine may have an overall inhibitory effect on the BLA that contributes to increased fear (Tye et al., 2011). Inhibiting acetylcholine may have a net excitatory effect on the BLA, explaining the acutely anxiolytic effect of cholinergic inhibition I observed in my experiments. Experiments ongoing in our laboratory have in fact shown mixed excitatory and inhibitory effects (approximately a 4:1 ratio excitatory:inhibitory) of optogenetic stimulation of cholinergic fibers on BLA neurons in *in vivo* recordings. Concurrent electrophysiological recordings would naturally complement the fear conditioning paradigm presented here to address this question.

Second, because acetylcholine interacts with a mixed complement of receptors of highly varying affinity and desensitization kinetics, the effects of acetylcholine are

likely to be highly dependent on both the amount and time course of its release. This is, perhaps, one reason underlying the variable results obtained in pharmacologically based studies of cholinergic effects on behavior (Kaplan & Moore, 2011). The affinity of muscarinic vs. nicotinic receptors for acetylcholine varies widely, and also depends on the specific receptor subtype or subunit composition. Therefore, the effects of acetylcholine are likely to be highly dose-dependent. It follows that at low concentrations of acetylcholine, the effects of muscarinic receptor activation will dominate. At higher concentrations, a mix of nicotinic and muscarinic effects will emerge, while at even higher concentrations, and over long time courses, the effects of receptor desensitization will manifest. A limitation of my current approaches is the lack of information on how much, and over what time course, acetylcholine is released from NBM projections under baseline conditions, both during and after fear leaning, and how the release profile changes with optogenetic stimulation or inhibition of NBM terminals within the BLA.

Finally, it is likely that the effects of acetylcholine are state-dependent. The effects of increasing or decreasing cholinergic signaling may differ depending on the baseline level of cholinergic activity and other factors that interact with the cholinergic system. For example, in behavioral experiments such as fear conditioning, the stress level of the animal prior to training affects levels of acetylcholine and other neuromodulators and has profound effects on the formation of fear memories (Campos, Fogaca, Aguiar, & Guimaraes, 2013).

While working on these experiments, I investigated possible ways to directly measure ACh concentrations in both in slice and *in vivo* in real-time. A variety of experimental methods including *in vivo* cellular and electrical sensors have been developed and implemented in recent years, but each of these techniques is somewhat complex and each is limited in its temporal and/or spatial resolution (Eray et al., 1995; Jabbari, Heli, Hajjizadeh, & Moosavi-Movahedi, 2008; Khan et al., 2013; Nguyen et al., 2010; Sattarahmady, Heli, & Moosavi-Movahedi, 2010). The ability to directly measure ACh concentrations under baseline conditions and after optogenetic stimulation or inhibition of cholinergic afferents would control for variability in expression levels of the optogenetic construct, offer information on the dose sensitivity of the effects of endogenous acetylcholine, and provide a direct measure of the dynamic range of the cholinergic system (Hasselmo & Sarter, 2011).

Collectively, my dissertation work reveals behaviorally relevant functional differences between thalamo- and cortico-BLA synaptic transmission and plasticity, and modulation by acetylcholine. Future experiments should seek to link the differences observed *in vitro* between cortico- and thalamo-BLA synaptic transmission and cholinergic modulation with the behavioral effects of stimulating cholinergic afferents in BLA observed *in vivo*. To dissect the role of cortical vs. thalamic inputs to BLA in fear learning and extinction, specific thalamic and cortical areas could be labeled with inhibitory optogenetic constructs. These inputs could then be selectively silenced during training or extinction learning. Current understanding of the relative contributions of these inputs relies primarily on studies using lesions or pharmacological silencing of

selected brain regions. However, with these methods, examination of the lesioned or silenced inputs after training is impossible. With optogenetic methods, labeled inputs could be stimulated or inhibited at various time points in a fear learning and extinction paradigm, then functionally examined *in vitro* to assess the differences in synaptic transmission and plasticity that occur at specific inputs during fear learning and other behaviors. Similarly, to link the cholinergic modulation of fear learning and extinction I observed in my behavioral experiments to differences in cholinergic modulation of thalamo- and cortico-BLA synaptic transmission and plasticity, animals could be trained in the fear conditioning paradigm described in Chapter 4, with or without cholinergic excitation or inhibition. On the following days, animals would be sacrificed for patch-clamp experiments to examine electrophysiological properties such as membrane excitability and synaptic transmission at thalamic and cortical inputs to BLA. If the effects of cholinergic stimulation or inhibition *in vivo* are the same as those previously observed in slice, then on average, cortico-BLA synapses would have higher release probability and/or evoked EPSC amplitudes, while thalamo-BLA synapses have lower release probabilities as compared to controls. Coupled with pharmacological blockade of specific cholinergic receptor subtypes, this type of experimentation would provide a more detailed understanding of synaptic integration and cholinergic modulation in the BLA.

Works Cited

Aggleton, J. P. (1992). *The Amygdala : neurobiological aspects of emotion, memory, and mental dysfunction*. New York: Wiley-Liss.

Aggleton, J. P. (2000). *The amygdala : a functional analysis* (2nd ed.). Oxford, OX ; New York: Oxford University Press.

Arroyo, S., Bennett, C., & Hestrin, S. (2014). Nicotinic modulation of cortical circuits. *Front Neural Circuits, 8*, 30. doi: 10.3389/fncir.2014.00030

Barazangi, N., & Role, L. W. (2001). Nicotine-induced enhancement of glutamatergic and GABAergic synaptic transmission in the mouse amygdala. *J Neurophysiol, 86*(1), 463-474.

Bard, P. (1928). A diencephalic mechanism for the expression of rage with special reference to the sympathetic nervous system. *Am J Physiol, 84*, 490-515.

Barik, J., & Wonnacott, S. (2009). Molecular and cellular mechanisms of action of nicotine in the CNS. *Handb Exp Pharmacol*(192), 173-207. doi: 10.1007/978-3-540-69248-5_7

Barot, S. K., Chung, A., Kim, J. J., & Bernstein, I. L. (2009). Functional imaging of stimulus convergence in amygdalar neurons during Pavlovian fear conditioning. *PLoS One, 4*(7), e6156. doi: 10.1371/journal.pone.0006156

Barros, D. M., Pereira, P., Medina, J. H., & Izquierdo, I. (2002). Modulation of working memory and of long- but not short-term memory by cholinergic mechanisms in the basolateral amygdala. *Behav Pharmacol, 13*(2), 163-167.

Barros, D. M., Ramirez, M. R., & Izquierdo, I. (2005). Modulation of working, short- and long-term memory by nicotinic receptors in the basolateral amygdala in rats. *Neurobiol Learn Mem, 83*(2), 113-118. doi: 10.1016/j.nlm.2004.10.001

Baysinger, A. N., Kent, B. A., & Brown, T. H. (2012). Muscarinic receptors in amygdala control trace fear conditioning. *PLoS One, 7*(9), e45720. doi: 10.1371/journal.pone.0045720

Blair, H. T., Sotres-Bayon, F., Moita, M. A., & Ledoux, J. E. (2005). The lateral amygdala processes the value of conditioned and unconditioned aversive stimuli. *Neuroscience, 133*(2), 561-569. doi: 10.1016/j.neuroscience.2005.02.043

Blair, H. T., Tinkelman, A., Moita, M. A., & LeDoux, J. E. (2003). Associative plasticity in neurons of the lateral amygdala during auditory fear conditioning. *Ann N Y Acad Sci, 985*, 485-487.

Bloem, B., Poorthuis, R. B., & Mansvelder, H. D. (2014). Cholinergic modulation of the medial prefrontal cortex: the role of nicotinic receptors in attention and regulation of neuronal activity. *Front Neural Circuits, 8*, 17. doi: 10.3389/fncir.2014.00017

Boccia, M. M., Blake, M. G., Baratti, C. M., & McGaugh, J. L. (2009). Involvement of the basolateral amygdala in muscarinic cholinergic modulation of extinction memory consolidation. *Neurobiol Learn Mem, 91*(1), 93-97. doi: 10.1016/j.nlm.2008.07.012

Buckley, N. J., Bonner, T. I., & Brann, M. R. (1988). Localization of a family of muscarinic receptor mRNAs in rat brain. *J Neurosci, 8*(12), 4646-4652.

Burstein, R., & Potrebic, S. (1993). Retrograde labeling of neurons in the spinal cord that project directly to the amygdala or the orbital cortex in the rat. *J Comp Neurol, 335*(4), 469-485. doi: 10.1002/cne.903350402

Campos, A. C., Fogaca, M. V., Aguiar, D. C., & Guimaraes, F. S. (2013). Animal models of anxiety disorders and stress. *Rev Bras Psiquiatr, 35 Suppl 2*, S101-111. doi: 10.1590/1516-4446-2013-1139

Cangioli, I., Baldi, E., Mannaioni, P. F., Bucherelli, C., Blandina, P., & Passani, M. B. (2002). Activation of histaminergic H3 receptors in the rat basolateral amygdala improves expression of fear memory and enhances acetylcholine release. *Eur J Neurosci, 16*(3), 521-528.

Carballo-Marquez, A., Boadas-Vaello, P., Villarejo-Rodriguez, I., Guillazo-Blanch, G., Marti-Nicolovius, M., & Vale-Martinez, A. (2011). Effects of muscarinic receptor antagonism in the basolateral amygdala on two-way active avoidance. *Exp Brain Res, 209*(3), 455-464. doi: 10.1007/s00221-011-2576-4

Cecchi, M., Passani, M. B., Bacciottini, L., Mannaioni, P. F., & Blandina, P. (2001). Cortical acetylcholine release elicited by stimulation of histamine H1 receptors in the nucleus basalis magnocellularis: a dual-probe microdialysis study in the freely moving rat. *Eur J Neurosci, 13*(1), 68-78.

Chapman, P. F., & Bellavance, L. L. (1992). Induction of long-term potentiation in the basolateral amygdala does not depend on NMDA receptor activation. *Synapse, 11*(4), 310-318. doi: 10.1002/syn.890110406

Cho, J. H., Bayazitov, I. T., Meloni, E. G., Myers, K. M., Carlezon, W. A., Jr., Zakharenko, S. S., & Bolshakov, V. Y. (2012). Coactivation of thalamic and cortical pathways induces input timing-dependent plasticity in amygdala. *Nat Neurosci, 15*(1), 113-122. doi: 10.1038/nn.2993

Christian, D. T., Alexander, N. J., Diaz, M. R., & McCool, B. A. (2013). Thalamic glutamatergic afferents into the rat basolateral amygdala exhibit increased presynaptic glutamate

function following withdrawal from chronic intermittent ethanol. *Neuropharmacology, 65*, 134-142. doi: 10.1016/j.neuropharm.2012.09.004

Dajas-Bailador, F., & Wonnacott, S. (2004). Nicotinic acetylcholine receptors and the regulation of neuronal signalling. *Trends Pharmacol Sci, 25*(6), 317-324. doi: 10.1016/j.tips.2004.04.006

Dani, J. A., & Bertrand, D. (2007). Nicotinic acetylcholine receptors and nicotinic cholinergic mechanisms of the central nervous system. *Annu Rev Pharmacol Toxicol, 47*, 699-729. doi: 10.1146/annurev.pharmtox.47.120505.105214

Davis, M. (1992). The role of the amygdala in fear and anxiety. *Annu Rev Neurosci, 15*, 353-375. doi: 10.1146/annurev.ne.15.030192.002033

Deutsch, S. I., Mohs, R. C., Levy, M. I., Rothpearl, A. B., Stockton, D., Horvath, T., . . . Davis, K. L. (1983). Acetylcholinesterase activity in CSF in schizophrenia, depression, Alzheimer's disease and normals. *Biol Psychiatry, 18*(12), 1363-1373.

Docherty, M., Bradford, H. F., & Wu, J. Y. (1987). Co-release of glutamate and aspartate from cholinergic and GABAergic synaptosomes. *Nature, 330*(6143), 64-66. doi: 10.1038/330064a0

Ehrlich, I., Humeau, Y., Grenier, F., Ciocchi, S., Herry, C., & Luthi, A. (2009). Amygdala inhibitory circuits and the control of fear memory. *Neuron, 62*(6), 757-771. doi: 10.1016/j.neuron.2009.05.026

El Mestikawy, S., Wallen-Mackenzie, A., Fortin, G. M., Descarries, L., & Trudeau, L. E. (2011). From glutamate co-release to vesicular synergy: vesicular glutamate transporters. *Nat Rev Neurosci, 12*(4), 204-216. doi: 10.1038/nrn2969

Eray, M., Dogan, N. S., Reiken, S. R., Sutisna, H., Van Wie, B. J., Koch, A. R., . . . Davis, W. C. (1995). A highly stable and selective biosensor using modified nicotinic acetylcholine receptor (nAChR). *Biosystems, 35*(2-3), 183-188.

Fuchs, R. A., Feltenstein, M. W., & See, R. E. (2006). The role of the basolateral amygdala in stimulus-reward memory and extinction memory consolidation and in subsequent conditioned cued reinstatement of cocaine seeking. *Eur J Neurosci, 23*(10), 2809-2813. doi: 10.1111/j.1460-9568.2006.04806.x

Gotti, C., & Clementi, F. (2004). Neuronal nicotinic receptors: from structure to pathology. *Prog Neurobiol, 74*(6), 363-396. doi: 10.1016/j.pneurobio.2004.09.006

Gotti, C., Moretti, M., Gaimarri, A., Zanardi, A., Clementi, F., & Zoli, M. (2007). Heterogeneity and complexity of native brain nicotinic receptors. *Biochem Pharmacol, 74*(8), 1102-1111. doi: 10.1016/j.bcp.2007.05.023

Gould, T. J. (2003). Nicotine produces a within-subject enhancement of contextual fear conditioning in C57BL/6 mice independent of sex. *Integr Physiol Behav Sci, 38*(2), 124-132.

Gould, T. J., & Lommock, J. A. (2003). Nicotine enhances contextual fear conditioning and ameliorates ethanol-induced deficits in contextual fear conditioning. *Behav Neurosci, 117*(6), 1276-1282. doi: 10.1037/0735-7044.117.6.1276

Gould, T. J., & Wehner, J. M. (1999). Nicotine enhancement of contextual fear conditioning. *Behav Brain Res, 102*(1-2), 31-39.

Hasselmo, M. E., & Sarter, M. (2011). Modes and models of forebrain cholinergic neuromodulation of cognition. *Neuropsychopharmacology, 36*(1), 52-73. doi: 10.1038/npp.2010.104

Heinbockel, T., & Pape, H. C. (2000). Input-specific long-term depression in the lateral amygdala evoked by theta frequency stimulation. *J Neurosci, 20*(7), RC68.

Hill, J. A., Jr., Zoli, M., Bourgeois, J. P., & Changeux, J. P. (1993). Immunocytochemical localization of a neuronal nicotinic receptor: the beta 2-subunit. *J Neurosci, 13*(4), 1551-1568.

Huang, Y. Y., & Kandel, E. R. (1998). Postsynaptic induction and PKA-dependent expression of LTP in the lateral amygdala. *Neuron, 21*(1), 169-178.

Huh, C. Y., Danik, M., Manseau, F., Trudeau, L. E., & Williams, S. (2008). Chronic exposure to nerve growth factor increases acetylcholine and glutamate release from cholinergic neurons of the rat medial septum and diagonal band of Broca via mechanisms mediated by p75NTR. *J Neurosci, 28*(6), 1404-1409. doi: 10.1523/JNEUROSCI.4851-07.2008

Hull, A. M. (2002). Neuroimaging findings in post-traumatic stress disorder. Systematic review. *Br J Psychiatry, 181*, 102-110.

Humeau, Y., Herry, C., Kemp, N., Shaban, H., Fourcaudot, E., Bissiere, S., & Luthi, A. (2005). Dendritic spine heterogeneity determines afferent-specific Hebbian plasticity in the amygdala. *Neuron, 45*(1), 119-131. doi: 10.1016/j.neuron.2004.12.019

Humeau, Y., & Luthi, A. (2007). Dendritic calcium spikes induce bi-directional synaptic plasticity in the lateral amygdala. *Neuropharmacology, 52*(1), 234-243. doi: 10.1016/j.neuropharm.2006.07.010

Humeau, Y., Shaban, H., Bissiere, S., & Luthi, A. (2003). Presynaptic induction of heterosynaptic associative plasticity in the mammalian brain. *Nature, 426*(6968), 841-845. doi: 10.1038/nature02194

Ito, H. T., & Schuman, E. M. (2008). Frequency-dependent signal transmission and modulation by neuromodulators. *Front Neurosci, 2*(2), 138-144. doi: 10.3389/neuro.01.027.2008

Jabbari, A., Heli, H., Hajjizadeh, M., & Moosavi-Movahedi, A. A. (2008). A nonenzymatic biosensor based on copper nanoparticles modified electrode for detection of acetylcholine. *Conf Proc IEEE Eng Med Biol Soc, 2008*, 2314-2317. doi: 10.1109/IEMBS.2008.4649661

Jiang, L., Emmetsberger, J., Talmage, D. A., & Role, L. W. (2013). Type III neuregulin 1 is required for multiple forms of excitatory synaptic plasticity of mouse cortico-amygdala circuits. *J Neurosci, 33*(23), 9655-9666. doi: 10.1523/JNEUROSCI.2888-12.2013

Jiang , L., Kundu, S., Lederman, J., Lopez-Hernandez, G., Ballinger, E., Fontanini, A., . . . Role, L. W. (2014 (in prep)). Cholinergic signaling enhances cortical-amygdala circuit activity and slows extinction of cued-fear behavior (in preparation).

Jiang, L., Lopez-Hernandez, G. Y., Lederman, J., Talmage, D. A., & Role, L. W. (2014). Optogenetic studies of nicotinic contributions to cholinergic signaling in the central nervous system. *Rev Neurosci*. doi: 10.1515/revneuro-2014-0032

Jiang, L., & Role, L. W. (2008). Facilitation of cortico-amygdala synapses by nicotine: activity-dependent modulation of glutamatergic transmission. *J Neurophysiol, 99*(4), 1988-1999. doi: 10.1152/jn.00933.2007

Johansen, J. P., Hamanaka, H., Monfils, M. H., Behnia, R., Deisseroth, K., Blair, H. T., & LeDoux, J. E. (2010). Optical activation of lateral amygdala pyramidal cells instructs associative fear learning. *Proc Natl Acad Sci U S A, 107*(28), 12692-12697. doi: 10.1073/pnas.1002418107

Kaplan, G. B., & Moore, K. A. (2011). The use of cognitive enhancers in animal models of fear extinction. *Pharmacol Biochem Behav, 99*(2), 217-228. doi: 10.1016/j.pbb.2011.01.009

Khan, A., Khan, A. A., Asiri, A. M., Rub, M. A., Azum, N., Rahman, M. M., . . . Ghani, S. A. (2013). A new trend on biosensor for neurotransmitter choline/acetylcholine--an overview. *Appl Biochem Biotechnol, 169*(6), 1927-1939. doi: 10.1007/s12010-013-0099-0

Kim, J., Lee, S., Park, K., Hong, I., Song, B., Son, G., . . . Choi, S. (2007). Amygdala depotentiation and fear extinction. *Proc Natl Acad Sci U S A, 104*(52), 20955-20960. doi: 10.1073/pnas.0710548105

Kim, J. J., & Jung, M. W. (2006). Neural circuits and mechanisms involved in Pavlovian fear conditioning: a critical review. *Neurosci Biobehav Rev, 30*(2), 188-202. doi: 10.1016/j.neubiorev.2005.06.005

Klein, R. C., & Yakel, J. L. (2006). Functional somato-dendritic alpha7-containing nicotinic acetylcholine receptors in the rat basolateral amygdala complex. *J Physiol, 576*(Pt 3), 865-872. doi: 10.1113/jphysiol.2006.118232

Kwon, J. T., & Choi, J. S. (2009). Cornering the fear engram: long-term synaptic changes in the lateral nucleus of the amygdala after fear conditioning. *J Neurosci, 29*(31), 9700-9703. doi: 10.1523/JNEUROSCI.5928-08.2009

Lalumiere, R. T., & McGaugh, J. L. (2005). Memory enhancement induced by post-training intrabasolateral amygdala infusions of beta-adrenergic or muscarinic agonists requires activation of dopamine receptors: Involvement of right, but not left, basolateral amygdala. *Learn Mem, 12*(5), 527-532. doi: 10.1101/lm.97405

LeDoux, J. (2007). The amygdala. *Curr Biol, 17*(20), R868-874. doi: 10.1016/j.cub.2007.08.005

LeDoux, J. E. (1993). Emotional memory: in search of systems and synapses. *Ann N Y Acad Sci, 702*, 149-157.

LeDoux, J. E. (2000). Emotion circuits in the brain. *Annu Rev Neurosci, 23*, 155-184. doi: 10.1146/annurev.neuro.23.1.155

Levin, E. D., McClernon, F. J., & Rezvani, A. H. (2006). Nicotinic effects on cognitive function: behavioral characterization, pharmacological specification, and anatomic localization. *Psychopharmacology (Berl), 184*(3-4), 523-539. doi: 10.1007/s00213-005-0164-7

Li, X. F., Stutzmann, G. E., & LeDoux, J. E. (1996). Convergent but temporally separated inputs to lateral amygdala neurons from the auditory thalamus and auditory cortex use different postsynaptic receptors: in vivo intracellular and extracellular recordings in fear conditioning pathways. *Learn Mem, 3*(2-3), 229-242.

Likhtik, E., Stujenske, J. M., Topiwala, M. A., Harris, A. Z., & Gordon, J. A. (2014). Prefrontal entrainment of amygdala activity signals safety in learned fear and innate anxiety. *Nat Neurosci, 17*(1), 106-113. doi: 10.1038/nn.3582

Lima, R. H., Radiske, A., Kohler, C. A., Gonzalez, M. C., Bevilaqua, L. R., Rossato, J. I., . . . Cammarota, M. (2013). Nicotine modulates the long-lasting storage of fear memory. *Learn Mem, 20*(3), 120-124. doi: 10.1101/lm.029900.112

Lin, J. Y., Lin, M. Z., Steinbach, P., & Tsien, R. Y. (2009). Characterization of engineered channelrhodopsin variants with improved properties and kinetics. *Biophys J, 96*(5), 1803-1814. doi: 10.1016/j.bpj.2008.11.034

Maggi, L., Sola, E., Minneci, F., Le Magueresse, C., Changeux, J. P., & Cherubini, E. (2004). Persistent decrease in synaptic efficacy induced by nicotine at Schaffer collateral-CA1 synapses in the immature rat hippocampus. *J Physiol, 559*(Pt 3), 863-874. doi: 10.1113/jphysiol.2004.067041

Mahanty, N. K., & Sah, P. (1999). Excitatory synaptic inputs to pyramidal neurons of the lateral amygdala. *Eur J Neurosci, 11*(4), 1217-1222.

Mansvelder, H. D., Keath, J. R., & McGehee, D. S. (2002). Synaptic mechanisms underlie nicotine-induced excitability of brain reward areas. *Neuron, 33*(6), 905-919.

Maren, S., & Quirk, G. J. (2004). Neuronal signalling of fear memory. *Nat Rev Neurosci, 5*(11), 844-852. doi: 10.1038/nrn1535

Matyas, F., Lee, J., Shin, H. S., & Acsady, L. (2014). The fear circuit of the mouse forebrain: connections between the mediodorsal thalamus, frontal cortices and basolateral amygdala. *Eur J Neurosci*. doi: 10.1111/ejn.12610

McDonald, A. J. (1998). Cortical pathways to the mammalian amygdala. *Prog Neurobiol, 55*(3), 257-332.

McDonald, A. J., & Mascagni, F. (2011). Neuronal localization of M2 muscarinic receptor immunoreactivity in the rat amygdala. *Neuroscience, 196*, 49-65. doi: 10.1016/j.neuroscience.2011.08.032

McGaugh, J. L. (2004). The amygdala modulates the consolidation of memories of emotionally arousing experiences. *Annu Rev Neurosci, 27*, 1-28. doi: 10.1146/annurev.neuro.27.070203.144157

McIntyre, C. K., Power, A. E., Roozendaal, B., & McGaugh, J. L. (2003). Role of the basolateral amygdala in memory consolidation. *Ann N Y Acad Sci, 985*, 273-293.

McKernan, M. G., & Shinnick-Gallagher, P. (1997). Fear conditioning induces a lasting potentiation of synaptic currents in vitro. *Nature, 390*(6660), 607-611. doi: 10.1038/37605

Mesulam, M. M. (1995). Cholinergic pathways and the ascending reticular activating system of the human brain. *Ann N Y Acad Sci, 757*, 169-179.

Milad, M. R., Rauch, S. L., Pitman, R. K., & Quirk, G. J. (2006). Fear extinction in rats: implications for human brain imaging and anxiety disorders. *Biol Psychol, 73*(1), 61-71. doi: 10.1016/j.biopsycho.2006.01.008

Mineur, Y. S., Somenzi, O., & Picciotto, M. R. (2007). Cytisine, a partial agonist of high-affinity nicotinic acetylcholine receptors, has antidepressant-like properties in male C57BL/6J mice. *Neuropharmacology, 52*(5), 1256-1262. doi: 10.1016/j.neuropharm.2007.01.006

Mishkin, M. (1986). The Amygdala: Sensory gateway to the emotions.

Muller, J. F., Mascagni, F., & McDonald, A. J. (2011). Cholinergic innervation of pyramidal cells and parvalbumin-immunoreactive interneurons in the rat basolateral amygdala. *J Comp Neurol, 519*(4), 790-805. doi: 10.1002/cne.22550

Muller, J. F., Mascagni, F., Zaric, V., & McDonald, A. J. (2013). Muscarinic cholinergic receptor M1 in the rat basolateral amygdala: ultrastructural localization and synaptic relationships to cholinergic axons. *J Comp Neurol, 521*(8), 1743-1759. doi: 10.1002/cne.23254

Nagumo, Y., Takeuchi, Y., Imoto, K., & Miyata, M. (2011). Synapse- and subtype-specific modulation of synaptic transmission by nicotinic acetylcholine receptors in the ventrobasal thalamus. *Neurosci Res, 69*(3), 203-213. doi: 10.1016/j.neures.2010.12.002

Nguyen, Q. T., Schroeder, L. F., Mank, M., Muller, A., Taylor, P., Griesbeck, O., & Kleinfeld, D. (2010). An in vivo biosensor for neurotransmitter release and in situ receptor activity. *Nat Neurosci, 13*(1), 127-132. doi: 10.1038/nn.2469

O'Malley, D. M., Sandell, J. H., & Masland, R. H. (1992). Co-release of acetylcholine and GABA by the starburst amacrine cells. *J Neurosci, 12*(4), 1394-1408.

Pan, B. X., Ito, W., & Morozov, A. (2009). Divergence between thalamic and cortical inputs to lateral amygdala during juvenile-adult transition in mice. *Biol Psychiatry, 66*(10), 964-971. doi: 10.1016/j.biopsych.2009.07.006

Pape, H. C., & Pare, D. (2010). Plastic synaptic networks of the amygdala for the acquisition, expression, and extinction of conditioned fear. *Physiol Rev, 90*(2), 419-463. doi: 10.1152/physrev.00037.2009

Pare, D. (2003). Role of the basolateral amygdala in memory consolidation. *Prog Neurobiol, 70*(5), 409-420.

Park, E. J., Nam, R. H., Choi, S., & Lee, C. J. (2004). Carbachol induces a form of long-term potentiation in lateral amygdala. *Neuroreport, 15*(8), 1339-1343.

Passani, M. B., Cangioli, I., Baldi, E., Bucherelli, C., Mannaioni, P. F., & Blandina, P. (2001). Histamine H3 receptor-mediated impairment of contextual fear conditioning and in-vivo inhibition of cholinergic transmission in the rat basolateral amygdala. *Eur J Neurosci, 14*(9), 1522-1532.

Pavesi, E., Gooch, A., Lee, E., & Fletcher, M. L. (2013). Cholinergic modulation during acquisition of olfactory fear conditioning alters learning and stimulus generalization in mice. *Learn Mem, 20*(1), 6-10. doi: 10.1101/lm.028324.112

Picciotto, M. R., Higley, M. J., & Mineur, Y. S. (2012). Acetylcholine as a neuromodulator: cholinergic signaling shapes nervous system function and behavior. *Neuron, 76*(1), 116-129. doi: 10.1016/j.neuron.2012.08.036

Pidoplichko, V. I., Prager, E. M., Aroniadou-Anderjaska, V., & Braga, M. F. (2013). alpha7-Containing nicotinic acetylcholine receptors on interneurons of the basolateral amygdala and their role in the regulation of the network excitability. *J Neurophysiol, 110*(10), 2358-2369. doi: 10.1152/jn.01030.2012

Power, A. E., McIntyre, C. K., Litmanovich, A., & McGaugh, J. L. (2003). Cholinergic modulation of memory in the basolateral amygdala involves activation of both m1 and m2 receptors. *Behav Pharmacol, 14*(3), 207-213. doi: 10.1097/01.fbp.0000073702.15098.21

Quirk, G. J., & Milad, M. R. (2010). Neuroscience: Editing out fear. *Nature, 463*(7277), 36-37. doi: 10.1038/463036a

Quirk, G. J., Repa, C., & LeDoux, J. E. (1995). Fear conditioning enhances short-latency auditory responses of lateral amygdala neurons: parallel recordings in the freely behaving rat. *Neuron, 15*(5), 1029-1039.

Ren, J., Qin, C., Hu, F., Tan, J., Qiu, L., Zhao, S., . . . Luo, M. (2011). Habenula "cholinergic" neurons co-release glutamate and acetylcholine and activate postsynaptic neurons via distinct transmission modes. *Neuron, 69*(3), 445-452. doi: 10.1016/j.neuron.2010.12.038

Ribeiro, A. M., Barbosa, F. F., Munguba, H., Costa, M. S., Cavalcante, J. S., & Silva, R. H. (2011). Basolateral amygdala inactivation impairs learned (but not innate) fear response in rats. *Neurobiol Learn Mem, 95*(4), 433-440. doi: 10.1016/j.nlm.2011.02.004

Rogan, M. T., Staubli, U. V., & LeDoux, J. E. (1997). Fear conditioning induces associative long-term potentiation in the amygdala. *Nature, 390*(6660), 604-607. doi: 10.1038/37601

Roldan, G., Cobos-Zapiain, G., Quirarte, G. L., & Prado-Alcala, R. A. (2001). Dose- and time-dependent scopolamine-induced recovery of an inhibitory avoidance response after its extinction in rats. *Behav Brain Res, 121*(1-2), 173-179.

Romanski, L. M., & LeDoux, J. E. (1992). Equipotentiality of thalamo-amygdala and thalamo-cortico-amygdala circuits in auditory fear conditioning. *J Neurosci, 12*(11), 4501-4509.

Roozendaal, B., van der Zee, E. A., Hensbroek, R. A., Maat, H., Luiten, P. G., Koolhaas, J. M., & Bohus, B. (1997). Muscarinic acetylcholine receptor immunoreactivity in the amygdala--II. Fear-induced plasticity. *Neuroscience, 76*(1), 75-83.

Rumpel, S., LeDoux, J., Zador, A., & Malinow, R. (2005). Postsynaptic receptor trafficking underlying a form of associative learning. *Science, 308*(5718), 83-88. doi: 10.1126/science.1103944

Sattarahmady, N., Heli, H., & Moosavi-Movahedi, A. A. (2010). An electrochemical acetylcholine biosensor based on nanoshells of hollow nickel microspheres-carbon microparticles-Nafion nanocomposite. *Biosens Bioelectron, 25*(10), 2329-2335. doi: 10.1016/j.bios.2010.03.031

Seguela, P., Wadiche, J., Dineley-Miller, K., Dani, J. A., & Patrick, J. W. (1993). Molecular cloning, functional properties, and distribution of rat brain alpha 7: a nicotinic cation channel highly permeable to calcium. *J Neurosci, 13*(2), 596-604.

Shin, R. M., Tsvetkov, E., & Bolshakov, V. Y. (2006). Spatiotemporal asymmetry of associative synaptic plasticity in fear conditioning pathways. *Neuron, 52*(5), 883-896. doi: 10.1016/j.neuron.2006.10.010

Shin, R. M., Tully, K., Li, Y., Cho, J. H., Higuchi, M., Suhara, T., & Bolshakov, V. Y. (2010). Hierarchical order of coexisting pre- and postsynaptic forms of long-term potentiation at synapses in amygdala. *Proc Natl Acad Sci U S A, 107*(44), 19073-19078. doi: 10.1073/pnas.1009803107

Shumyatsky, G. P., Malleret, G., Shin, R. M., Takizawa, S., Tully, K., Tsvetkov, E., . . . Bolshakov, V. Y. (2005). stathmin, a gene enriched in the amygdala, controls both learned and innate fear. *Cell, 123*(4), 697-709. doi: 10.1016/j.cell.2005.08.038

Sierra-Mercado, D., Padilla-Coreano, N., & Quirk, G. J. (2011). Dissociable roles of prelimbic and infralimbic cortices, ventral hippocampus, and basolateral amygdala in the expression and extinction of conditioned fear. *Neuropsychopharmacology, 36*(2), 529-538. doi: 10.1038/npp.2010.184

Siggins, G. R. (1979). Neurotransmitters and neuromodulators and their mediation by cyclic nucleotides. *Adv Exp Med Biol, 116*, 41-64.

Sigurdsson, T., Doyere, V., Cain, C. K., & LeDoux, J. E. (2007). Long-term potentiation in the amygdala: a cellular mechanism of fear learning and memory. *Neuropharmacology, 52*(1), 215-227. doi: 10.1016/j.neuropharm.2006.06.022

Spencer, D. G., Jr., Horvath, E., & Traber, J. (1986). Direct autoradiographic determination of M1 and M2 muscarinic acetylcholine receptor distribution in the rat brain: relation to cholinergic nuclei and projections. *Brain Res, 380*(1), 59-68.

Sugita, S., Uchimura, N., Jiang, Z. G., & North, R. A. (1991). Distinct muscarinic receptors inhibit release of gamma-aminobutyric acid and excitatory amino acids in mammalian brain. *Proc Natl Acad Sci U S A, 88*(6), 2608-2611.

Swanson, L. W. (2003). The amygdala and its place in the cerebral hemisphere. *Ann N Y Acad Sci, 985*, 174-184.

Tinsley, M. R., Quinn, J. J., & Fanselow, M. S. (2004). The role of muscarinic and nicotinic cholinergic neurotransmission in aversive conditioning: comparing pavlovian fear conditioning and inhibitory avoidance. *Learn Mem, 11*(1), 35-42. doi: 10.1101/lm.70204

Tsvetkov, E., Carlezon, W. A., Benes, F. M., Kandel, E. R., & Bolshakov, V. Y. (2002). Fear conditioning occludes LTP-induced presynaptic enhancement of synaptic transmission in the cortical pathway to the lateral amygdala. *Neuron, 34*(2), 289-300.

Tye, K. M., Prakash, R., Kim, S. Y., Fenno, L. E., Grosenick, L., Zarabi, H., . . . Deisseroth, K. (2011). Amygdala circuitry mediating reversible and bidirectional control of anxiety. *Nature, 471*(7338), 358-362. doi: 10.1038/nature09820

van der Zee, E. A., & Luiten, P. G. (1999). Muscarinic acetylcholine receptors in the hippocampus, neocortex and amygdala: a review of immunocytochemical localization in relation to learning and memory. *Prog Neurobiol, 58*(5), 409-471.

Vazdarjanova, A., & McGaugh, J. L. (1999). Basolateral amygdala is involved in modulating consolidation of memory for classical fear conditioning. *J Neurosci, 19*(15), 6615-6622.

Washburn, M. S., & Moises, H. C. (1992). Muscarinic responses of rat basolateral amygdaloid neurons recorded in vitro. *J Physiol, 449*, 121-154.

Watanabe, Y., Ikegaya, Y., Saito, H., & Abe, K. (1995). Roles of GABAA, NMDA and muscarinic receptors in induction of long-term potentiation in the medial and lateral amygdala in vitro. *Neurosci Res, 21*(4), 317-322.

Weiskrantz, L. (1956). Behavioral changes associated with ablation of the amygdaloid complex in monkeys. *J Comp Physiol Psychol, 49*(4), 381-391.

Wess, J. (2003). Novel insights into muscarinic acetylcholine receptor function using gene targeting technology. *Trends Pharmacol Sci, 24*(8), 414-420. doi: 10.1016/S0165-6147(03)00195-0

Williams, S. C., & Deisseroth, K. (2013). Optogenetics. *Proc Natl Acad Sci U S A, 110*(41), 16287. doi: 10.1073/pnas.1317033110

Wonnacott, S., Drasdo, A., Sanderson, E., & Rowell, P. (1990). Presynaptic nicotinic receptors and the modulation of transmitter release. *Ciba Found Symp, 152*, 87-101; discussion 102-105.

Wonnacott, S., Sidhpura, N., & Balfour, D. J. (2005). Nicotine: from molecular mechanisms to behaviour. *Curr Opin Pharmacol, 5*(1), 53-59. doi: 10.1016/j.coph.2004.12.002

Woolf, N. J. (1991). Cholinergic systems in mammalian brain and spinal cord. *Prog Neurobiol, 37*(6), 475-524.

Yajeya, J., De La Fuente, A., Criado, J. M., Bajo, V., Sanchez-Riolobos, A., & Heredia, M. (2000). Muscarinic agonist carbachol depresses excitatory synaptic transmission in the rat basolateral amygdala in vitro. *Synapse, 38*(2), 151-160. doi: 10.1002/1098-2396(200011)38:2<151::AID-SYN6>3.0.CO;2-K

Yizhar, O., Fenno, L. E., Davidson, T. J., Mogri, M., & Deisseroth, K. (2011). Optogenetics in neural systems. *Neuron, 71*(1), 9-34. doi: 10.1016/j.neuron.2011.06.004

Young, M. B., & Thomas, S. A. (2014). M1-muscarinic receptors promote fear memory consolidation via phospholipase C and the M-current. *J Neurosci, 34*(5), 1570-1578. doi: 10.1523/JNEUROSCI.1040-13.2014

Yun, A. J., Bazar, K. A., Lee, P. Y., Gerber, A., & Daniel, S. M. (2005). The smoking gun: many conditions associated with tobacco exposure may be attributable to paradoxical compensatory autonomic responses to nicotine. *Med Hypotheses, 64*(6), 1073-1079. doi: 10.1016/j.mehy.2004.11.040

Zaborszky, L. (2002). The modular organization of brain systems. Basal forebrain: the last frontier. *Prog Brain Res, 136*, 359-372.